

AD-A253 246



RL TR-92-5  
Final Technical Report  
January 1992

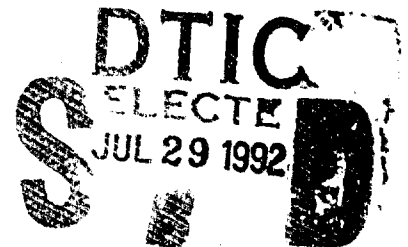


2

# 10KW L-BAND AMPLIFIER TUBES FOR EFFICIENT AND RELIABLE TROPOSCATTER COMMUNICATION TRANSMITTER SYSTEMS

Varian Associates, Inc.

Edward L. Eisen, Mike Chase, Merrald Schrader, Don Preist



*APPROVED FOR PUBLIC RELEASE; DISTRIBUTION UNLIMITED.*

02 7 21 153

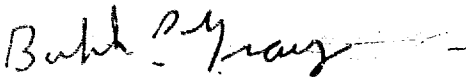


Rome Laboratory  
Air Force Systems Command  
Griffiss Air Force Base, NY 13441-5700

This report has been reviewed by the Rome Laboratory Public Affairs Office (PA) and is releasable to the National Technical Information Service (NTIS). At NTIS it will be releasable to the general public, including foreign nations.

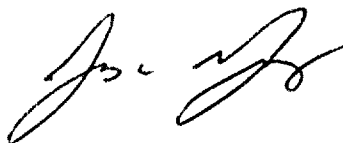
RL-TR-92-5 has been reviewed and is approved for publication.

APPROVED:



BOBBY R. GRAY  
Project Engineer

FOR THE COMMANDER:



JAMES W. YOUNGBERG, LT COL, USAF  
Deputy Director  
Surveillance and Photonics Directorate

If your address has changed or if you wish to be removed from the Rome Laboratory mailing list, or if the addressee is no longer employed by your organization, please notify RL(OCTI) Griffiss AFB, NY 13441-5700. This will assist us in maintaining a current mailing list.

Do not return copies of this report unless contractual obligations or notices on a specific document require that it be returned.

# REPORT DOCUMENTATION PAGE

Form Approved  
OMB No. 0704-0188

Public reporting burden for this collection of information is estimated to average 1 hour per response, including the time for reviewing instructions, searching existing data sources, gathering and maintaining the data needed, and completing and reviewing the collection of information. Send comments regarding this burden estimate or any other aspect of this collection of information, including suggestions for reducing this burden, to Washington Headquarters Services, Directorate for Information Operations and Reports, 1215 Jefferson Davis Highway, Suite 1204, Arlington, VA 22202-4302, and to the Office of Management and Budget, Paperwork Reduction Project (0704-0188), Washington, DC 20503.

1. AGENCY USE ONLY (Leave Blank)		2. REPORT DATE December 1991	3. REPORT TYPE AND DATES COVERED Final Apr 83 - Mar 87	
4. TITLE AND SUBTITLE 10KW L-BAND AMPLIFIER TUBES FOR EFFICIENT AND RELIABLE TROPOSCATTER COMMUNICATION TRANSMITTER SYSTEMS			5. FUNDING NUMBERS C - F30602-83-C-0149 PE - 33126F PR - 2157 TA - 03 WU - 14	
6. AUTHOR(S) Edward L Eisen, Mike Chase, Merrald Schrader, Don Priest			8. PERFORMING ORGANIZATION REPORT NUMBER	
7. PERFORMING ORGANIZATION NAME(S) AND ADDRESS(ES) Varian Associates Inc 611 Hansen Way Palo Alto CA 93403 Varian Associates Inc EIMAC Division 311 Industrial Way San Carlos CA 94070			10. SPONSORING/MONITORING AGENCY REPORT NUMBER RL-TR-92-5	
9. SPONSORING/MONITORING AGENCY NAME(S) AND ADDRESS(ES) Rome Laboratory (OCTP) Griffiss AFB NY 13441-5700 Defense Communications Agency Washington DC 20305			11. SUPPLEMENTARY NOTES Rome Laboratory project engineer: Bobby R Gray/OCTP/(315) 330-4381	
12a. DISTRIBUTION/AVAILABILITY STATEMENT Approved for public release; distribution unlimited.			12b. DISTRIBUTION CODE	
13. ABSTRACT (Maximum 200 words) The purpose of this program was to develop two advanced development model high power amplifier tubes specifically for troposcatter communication application. Varian Associates was awarded a single contract to develop a klystron model tube and a klystrode model tube. Critical elements of the specification for the two tubes were (a) power output 10kw, (b) 10 MHz electronics bandwidth, (c) 750-980 MHz tuning range and (d) efficiency 50%. The challenge for the klystron design was to be able to maintain efficiency in excess of 50% over the full 10 MHz bandwidth. This was accomplished with an eight cavity design. The klystrode challenge required designing a new grid shape that integrates a converging electron beam with a cavity with a minimal magnetic field focusing. Results of the program were that basically most of the performance specifications were demonstrated. However, the klystron showed a sharp drop-off in power at 840 MHz due to a second harmonic cavity mode. The klystrode has considerably less gain than the existing klystron and thus additional RF drive is required.				
14. SUBJECT TERMS Klystron, Klystrode, High Efficiency, Wide Bandwidth, Reliable, Troposcatter Communication			15. NUMBER OF PAGES	
			16. PRICE CODE	
17. SECURITY CLASSIFICATION OF REPORT UNCLASSIFIED	18. SECURITY CLASSIFICATION OF THIS PAGE UNCLASSIFIED	19. SECURITY CLASSIFICATION OF ABSTRACT UNCLASSIFIED	20. LIMITATION OF ABSTRACT UL	

## TABLE OF CONTENTS

<u>Section</u>	<u>Page</u>
1.0 EXECUTIVE SUMMARY . . . . .	1
1.1 Introduction . . . . .	1
1.2 10 KW L-Band Klystron . . . . .	1
1.3 10 KW L-Band Klystrode . . . . .	3
2.0 10 KW L-BAND KLYSTRON . . . . .	6
2.1 Introduction . . . . .	6
2.1.1 Program Objective . . . . .	6
2.1.2 Typical Performance of Klystrons Now in Use . . . . .	6
2.1.3 Perspective of Klystron Now in Service . . . . .	7
2.1.4 Work Completed During First Half of Program . . . . .	7
2.1.5 Work Completed During Second Half of Program . . . . .	7
2.2 Design Study for Improved Performance in Terms of Instantaneous Bandwidth and Efficiency . . . . .	8
2.2.1 Instantaneous Bandwidth . . . . .	8
2.2.1.1 Basic Design Criteria . . . . .	8
2.2.1.2 Beam Resistance . . . . .	8
2.2.1.3 Beam-Coupling Coefficient . . . . .	9
2.2.1.4 Characteristic Cavity Impedance . . . . .	10
2.2.2 Efficiency . . . . .	12
2.2.2.1 Basic Design Criteria . . . . .	12
2.2.2.2 Drift Lengths, Cavity Interaction Gap Lengths and Drift Tube Diameter . . . . .	12
2.2.3 Determination of the Complete Klystron Circuit Configuration . . . . .	13
2.2.3.1 The Four-Cavity Configuration . . . . .	13
2.2.3.2 The Five-Cavity Configuration . . . . .	13
2.2.3.3 The Six-Cavity Configuration . . . . .	14
2.2.4 Determination of the RF Output Circuit . . . . .	14
2.2.4.1 Double-Tuned RF Output Circuits . . . . .	14
2.2.4.2 External RF Output Circuits . . . . .	14
2.2.4.3 The Integral RF Output Circuit (Inductive Sliding Short Tuning) . . . . .	17
2.2.4.4 The Integral RF Output Circuit (Capacitive Tuning) . . . . .	17

2.2.5	Klystron Design Summary . . . . .	20
2.3	Design Review of the Major Klystron Assemblies . . . . .	20
2.3.1	The Electron Gun . . . . .	20
2.3.2	The RF Cavity Tuner Mechanism . . . . .	29
2.3.3	The Collector . . . . .	29
2.3.4	The Electromagnet . . . . .	32
2.3.5	The Electrical Design . . . . .	32
2.3.6	The Mechanical Design . . . . .	32
2.4	Performance Tests . . . . .	37
2.4.1	Electron Beam Performance . . . . .	37
2.4.2	Klystron RF Amplification Performance . . . . .	37
2.4.3	Overall Klystron Performance . . . . .	59
2.5	Design Refinements for Future Engineering Development Model . . . . .	70
2.5.1	Introduction . . . . .	70
2.5.2	RF Output Circuit Loading for Improved Efficiency . . . . .	70
2.5.3	Loading of the Driver Cavities for the Desired Bandwidth . . . . .	71
2.5.4	Vapor-Phase Collector . . . . .	71
2.5.5	Magnetic Field Refinements . . . . .	71
2.5.6	Mechanical Refinements . . . . .	72
2.5.7	Elimination of Interfering Harmonic Mode . . . . .	72
2.6	Conclusions . . . . .	72
3.0	10 KW L-BAND KLYSTRODE . . . . .	74
3.1	Introduction . . . . .	74
3.1.1	Program Objectives . . . . .	74
3.1.2	Work Completed During First Half of Program . . . . .	74
3.1.3	Work Completed During Second Half of Program . . . . .	75
3.2	Design Review of Critical Sub Assemblies . . . . .	76
3.2.1	The Input Circuit . . . . .	76
3.2.2	The Input Coupler . . . . .	76
3.2.3	The Electron Gun . . . . .	79
3.2.4	The Output Circuit . . . . .	80
3.2.5	The Focusing System and the Collector . . . . .	81
3.2.6	The Complete Klystrode Amplifier . . . . .	83
3.2.7	Subsystem Support . . . . .	83
3.3	Performance Tests . . . . .	83
3.3.1	DC Beam Performance . . . . .	83
3.3.2	Klystrode RF Amplification Performance . . . . .	90

3.3.3	Efficiency Results . . . . .	90
3.3.4	Bandwidth Data . . . . .	94
3.4	Problems Encountered During the Program . . . . .	94
3.5	Future Engineering Programs . . . . .	97
3.5.1	Complete Amplifier Characterization . . . . .	97
3.5.2	Input Coupling . . . . .	97
3.5.3	Collector Improvements . . . . .	97
3.5.4	Permanent Pole Magnet . . . . .	98
3.5.5	Productization . . . . .	98
3.6	Summary and Conclusions . . . . .	98

**DTIC QUALITY INSPECTED 2**

<b>Accession For</b>	
NTIS GRA&I	<input checked="" type="checkbox"/>
DTIC TAB	<input type="checkbox"/>
Unannounced	<input type="checkbox"/>
Justification _____	
By _____	
Distribution/	
<b>Availability Codes</b>	
Dist.	Avail and/or Special
A-1	

LIST OF TABLES

<u>Table</u>		<u>Page</u>
1	Nominal Performance Specifications and Design Parameters for an Efficient, Reliable, High-Power UHF Amplifier . . . . .	22
2	Summary of the VKP-7865 Klystron Amplifier RF Performance . . . . .	41
3	Counter Readings for Each Cavity to Set $F_0$ in 5 MHz Steps . . . . .	69
4	X2255 General Operating Specifications . . . . .	88

## LIST OF ILLUSTRATIONS

<u>Figure</u>	<u>Page</u>
2-1     A Cross-Section View of a Typical Klystron RF Cavity with Cylindrical Geometry . . . . .	11
2-2     Efficiency as a Function of R/Q in the Output Cavity . . . . .	15
2-3     General Layout of a Typical External RF Cavity . . .	16
2-4     General Layout of an Integral RF Cavity with Rectangular Geometry . . . . .	18
2-5     General Layout of an Integral RF Cavity with Cylindrical Geometry . . . . .	19
2-6     R/Q as a Function of Frequency for Three Different RF Cavity Types . . . . .	21
2-7     Beam Analyzer Test Results for the Electrostatically Focused Electron Beam, $I_{\text{cat}} = 0$ . . . . .	24
2-8     Beam Diameter Variation as a Function of Axial Distance for the Electrostatically Focused Beam of Fig 2-1 . . . . .	25
2-9     Beam Analyzer Test Results for the Beam of Fig 2-1 With Magnetic Focusing, $I_{\text{cat}} = 12.9$ A . . . . .	26
2-10    Beam Diameter Variation as a Function of Axial Distance for the Magnetically Focused Beam of Fig 2-3 . . . . .	27
2-11    Three Dimensional Plots of the Electron Beam Current Density Profile . . . . .	28
2-12    Comparison of R/Q vs Frequency for Two Different Cavity Geometries and Tuner Types . . . . .	30
2-13    Layout of the Capacitive Tuner in the Cylindrical RF Cavity . . . . .	31
2-14    VYW-7865 Magnetic Field Goal Curve . . . . .	33
2-15    The VYW-7865 Electromagnet With the VKP-7865 Klystron Installed . . . . .	34
2-16    The VKP-7865 Klystron Amplifier . . . . .	35

2-17	The VKP-7865 Klystron Amplifier Rotated . . . . .	36
2-18	Power Output vs Frequency Curves (S) and (B) at $F_0 = 755$ MHz . . . . .	39
2-19	Power Output vs Frequency Curve (C) at $F_0 = 755$ MHz .	40
2-20	Power Output vs Frequency Curves (A) and (B) at $F_0 = 780$ MHz . . . . .	42
2-21	Power Output vs Frequency Curve (C) at $F_0 = 780$ MHz .	43
2-22	Power Output vs Frequency Curves (A) and (B) at $F_0 = 810$ MHz . . . . .	44
2-23	Power Output vs Frequency Curve (C) at $F_0 = 810$ MHz .	45
2-24	Power Output vs Frequency Curves (A) and (B) at $F_0 = 845$ MHz . . . . .	46
2-25	Power Output vs Frequency Curve (C) at $F_0 = 845$ MHz .	47
2-26	Power Output vs Frequency Curves (A) and (B) at $F_0 = 870$ MHz . . . . .	48
2-27	Power Output vs Frequency Curve (C) at $F_0 = 870$ MHz .	49
2-28	Power Output vs Frequency Curves (A) and (B) at $F_0 = 900$ MHz . . . . .	50
2-29	Power Output vs Frequency Curve (C) at $F_0 = 900$ MHz .	51
2-30	Power Output vs Frequency Curves (A) and (B) at $F_0 = 930$ MHz . . . . .	52
2-31	Power Output vs Frequency Curve (C) at $F_0 = 930$ MHz .	53
2-32	Power Output vs Frequency Curves (A) and (B) at $F_0 = 960$ MHz . . . . .	54
2-33	Power Output vs Frequency Curve (C) at $F_0 = 960$ MHz .	55
2-34	Power Output vs Frequency Curves (A) and (B) at $F_0 = 985$ MHz . . . . .	56
2-35	Power Output vs Frequency Curve (C) at $F_0 = 985$ MHz .	57
2-36	Power Output vs Frequency at $F_0 = 840$ MHz, 4th Cavity Harmonic Mode Shown . . . . .	58
2-37	Power Output vs Drive Power at $F_0 = 755$ MHz . . . . .	60

2-38	Power Output vs Drive Power at $F_0 = 870$ MHz . . . . .	61
2-39	Power Output vs Drive Power at $F_0 = 985$ MHz . . . . .	62
2-40	Tuning Curve for Cavity #1 . . . . .	63
2-41	Tuning Curve for Cavity #2 . . . . .	64
2-42	Tuning Curve for Cavity #3 . . . . .	65
2-43	Tuning Curve for Cavity #4 . . . . .	66
2-44	Tuning Curve for Cavity #5 . . . . .	67
2-45	Tuning Curve for Cavity #6 . . . . .	68
3-1	X2255 Klystrode Device . . . . .	77
3-2	Schematic of Klystrode Device . . . . .	78
3-3	X2255 Electron Gun Structure . . . . .	80
3-4	Double Tuned Output Circuit . . . . .	82
3-5	Axial Magnetic Field (Electromagnet) . . . . .	84
3-6	Klystrode in Its Experimental Circuit . . . . .	85
3-7	Electrical Subsystems . . . . .	86
3-8	Cooling Subsystems . . . . .	87
3-9	DC Triode Curves . . . . .	89
3-10	RF Output Power and Beam Current vs RF Drive Curve . . . . .	91
3-11	Efficiency vs Center Frequency Curve . . . . .	92
3-12	Efficiency vs Bandwidth Curve . . . . .	93
3-13	Output Response at 920 MHz . . . . .	95
3-14	Output Response at 800 MHz . . . . .	96
3-15	Axial Magnetic Field (Permanent Magnet) . . . . .	99

## 1.0 EXECUTIVE SUMMARY

### 1.1 Introduction

The objective of this program was to develop an efficient and reliable high-power amplifier and its focusing system for use in a troposcatter communications system. Two separate approaches were undertaken in designing this power amplifier. The Final Technical Reports detail design and testing of a Klystron and a Klystrode Amplifier for operation in the 755 to 985 MHz band. These reports were submitted on the dates indicated.

a. "A 10 KW L-Band Klystron as an Efficient, Reliable, High-Power Amplifier", May 1986.

b. "A 10 KW L-Band Klystrode Amplifier for Efficient Wideband Troposcatter Applications", April 1988.

Following are summaries of these two reports and are included as sections 2 and 3 of this combined document.

### 1.2 10 KW L-Band Klystron

An Advanced Development Model of a high power Klystron Amplifier was developed, built and tested. Performance met all customer specifications including a 755 to 985 MHz tuning range, a 9 MHz (-1 dB) instantaneous bandwidth, 35 dB minimum gain, 12 kW CW minimum RF power output, and 50 percent minimum efficiency.

The Klystron has six (6) integral cavities with capacitive tuners, coaxial RF output and input lines, a diode gun system forming a converging electron beam, and a water cooled collector and body. A water cooled electromagnet was developed for beam focusing.

Electron gun design goals included 12 kV DC maximum capability at a nominal  $1 \times 10^{-6}$  A/V<sup>3/2</sup> and a cathode-beam area convergence ratio of 4:1. An impregnated tungsten matrix cathode was chosen. Gun performance with magnetic focusing was evaluated in a beam analyzer at reduced beam voltage.

Two cavity types were evaluated: 1) a cylindrical shape with a capacitive tuner and 2) a rectangular shape with an inductive tuner. Coupling its high characteristic impedance (R/Q) with its compact size and tuning range made the cylindrical shape with capacitive tuner the best choice for all six (6) resonators.

A water cooled focusing magnet was developed for this application. Special tuner counter mechanisms were installed on the outside of

the magnet. Greatest klystron efficiency was achieved with reduced field in the vicinity of the output cavity.

Extensive full and reduced power testing of the Advanced Development Model was performed. The electron beam was evaluated with and without RF. Typical DC and RF transmissions were 99.5 percent and 98.9 percent respectively. The beam showed excellent stability under extreme conditions of magnetic field and RF drive. Beam perveance was a nominal  $1.1 \times 10^{-6} \text{ A/V}^{3/2}$ .

It was found during preliminary testing that in order to meet efficiency and instantaneous bandwidth requirements simultaneously, the RF input drive power had to be reduced approximately 2 dB from that required for full saturated power output. After discussions with cognizant RADC and Mitre Corporation engineering personnel, it was established that the klystron would almost never be operated at full saturated power output, but rather at a level .9 dB below the full saturated power output.

Consequently, to demonstrate performance under several conditions, bandwidth and power output were measured at:

- a. Saturated center frequency power output of 16 kW CW minimum
- b. Same as (a) except drive power now reduced to give nominal 13 kW CW power output (Saturation -.9dB)
- c. Same as (a) except drive power now adjusted to simultaneously meet or exceed 50 percent minimum efficiency, 35 dB minimum gain, 9 MHz (-1 dB) minimum bandwidth, and 12 kW CW minimum power output.

These tests were done at 755, 780, 810, 845, 870, 900, 930, 960, and 985 MHz. The goals of (c) above were met or exceeded at all test frequencies. Additional testing was performed to determine the klystron efficiency at lower DC beam power levels. Output loading experiments were also made under certain conditions to observe the effect on efficiency.

A second harmonic mode associated with the fourth cavity was discovered in the form of a large notch in the bandpass when the tube was operating in the vicinity of 840 MHz. To prevent possible damage, the klystron should not be tuned for operation at center frequencies between 830 and 850 MHz.

During a possible follow on phase to this program, an Engineering Model Klystron should include the following design requirements:

- a. Increase efficiency by optimizing the output cavity loading.

- b. Simplify tube construction by reducing driver cavity loading.
- c. Redesign the collector to provide vapor-phase cooling.
- d. Reduce the 4th and 5th coil windings of the electromagnet to achieve desired magnetic field shape.
- e. Redesign the output polepieces of the klystron and electromagnet to reduce klystron weight and make polepiece handling easier.
- f. Redesign the tuner counter to eliminate flexing of the engaging shaft and bearing assembly.
- g. If possible, eliminate or reduce the effects of the 2nd harmonic mode associated with the 4th RF cavity.

### 1.3 10 KW L-Band Klystrode

A Klystrode Amplifier for Troposcatter Communications Systems operating in the 755 to 795 MHz range was designed, built and tested. The various subsections of a Klystrode Amplifier are the input circuit, electron gun, output circuit, collector, and focusing system. These subsections have interdependent design problems.

The "bell" type input circuit was scaled directly from that of the television configuration. The RF drive is coupled to the grid bell by way of a capacitive probe. A convergent gun structure with a pyrolytic graphite control grid was used. This control grid density modulates the electron beam as opposed to velocity modulating it. Grid fabrication was a major problem. After extended delays relating to computer programming and hardware for cutting the grids, the final solution was completely satisfactory.

The external output cavity used on the Klystrode is an iris coupled double tuned structure. The output window was eventually fabricated from BeO ceramic because of early failures with AD-99 high purity alumina.

The collector on this experimental tube is the same water cooled collector used on the 300 kW television klystrode. It is recognized that the collector is overrated for this application but was selected because it was expedient and inexpensive.

The electron beam must be focused from cathode to collector. Being short in length, the Klystrode tube requires only one focusing magnet. With the gun pushed up into the conical anode, it was

possible to use a conical polepiece leading to a smaller aperture and less magnet power than would otherwise be required.

The following is a list of Klystrode general operating specifications:

Beam Voltage	16 to 18 kW
Grid Bias Voltage Range	-30 to -80 Volts
Cathode Heater Voltage	7.0 Volts
Cathode Heater Current	10.8 Amps
Maximum Allowable Gas Current	100 uAmps
Magnet Voltage	35 Volts
Magnet Current	5 Amps
Collector Cooling Water Flow	25 gpm @ 25 psi
Body Cooling Water Flow	1.5 gpm @ 25 psi
Input Circuit and Cathode Cooling Air Flow	10 cfm @ 2 in of H <sub>2</sub> O
Output Circuit Cooling Air Flow	100 cfm @ 1 in of H <sub>2</sub> O

The Final Technical Report includes Klystrode performance data. The first critical performance test for the klystrode is measurement of the triode characteristics of the gun. A graph of beam and grid currents as functions of grid voltage at 17.5 kV anode voltage is presented. The plot shows that grid current is never greater than 23% of beam current in the range of measured grid voltages. Grid-cathode cutoff voltage is 75 volts negative.

Most of the data measured for the klystrode amplifier is around two frequencies: 800 and 920 MHz. The device's performance at higher frequencies was not measured due to the unavailability of RF drive above 930 MHz. Bandpass was plotted at both frequencies and included in the final report. At 920 MHz, center frequency power output and efficiency are 12 kW and 50%, respectively. Corresponding values at 800 MHz are 12 kW and 56%.

Additional data is included for 920 MHz with the circuit adjusted for .5 dB, 10 MHz bandwidth, it appears that center frequency output saturation occurs at slightly greater than 12 kW. Power gain is about 19.6 dB.

Time and funding did not allow completion of this job. Measured data is not complete and a program is necessary to complete the measurements across the operational band. This will allow generation of tuning curves and tables. There are also several subsystems which could be improved with further work.

Future engineering programs should also include:

- a. Improvement of the input coupling system
- b. Development of a vapor or air cooled collector

c. Replacement of the electromagnet with a permanent magnet focusing system

d. Productizing the experimental device and hardware for reason of usability, maintainability, and safety.

## 2.0 10 KW L-BAND KLYSTRON

### 2.1 Introduction

#### 2.1.1 Program Objective

The objective of this program was the development of an efficient and reliable high-power klystron amplifier and its focusing system for use in a troposcatter radio communications system. The klystron was to be tunable from 755 MHz to 985 MHz and provide a minimum (-1 dB) instantaneous bandwidth of 9 MHz. The minimum power output was to be 12 KW CW and the minimum dc to rf conversion efficiency was to be 50%. All operating parameters (voltages, currents, etc.) were to be compatible with the existing equipment used in the communications system. The many advances which have been made in the manufacture and performance of klystrons, since the original installation of the present communications system, was utilized, as needed, to help fulfill the program objectives.

This program is an outgrowth of similar programs in which high-power klystrons, operating in the C-band and S-band frequency ranges, were developed. The final report for the S-band program, report no. CSA-76-8072-F, written in 1980 under contract DAAB07-76-C-8072, was used as a reference for this program. In the area of tube/system compatibility, this report was used extensively. The report also contains a proposed paper design for an L-band klystron which was investigated, but was rejected in favor of a more suitable design based on the present day technology.

#### 2.1.2 Typical Performance of Klystrons Now in Use

One tube, presently used in the troposcatter radio communications system, is the 4KL50000LR. The 4KL50000LR is a four-cavity klystron of the external rf cavity type, tunable over the 755 to 985 MHz range. Typical performance for this tube, when tuned for high-efficiency operation at 755 MHz is:

Power Output	12 kW CW
Instantaneous Bandwidth (-1 dB)	1 MHz
Gain	49 dB
DC to RF Conversion Efficiency	40%

Typical performance for this tube when tuned for broadband operation at 755 MHz is:

Power Output	10 kW CW
Instantaneous Bandwidth (-1 dB)	4 MHz
Gain	37 dB
DC to RF Conversion Efficiency	31%

The 4KM5000LR can be tuned for considerably more instantaneous bandwidth, at the cost of reduced gain, power output, and efficiency.

### 2.1.3 Perspective of Klystron Now in Service

The 4KM5000LR was developed using the best design knowledge available in the late 1950s, but the tube cannot deliver the required performance to meet the objectives of this program. If a redesign effort were initiated, the original design parameters would be evaluated relative to tube technology developed since this tube was introduced. Substantial redesign would be expected and consequently, such an approach is unattractive as a starting point for this program.

However, in the intervening years since the introduction of the 4KM5000LR, sophisticated computer programs have been developed to analyze both small-signal and large-signal performance of rf excited electron beams. Coupled with new design concepts, these computer programs provide the tools to create a present day state-of-the-art klystron to meet today's program objectives.

### 2.1.4 Work Completed During the First Half of the Program

The first half of the program was spent doing research and development relating to the electrical and mechanical design of the klystron. The required combination of wide tunability, wide instantaneous bandwidth, and high efficiency presented special problems at the desired rf power output level. An rf cavity with a large characteristic impedance,  $R/Q$ , and a wide tuning range needed to be developed in order to satisfy the above requirements. The basic klystron architecture and the electron beam to rf cavity coupling circuit were developed. The ceramic coaxial rf output window was designed, fabricated, and cold-tested. Work was begun on the development of the electron gun, the water cooled collector, and the rf cavities and their tuning mechanisms. The mechanical layout of the klystron was also being developed during this time, as well as, many of the piece part drawings needed for parts fabrication.

### 2.1.5 Work Completed During the Second Half of the Program

The second half of the program was spent completing the development of the electron gun, the water cooled collector, the rf cavities and their tuning mechanisms, and the electromagnet for the focusing of the electron beam. All documentation, necessary for piece part and assembly fabrication, were completed and all parts were ordered and received. Klystron construction, cold-testing, final assembly, bake-out, and hot-testing were also completed during this time.

## 2.2 Design Study for Improved Performance in Terms of Instantaneous Bandwidth and Efficiency

### 2.2.1 Instantaneous Bandwidth

#### 2.2.1.1 Basic Design Criteria

Within practical limits, the instantaneous bandwidth of a klystron is not generally limited by the bandwidth of the individual driver cavities unless very high gain is desired. Ignoring gain, the driver cavities can be loaded and staggered in frequency, so that a klystron may provide extremely wide instantaneous bandwidth, limited only by the instantaneous bandwidth capability of its output circuit. However, when high efficiency is required as well as a specified minimum instantaneous bandwidth, the klystron design parameters  $Q$  (loaded),  $R/Q$ ,  $M$ , and  $R_o$ , plus the klystron circuit configuration are the controlling factors (see text below).

At 755 MHz, an output cavity  $Q$  (loaded) no greater than 40, is required to meet the instantaneous bandwidth requirement of 9 MHz (-1 dB). This value is determined using Equation (1). Equation (1) is derived from the impedance-bandwidth equation for a single-tuned resonant cavity.

$$Q \text{ (loaded)} = 0.509 \times F_o / (-1 \text{ dB}) \text{ Bandwidth} \quad (1)$$

To realize optimum performance from a klystron with an output cavity loaded for a specific instantaneous bandwidth, a long and tedious set of calculations must be performed to optimize the klystron design parameters and the klystron configuration for the specified  $Q$  (loaded). Fortunately, computer programs now exist which simulate small-signal and large-signal klystron performance; making these calculations relatively simple. As with any computer program, an initial set of the klystron design parameters must be used as a starting point. The  $Q$  (loaded) has already been determined from Equation (1) and an empirical relationship, based on optimum performance, exists between the  $Q$  (loaded) and the other three klystron design parameters. This relationship states that the  $Q$  (loaded) of the output cavity is proportional to the beam resistance,  $R_o$ , and inversely proportional to the beam coupling coefficient,  $M$ , and the characteristic cavity impedance,  $R/Q$ . Choosing the appropriate combination of values for  $R_o$ ,  $M$ , and  $R/Q$ , which will satisfy the empirical relationship above, requires a complete analysis of the system operating parameters, klystron performance specifications, and the output cavity geometry.

#### 2.2.1.2 Beam Resistance

The beam resistance,  $R_o$ , is defined by the ratio of the dc beam voltage to the dc beam current and the value becomes fixed when the

power output, efficiency, and perveance are specified. To calculate the beam resistance, the values for the beam voltage and the beam current must first be computed.

The beam power is defined by the product of the beam voltage and the beam current. For the required power output of 12 kW and dc to rf conversion efficiency of 50%, the beam power,  $P_b$ , required is 24 kW.

$$P_b = I_b \times E_b = 24 \text{ kW} \quad (2)$$

The beam current is related to the beam voltage by the simple diode equation shown as equation (3).

$$I_b = K \times (E_b)^{3/2} \quad (3)$$

Substituting (3) in (2)

$$P_b = K \times (E_b)^{5/2} \quad (4)$$

Letting  $K = 1.0 \times 10^{-6} \text{ A/V}^{3/2}$  in (4) gives:

$$E_b = 14.2 \text{ kV} \quad (5)$$

Let  $E_b = 14 \text{ kV}$  and then (3) gives:

$$I_b = 1.66 \text{ A} \quad (6)$$

The beam resistance is then calculated as:

$$R_o = 14000 / 1.66 = 8,434 \text{ ohms} \quad (7)$$

The choice of the beam perveance,  $K$ , is based on a compromise of the requirements for efficiency and bandwidth, as well as the requirement for a beam voltage and beam current which are compatible with the present system power supplies. In general, klystrons with low perveance provide high efficiency and narrow instantaneous bandwidths and klystrons with high perveance provide wide instantaneous bandwidths and lower efficiency.

### 2.2.1.3 Beam-Coupling Coefficient

The beam-coupling coefficient,  $M$ , is defined by the ration of the peak rf current induced in the cavity gap to the peak rf current on the beam in the gap. The factors which control the value of  $M$  include the drift tube diameter, the beam diameter, the interaction gap length, the beam voltage and the frequency.

The drift tube diameter is small to maximize  $M$  and to minimize the interaction gap capacitance for good tunability and high  $R/Q$ , but

not so small as to require excessive magnetic field strength to focus the electron beam. For this program, a drift tube diameter of 0.562 inch provides the best compromise.

The beam diameter is specified by the filling factor which is a fixed percentage of the drift tube diameter. For most tubes designed today, a filling factor of 65% is used. Based on a drift tube diameter of 0.562 inch and a filling factor of 65%, the beam diameter is 0.365 inch.

The cavity interaction gap is the region where the electrons in the beam interact with the rf fields in the cavity. The gap is large, again, to minimize the gap capacitance for good tunability and high R/Q; but not so large as to degrade M significantly. For this program, the gap length is 0.525 inch and this is a little less than 1.0 radians at 755 MHz.

With the drift tube diameter, beam diameter, and the gap length set, the value of M varies from 0.91 to 0.85 over the 755 MHz to 985 MHz frequency range when a beam voltage of 14 kV is used in the calculation. The theoretical maximum value for M is 1.0, but this value is never realized. The values for M could be increased by reducing the gap length, but the requirement for minimum gap capacitance is felt to be more important for this program and the values of M achieved will provide adequate performance.

#### 2.2.1.4 Characteristic Cavity Impedance

The characteristic cavity impedance, R/Q, is a cavity quality factor which influences circuit performance in terms of bandwidth, gain, and efficiency. A cavity's R/Q is defined as:

$$R/Q = (L/C)^{1/2} \quad (8)$$

Where L is the cavity inductance and C is the cavity capacitance.

Figure 2-1 illustrates a cross-sectional view of a typical rf cavity with cylindrical geometry. An inductive path, P, is shown in heavy outline. If the inductive path is revolved about the Z-axis, the total cavity inductance is defined. The cavity inductance increases only when the length of P increases. The cavity capacitance is the sum of C1 and C2. C1 is the capacitance between the cavity top and the cavity bottom and C2 is the interaction gap capacitance. Within limits, the cavity capacitance decreases when the cavity height, H, and/or the gap length, G, is increased and it also decreases when the cavity diameter, D, and/or the drift tube diameter, d, is decreased.

Since the cavity inductance and the cavity capacitance are determined solely by cavity geometry, the cavity R/Q is determined solely by the cavity geometry. The cavity R/Q is maximized when

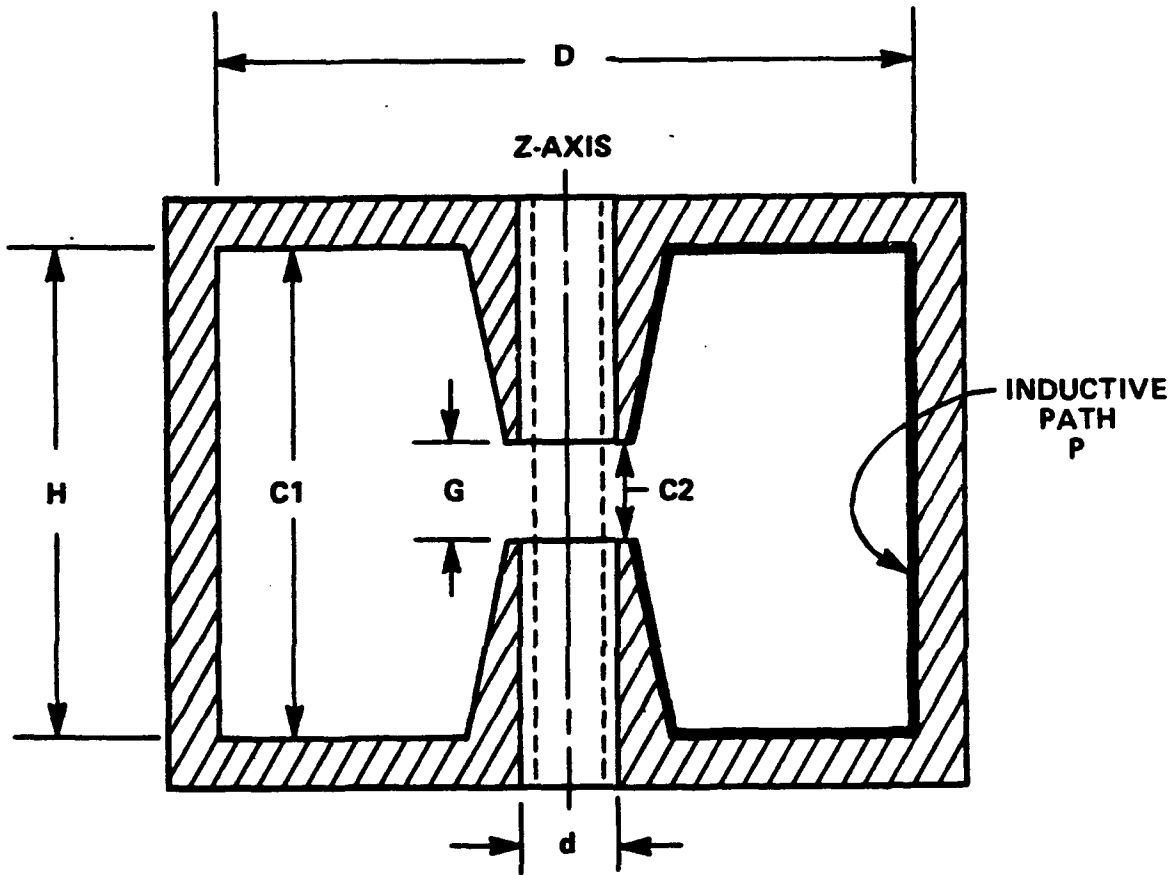


FIGURE 2-1. A CROSS-SECTION VIEW OF A TYPICAL KLYSTRON RF CAVITY WITH CYLINDRICAL GEOMETRY

the cavity inductance is maximized and the cavity capacitance is minimized. Since the cavity geometry is the only constraint on the R/Q, great effort has been spent on the tailoring of the cavity geometry in order to maximize the available R/Q. The larger the R/Q is, the lower the output cavity Q (loaded) may be, which will result in greater instantaneous bandwidth capability with high-efficiency operation.

## 2.2.2 Efficiency

### 2.2.2.1 Basic Design Criteria

The efficiency of a klystron is a measure of its ability to convert the dc (kinetic) energy in the beam to rf (electromagnetic) energy in the output circuit. To achieve high efficiency, the electron beam must be sufficiently bunched, such that each bunch is optimum when it reaches the output cavity interaction gap. Once this is achieved, a sufficiently high-beam coupling coefficient must exist to allow the efficient transfer of energy from the beam to the output cavity.

Again, the klystron dimensions are the controlling factors in achieving a high-efficiency klystron design. In particular, the drift lengths between cavity gaps, the cavity interaction gap lengths and the drift tube diameter must be optimized to realize high-efficiency performance.

### 2.2.2.2 Drift Lengths, Cavity Interaction Gap Lengths and Drift Tube Diameter

A drift length is defined as the distance from the center of one cavity interaction gap to the center of the next cavity interaction gap. The cavity interaction gap is the region where the electron beam interacts with the rf fields in the cavity. The drift lengths provide the proper positioning of the cavity interaction gaps, so that the electron beam may be properly bunched and the energy in the bunches may be efficiently extracted by the output circuit. The length of the interaction gaps and the drift tube diameter are important factors in determining the beam coupling coefficient and the beam coupling coefficient determines how effective the interaction will be between the beam and the cavity. Proper optimization of these parameters is critical to the optimum extraction of energy from the electron beam by the output circuit.

### 2.2.3 Determination of the Complete Klystron Circuit Configuration

#### 2.2.3.1 The Four-Cavity Configuration

The 4KM50000LR is a four-cavity design which provides typical performance for a tube designed in the late 50's. Today, the four-cavity klystron is most often used when high gain and efficiency are desired, but wide instantaneous bandwidth is not a requirement. Broadband tuning of a four-cavity klystron is possible at the cost of reduced gain and efficiency. The broadband tuning of the driver cavities causes the reduction in gain, but the increased output circuit loading, which is required to take advantage of the broadband tuning of the driver cavities, may affect efficiency because the lower Q (loaded) may require an increase in the R/Q to maintain the same efficiency. This condition is not limited to four-cavity designs but is true for any output circuit of the single-tuned resonator variety. For this program, the use of a four-cavity design is not desirable because of the low gain characteristic under broadband conditions.

#### 2.2.3.2 The Five-Cavity Configuration

More recently, five-cavity designs have been used to increase the gain-bandwidth performance of klystrons. An extra driver cavity is added to help support the output circuit bandpass under broadband tuning conditions and it also provides an extra stage of small signal gain. However, the addition of another in-band driver cavity does not significantly enhance the tube efficiency.

If the R/Q could be increased indefinitely, the output circuit could be loaded to provide ever increasing instantaneous bandwidths and the tube efficiency would remain relatively constant. However, infinite R/Q is not reality and if the output circuit is loaded too heavily relative to the available R/Q, the output circuit performance will suffer in terms of efficiency.

The efficiency of a five-cavity tube generally runs around 50% to 54% under optimum conditions. For this program, the instantaneous bandwidth requirements are so large at the low end of the frequency tuning range, that the optimum R/Q for the Q (loaded) needed to achieve the bandwidth requirement, cannot be realized in any cavity configuration designed to meet all the program performance requirements. Therefore, some degradation in efficiency will be experienced due to insufficient R/Q. For a five-cavity design this could result in an efficiency significantly below 50%, which makes the design unattractive for this program.

### 2.2.3.3 The Six-Cavity Configuration

As previously mentioned, the efficiency of a klystron is largely controlled by how effectively the electron beam is bunched and how effectively the energy in the bunches is extracted by the output circuit. The extraction of energy is mainly controlled by the beam coupling coefficient and not much can be done to further optimize  $M$  to increase performance in this area. However, it is possible to enhance the beam bunching which results in more energy per bunch. This enhancement is accomplished by the addition of a second inductively tuned driver cavity, so that two such cavities precede the output cavity. With the enhanced efficiency provided by the six-cavity design, efficiencies of 50% or more are achievable across the 755 MHz to 985 MHz tuning range. Therefore, the six-cavity design is a viable approach in meeting the improved performance requirements of this program.

Figure 2-2 illustrates the relationship between efficiency and  $R/Q$  for the output cavity of a six-cavity klystron at 755 MHz. The  $Q$  (loaded) was held constant at 40 while the  $R/Q$  was varied and the frequency of the inductively tuned cavities was adjusted to optimize the efficiency at each value of  $R/Q$ . The efficiencies shown in Figure 2-2 are computer predicted and tend to be high by approximately ten percent of values for real klystron efficiencies.

### 2.2.4 Determination of the RF Output Circuit

#### 2.2.4.1 Double-Tuned RF Output Circuits

The above discussion of improved performance assumed the rf output circuit to be of the single-tuned variety. The use of double-tuned rf output circuits (filter-loaded and/or extended interaction), while providing exceptional instantaneous bandwidth capability, have not been deemed appropriate for use in this program because these circuits are generally tunable over wide tuning ranges.

#### 2.2.4.2 External RF Output Circuits

It was originally thought that an external rf output cavity could provide the required performance for this program. Figure 2-3 illustrates the general layout of an external rf cavity. It was assumed that the  $R/Q$  of inductively tuned external rf cavities increased with decreasing frequency and that this characteristic would aid in maintaining high-efficiency operation for the required instantaneous bandwidth at the low frequency end of the tuning range. Subsequent cold-testing of several external cavities proved this assumption to be false. In fact, the  $R/Q$  degrades to such a degree at the low frequency end of the tuning range, that the external cavity approach was abandoned. It appears that although the inductance (cavity length) at the low frequency end of the

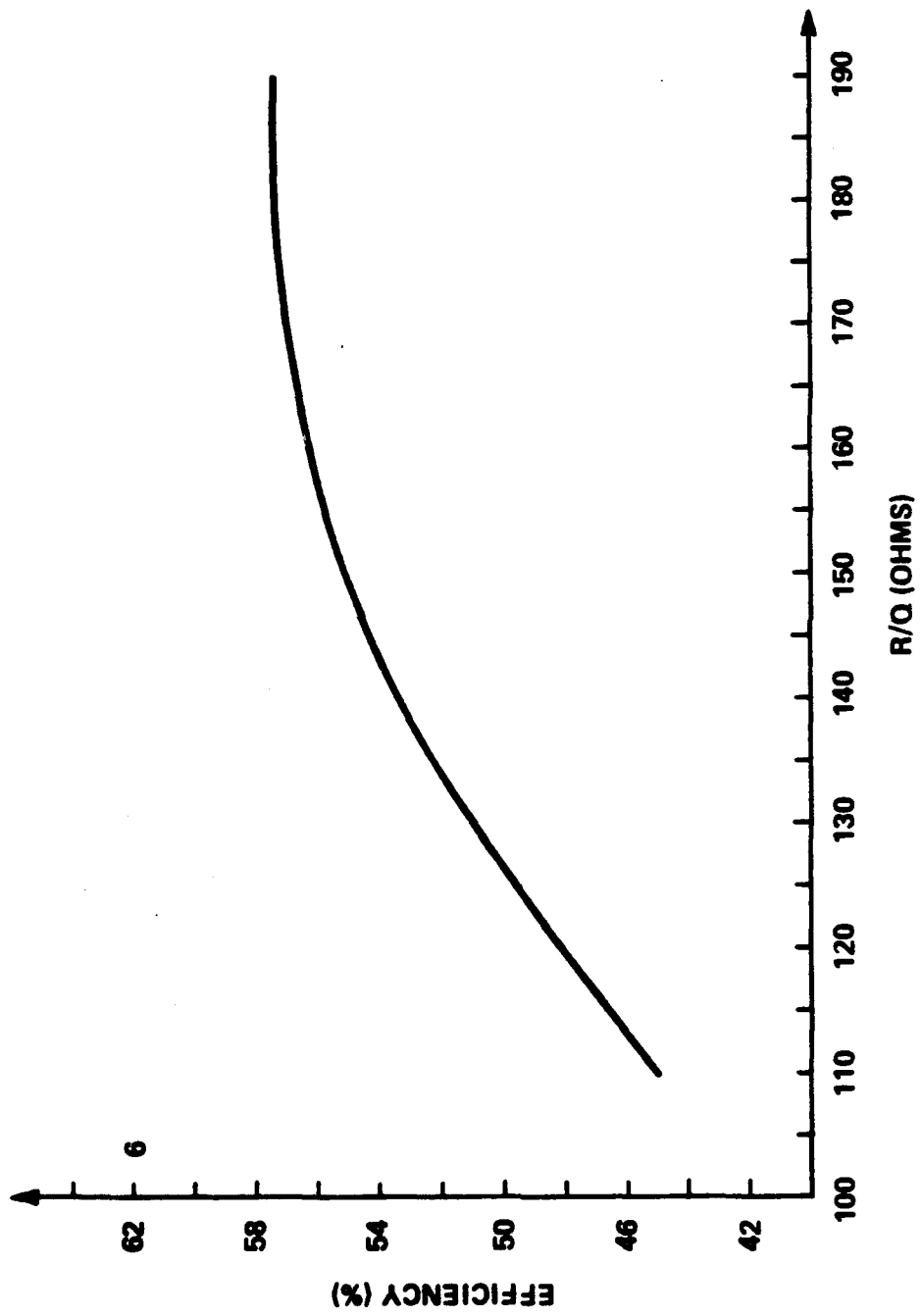


FIGURE 2-2. EFFICIENCY AS A FUNCTION OF R/Q IN THE OUTPUT CAVITY

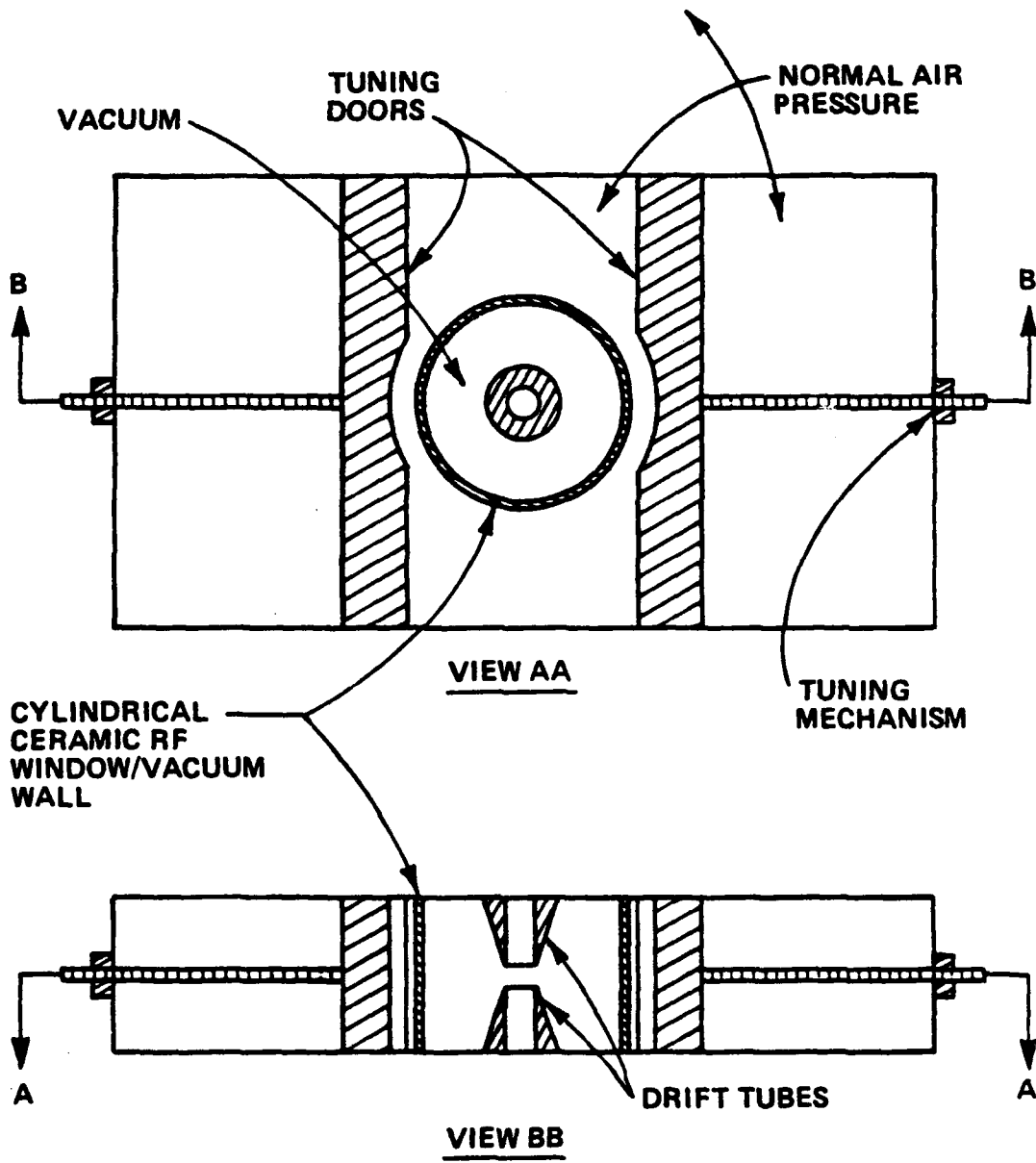


FIGURE 2-3. GENERAL LAYOUT OF A TYPICAL EXTERNAL RF CAVITY

tuning range is increasing, the capacitance between the cavity top wall and bottom wall is increasing faster and the relationship  $R/Q = (L/C)^{1/2}$  is affected in an adverse manner. This characteristic is due to the rectangular geometry of the external rf cavity. Another factor which causes a degrading of the R/Q for this cavity type is the presence of the ceramic cylinder concentric with the drift tube. This ceramic is utilized as a vacuum wall and as an rf window between the interaction gap and the rf cavity. The presence of this ceramic greatly increases the cavity capacitance.

#### 2.2.4.3 The Integral RF Output Circuit (Inductive Sliding Short Tuning)

An integral cavity, such as that illustrated in Figure 2-4, is different from an external cavity in that the differential pressure exerted on the cavity wall of an integral cavity is not zero. This is due to the absence of the cylindrical ceramic window used in the external cavity to contain the vacuum. The integral cavity wall is a vacuum wall and must be capable of supporting the forces caused by the differential pressure.

The use of sliding short tuners dictates a rectangular cavity geometry and the maintenance of very flat cavity walls to insure good tuner contact. At high frequencies this presents no problems because the cavity size is small. However, for the low-frequency operation required in this program, the cavity size is large (15.5" by 8.5" by 3.0") and strong materials, which do not warp at the brazing and exhaust temperatures, are generally very expensive and not readily available. The use of very thick copper for the cavity walls would provide the required surface conditions through the brazing and exhaust cycles, but the resulting cavity weight would be excessive.

The R/Q is still degraded for this cavity type because of the rectangular geometry, but the R/Q is higher than that for an external rf cavity because of the absence of the cylindrical ceramic window used in the external rf cavity to contain the vacuum. This type of cavity is deemed unsuitable for use in this program due to the mechanical problems and the low R/Q associated with it at low frequencies.

#### 2.2.4.4 The Integral RF Output Circuit (Capacitive Tuning)

The use of capacitive tuning in an integral cavity, as illustrated in Figure 2-5, eliminates the need for a rectangular cavity geometry. Instead, a cylindrical cavity geometry is used, and since this type of geometry creates a strong structure, thinner materials are used for the cavity walls with a corresponding reduction in

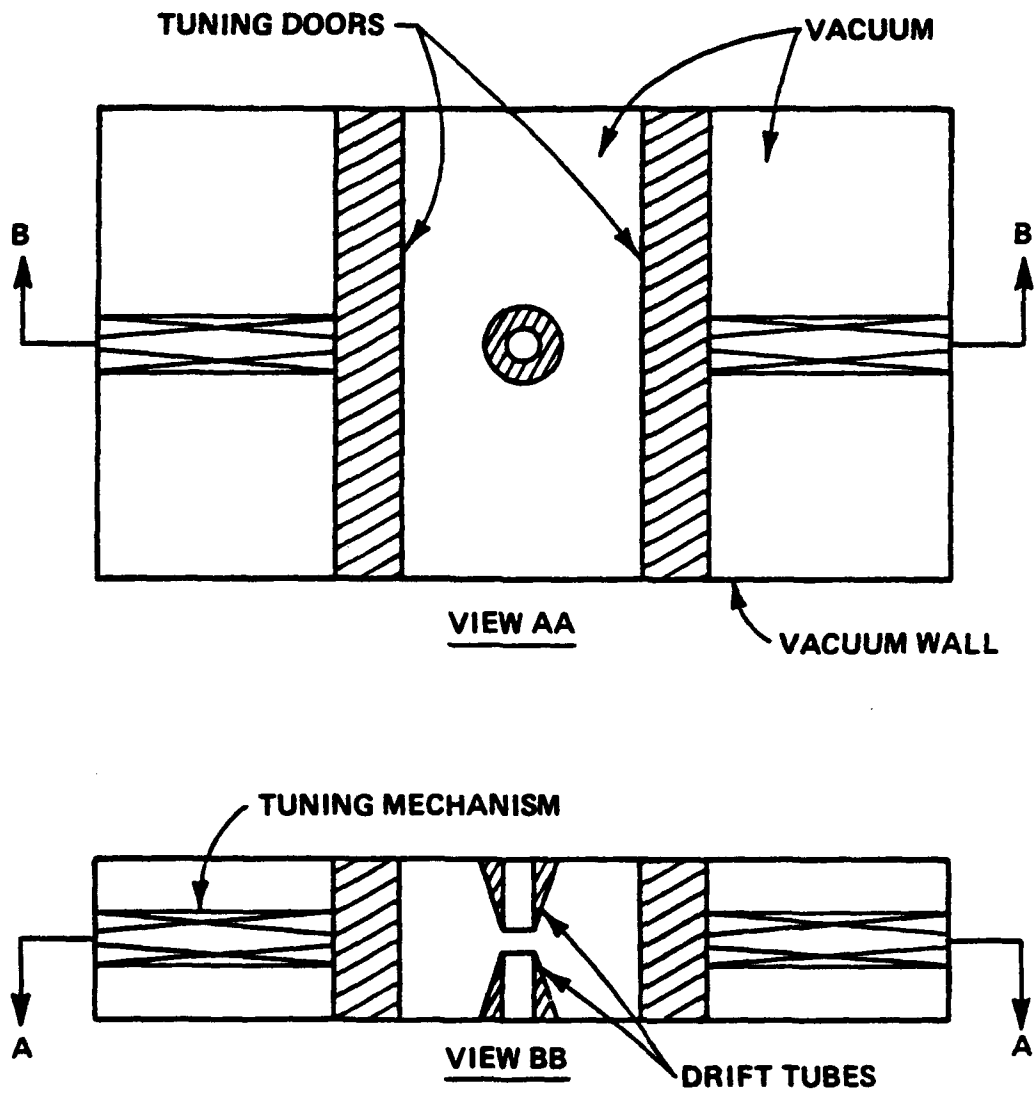


FIGURE 2-4. GENERAL LAYOUT OF AN INTEGRAL RF CAVITY WITH RECTANGULAR GEOMETRY

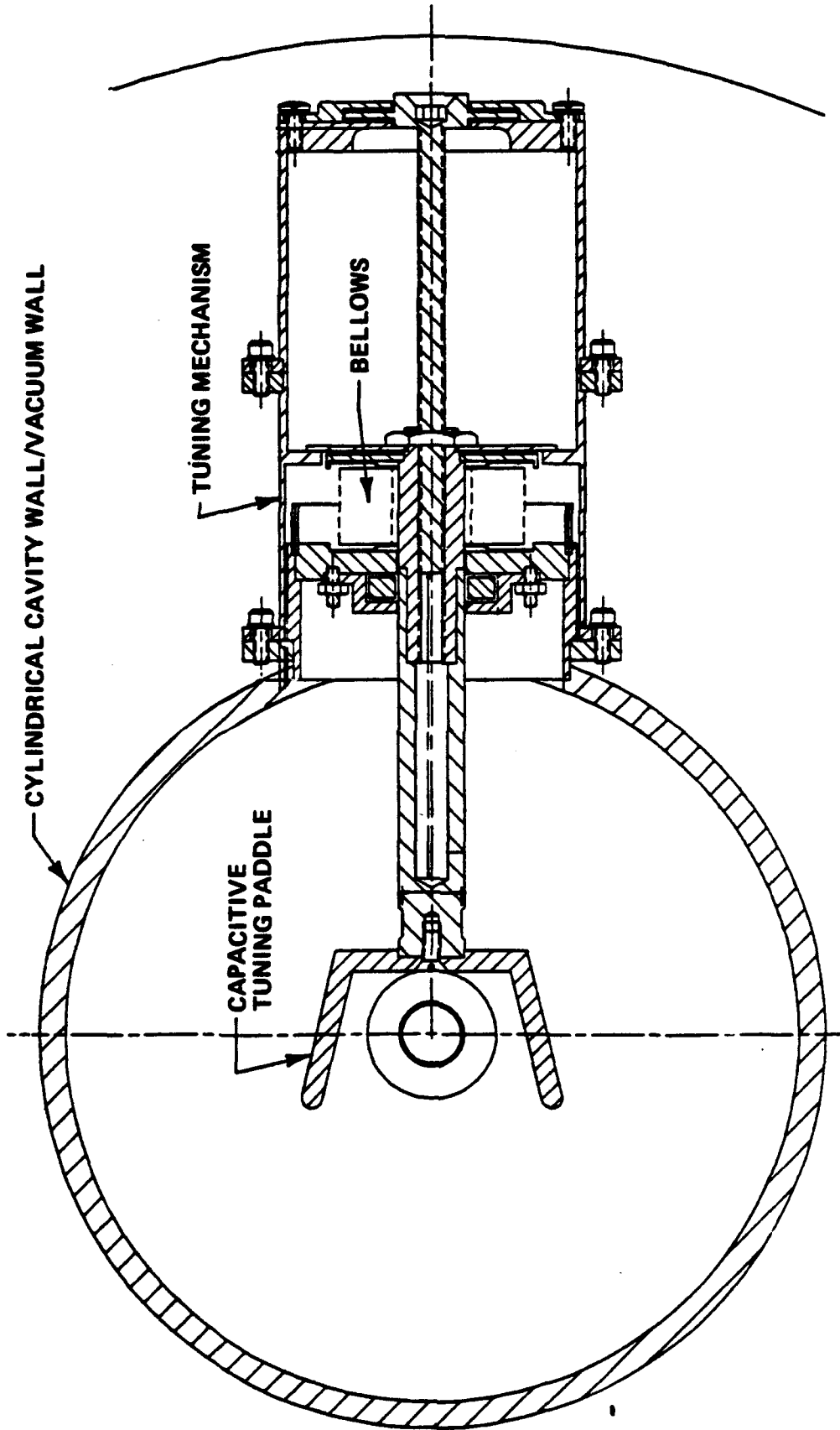


FIGURE 2-5. GENERAL LAYOUT OF AN INTEGRAL RF CAVITY WITH CYLINDRICAL GEOMETRY

weight of the cavity. Another desirable feature of the cylindrical geometry and capacitive tuning is that it results in a more compact cavity design and a simpler tuning mechanism, as compared to the rectangular geometry with inductive tuning covering the same frequency range.

One problem with the capacitive tuner is that it uses the addition of capacitance to lower the frequency of the cavity. This effect is the opposite of that which is desired, since R/Q decreases with increasing capacitance and the R/Q needs to be large at the low-frequency end of the tuning range. However, all the cavity types, whether inductively or capacitively tuned, have the same undesirable characteristic.

The measurement of R/Q, using cold-test techniques, was performed on the last three cavity types mentioned. The results of those measurements are displayed graphically in Figure 2-6. It is seen that the capacitively tuned cavity provides better R/Q at the low frequency end of the tuning range than any of the other cavity types.

The integral cylindrical cavity tuned by a capacitive tuner is deemed the best rf output cavity and tuning mechanism for achieving the performance objectives of this program. They provide the best R/Q at the low frequency end of the tuning range and will help keep the klystron light in weight and compact in size. Use of this cavity type for the driver cavities is also desirable for similar reasons.

#### 2.2.5 Klystron Design Summary

The klystron developed in this program will be a six-cavity design which will incorporate two inductively tuned cavities to enhance the dc to rf conversion efficiency. The rf circuits will be integral cavities with cylindrical geometry and the frequency of the cavities will be tuned by means of a capacitive tuner. A summary of the klystron performance specifications and design parameters is presented in Table 1.

### 2.3 Design Review of the Major Klystron Assemblies

#### 2.3.1 The Electron Gun

The electron gun was designed with a nominal beam micro-perveance of  $1.0 \text{ A}/(\text{V})^{1.5}$  which provided a good compromise between high efficiency and wide instantaneous bandwidth. This micro-perveance also allowed for beam voltages and beam currents which were well within the range of the existing system power supplies. A

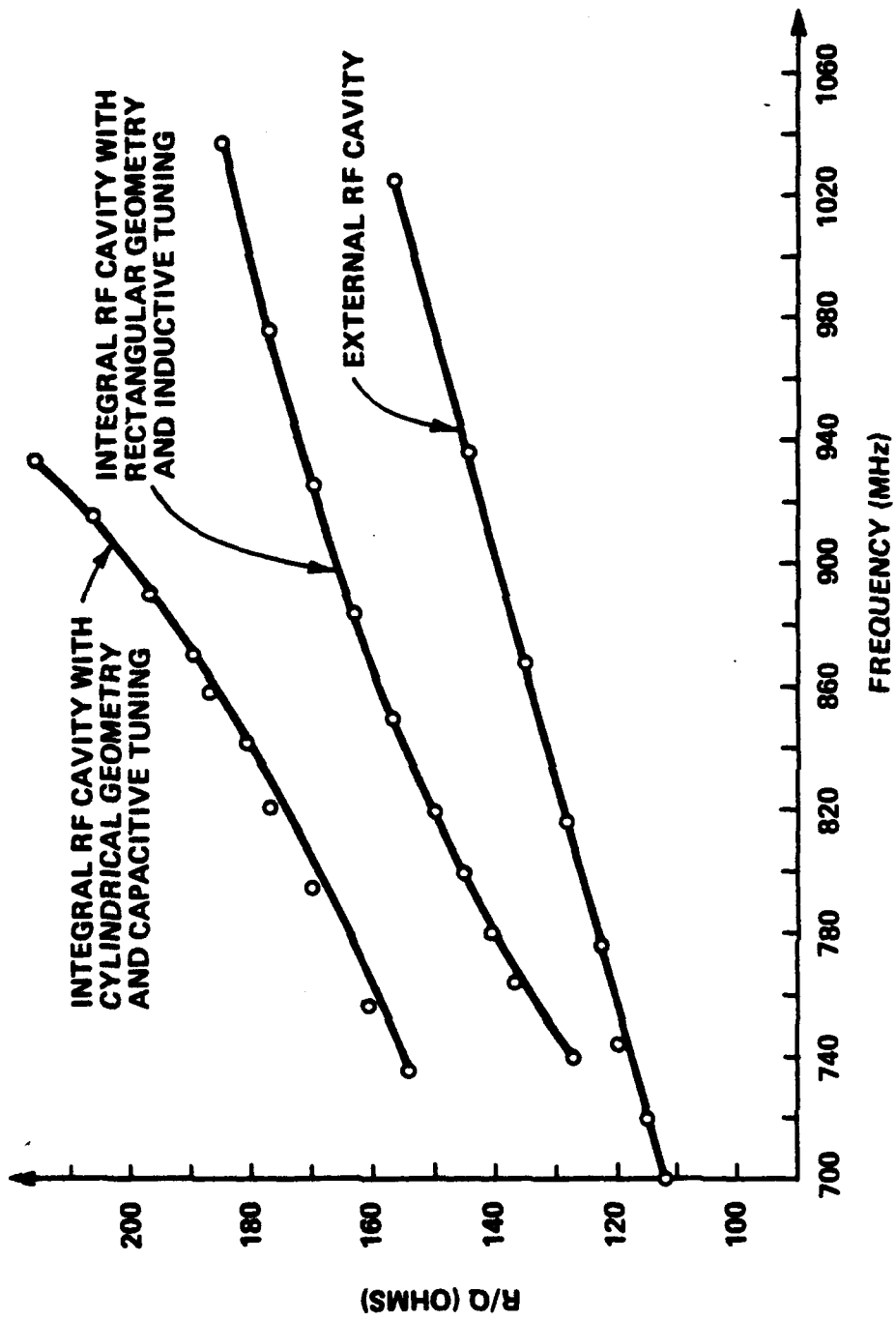


FIGURE 2-6. R/Q AS A FUNCTION OF FREQUENCY FOR THREE DIFFERENT RF CAVITY TYPES

Table 1

Nominal Performance Specifications and Design Parameters  
for an Efficient, Reliable, High-Power UHF Amplifier

<u>Symbol</u>	<u>Parameter</u>	<u>Value</u>	<u>Units</u>
Po	Power Output	12.0	kW
F1 to F2	Tuning Range	755-985	MHz
BW	Instantaneous Bandwidth (-1dB)	9.0	MHz
	Efficiency	50.0	%
Eb	Beam Voltage	14.0	kV
Ib	Beam Current	1.66	A
K	Perveance	$1.0 \times 10^{-6}$	A/V <sup>3/2</sup>
Bed1		0.92-1.2	rad
Bed2	Normalized	0.92-1.2	rad
Bed3	Gap	0.92-1.2	rad
Bed4	Lengths	0.92-1.2	rad
Bed5		0.92-1.2	rad
Bed6		0.92-1.2	rad
BqL1-2		64-83	deg
BqL2-3	Normalized	82-105	deg
BqL3-4	Drift	69 to 89	deg
BqL4-5	Lengths	42 to 54	deg
BqL5-6		37 to 48	deg
R/Q1		170-230	ohms
R/Q2	Characteristic	170-230	ohms
R/Q3	Cavity	170-230	ohms
R/Q4	Impedances	170-230	ohms
R/Q5		120-180	ohms
R/Q6		155-220	ohms

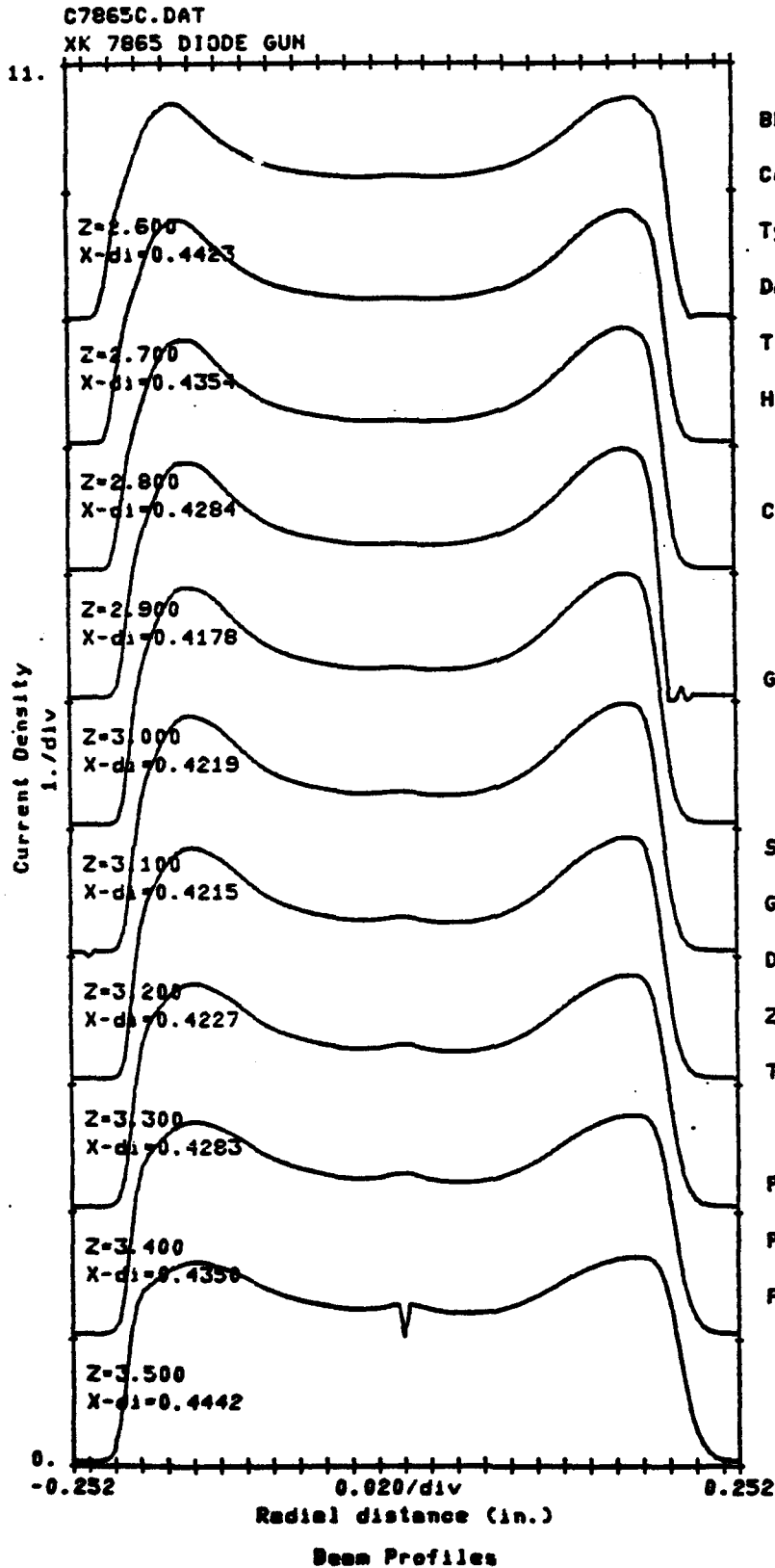
micro-perveance of  $1.0 \text{ A}/(\text{V})^{1.5}$  and the maximum allowed beam voltage of 15 KVdc results in a beam current of 1.84 Adc.

The choice of cathode size and type was made based on the requirements of cathode current loading, cathode ruggedness, long service life, and simplicity of the beam focusing circuit. The cathode diameter chosen was 1.5 inches. This provides an approximate surface area of 11.39 square centimeters and at an operational level of 1.84 Amperes, places the cathode loading at an extremely conservative 0.161 Amperes/square centimeter. This loading permitted the choice of either an oxide cathode or the impregnated tungsten matrix type.

Although the oxides type is the least expensive, it is more susceptible to emission loss due to contamination and is less mechanically rugged than the impregnated tungsten matrix type. Therefore, the impregnated tungsten matrix type cathode was chosen for use in this tube.

In addition, the choice of a 1.5 inch diameter cathode, to provide the desired beam diameter of 0.375 inches, results in a beam diameter convergence of 4. Designs with this convergence require only very simple and easily built electrostatic and magnetic optical focusing systems.

The mechanical and optical structures for the gun were scaled from an existing design of known excellent performance. The actual gun to be used on the tube was built and then tested in the electron beam analyzer. Results from the beam analyzer are shown in Figures 2-7 through 2-11. Figure 2-7 shows the electron beam current density profiles for the electrostatically focused beam ( $I_{sol}=0$ ). Each curve represents a profile, taken across the beam diameter coincident with the x-axis, for different positions along the z-axis (the direction of beam travel). Figure 2-8 provides information on average beam diameter and the percentage of beam diameter variation, (ripple) between two specified positions along the z-axis. For this case the ripple was calculated between  $z=2.6$  and  $z=3.5$  inches. Figure 2-9 provides similar information as Figure 2-7 except  $I_{sol}$  no longer equals zero. The appropriate magnetic focusing field has been applied to confine the beam to its proper diameter. Current density profiles were taken across diameters coincident with the x-axis (solid curve) and the y-axis (dotted curve) to verify the beam symmetry. Figure 2-10 shows the average beam diameters and ripple for the data in Figure 2-9. Figure 2-11 shows a three dimensional representation of the electron beam current density profile for a given z-axis position. This picture provides a good verification of the uniformity of emission from the cathode.



BEAM ANALYZER TEST PARAMETERS

Code NK 7865 DIODE GUN

Type T-2 R-2a

Date 4-NOV-85

Time 8:00 AM

HEATER: Eh 6.25

Ih 17.27 AMP.

CATHODE: Ek 14.0 KV

Ik 1.885 AMP.

$\mu$ Perv 1.138

GRID: Bias

Egt Pulse

IRON-0-REF. = 2.411

Solenoid: Is 0

Gun Coil: Ig 0

Delta K-A 1.095

Zero ref. 2.538 INCHES

TARGET: Type 1.3 INCHES

Pinhole diam. 0.0095

Pressure:  $2.0 \times 10^{-8}$

Pulser: ETM P-297

Page 1 of 1

FIGURE 2-7. BEAM ANALYZER TEST RESULTS FOR THE ELECTROSTATICALLY FOCUSED ELECTRON BEAM,  $I_{sol} = 0$

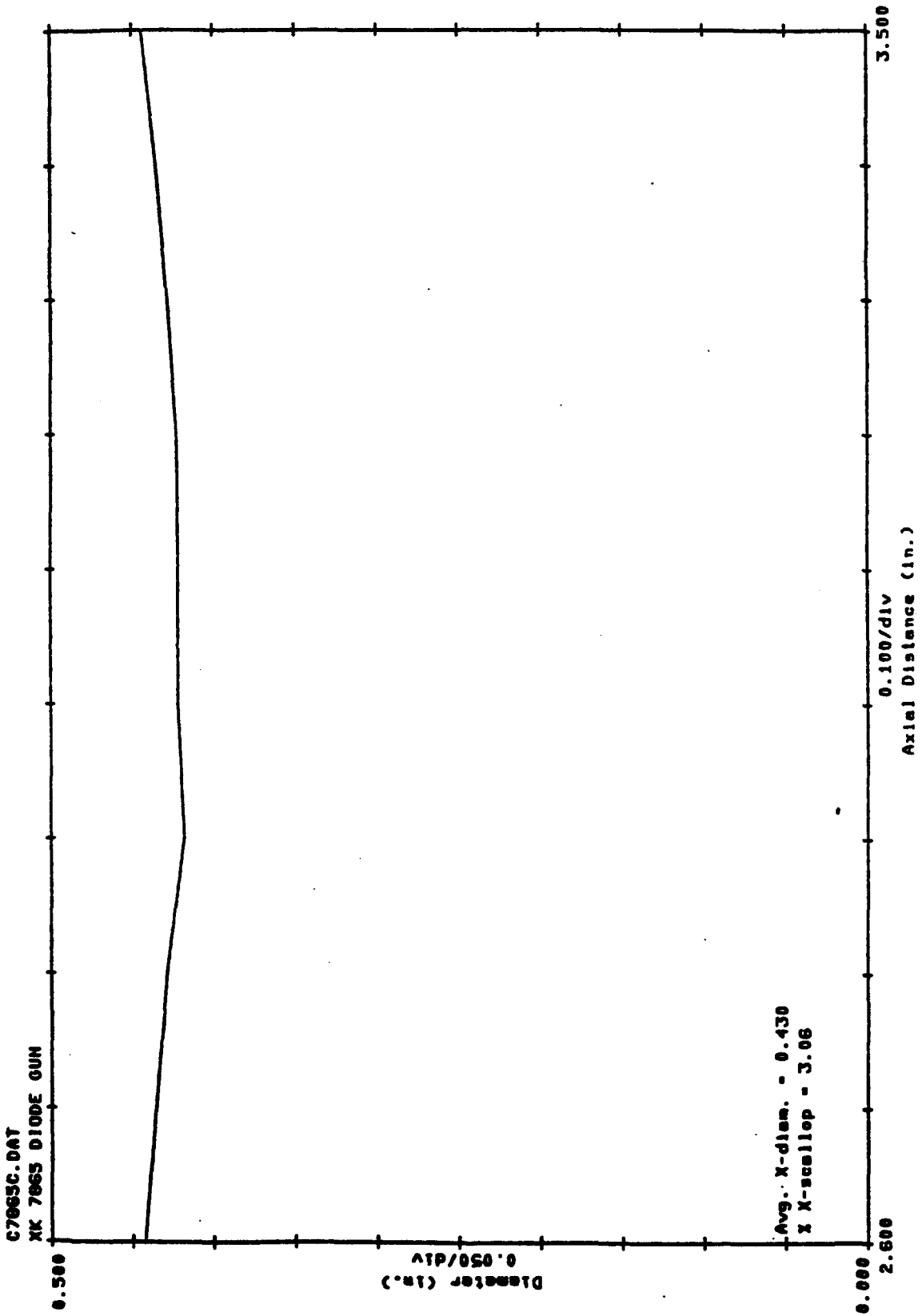
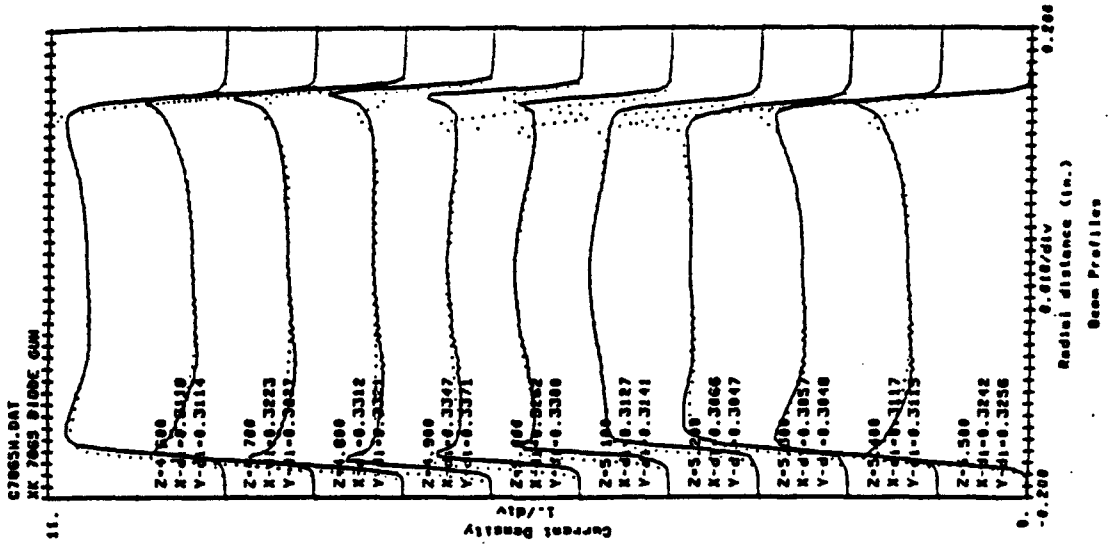
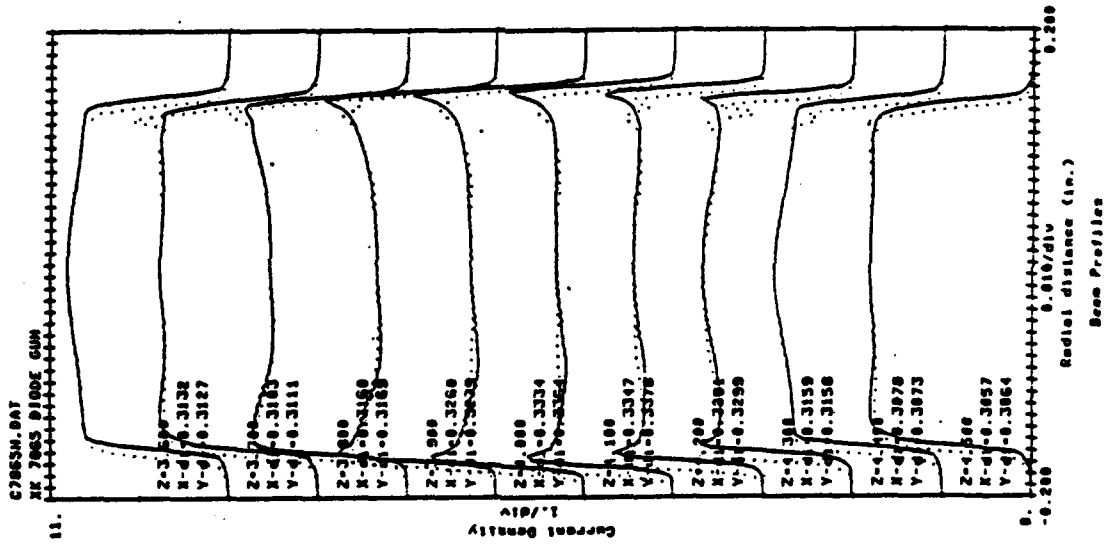
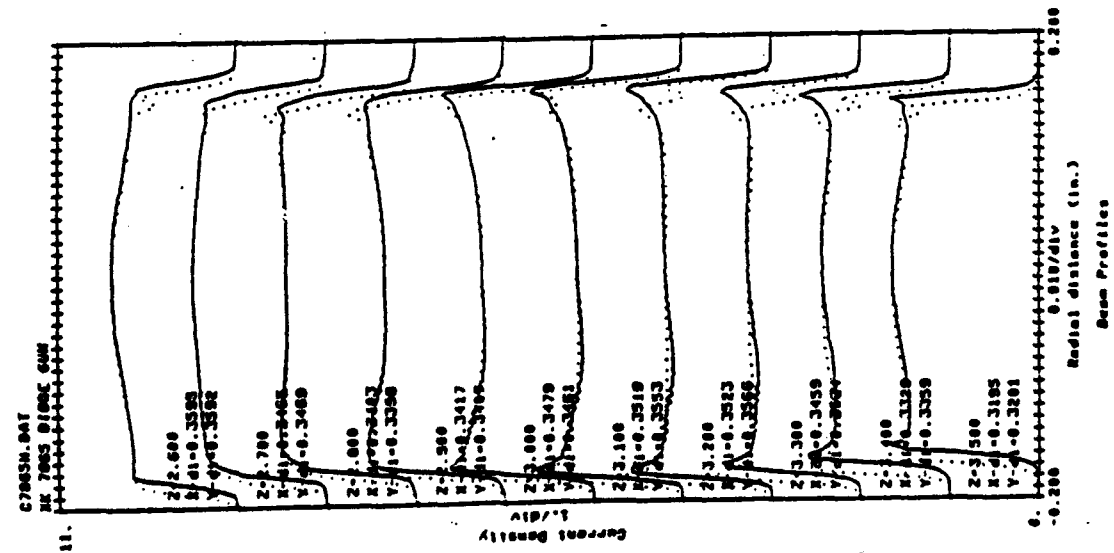


FIGURE 2-8. BEAM DIAMETER VARIATION AS A FUNCTION OF AXIAL DISTANCE FOR THE ELECTROSTATICALLY FOCUSED BEAM OF FIGURE 2-1



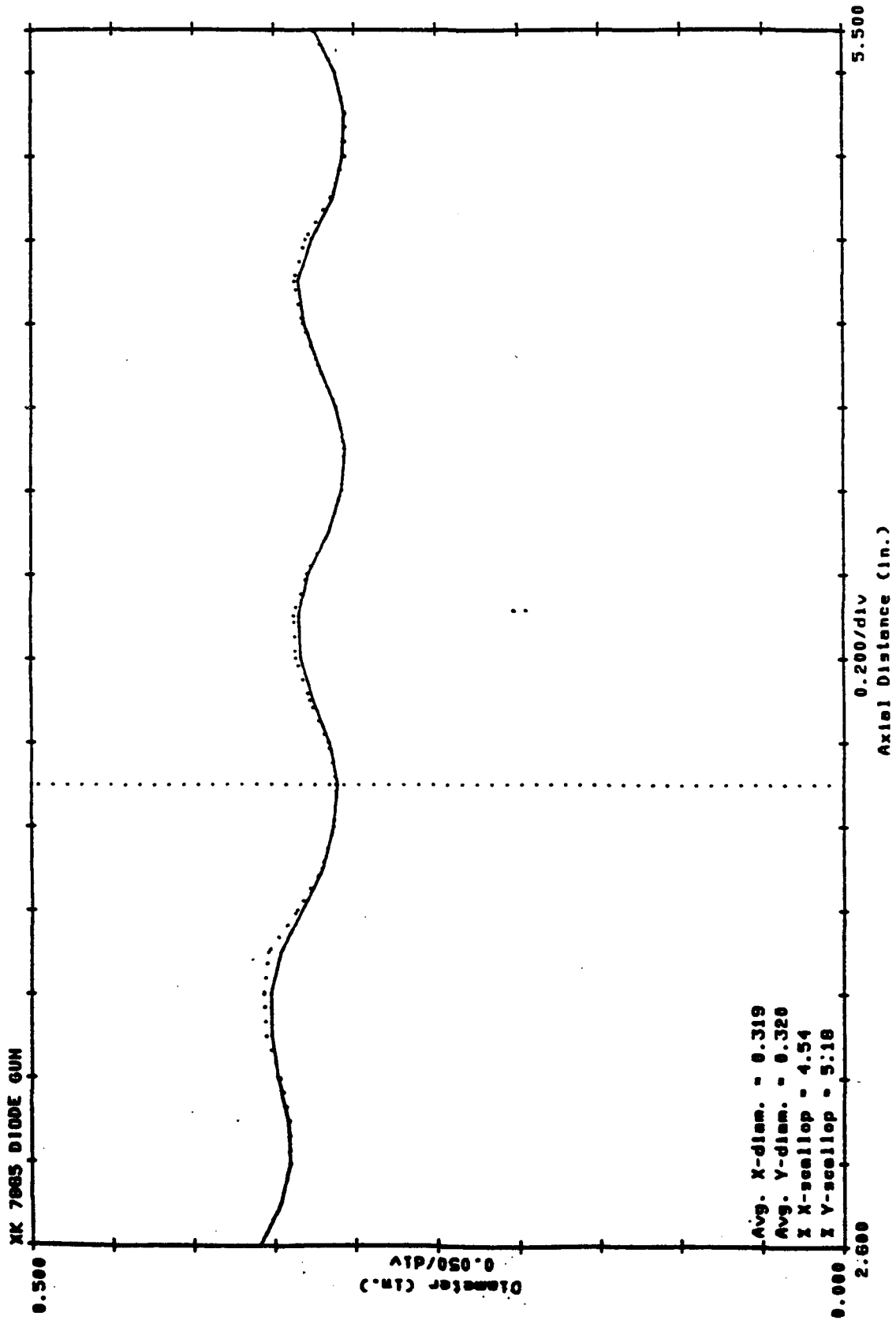


FIGURE 2-10. BEAM DIAMETER VARIATION AS A FUNCTION OF AXIAL DISTANCE FOR THE MAGNETICALLY FOCUSED BEAM OF FIGURE 2-3

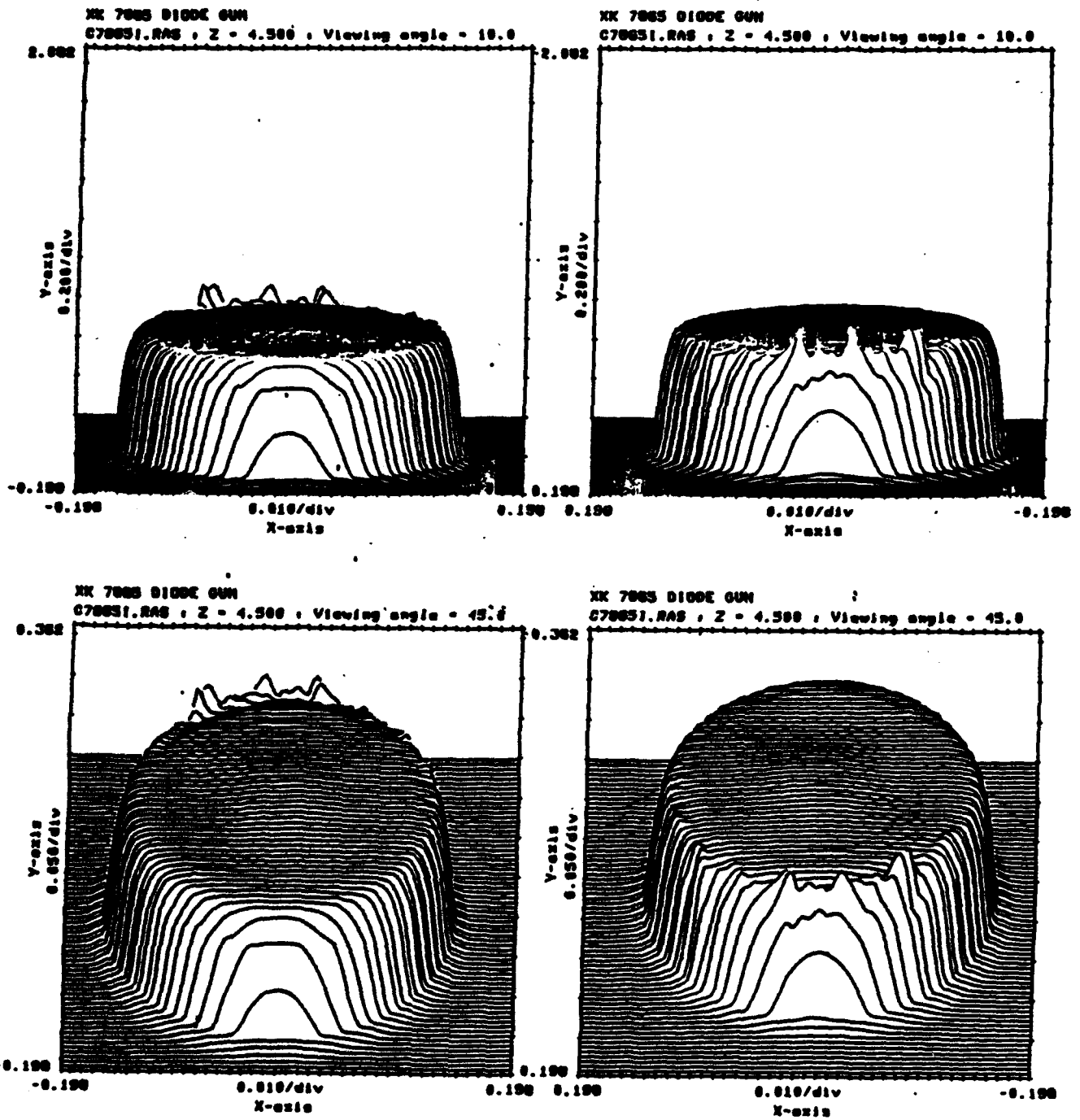


FIGURE 2-11. THREE DIMENSIONAL PLOTS OF THE ELECTRON BEAM CURRENT DENSITY PROFILE

### 2.3.2 The RF Cavity Tuner Mechanism

The tuner chosen for this klystron was the capacitive type. The factors governing this choice were the required tuning range, the desire for maximum R/Q as a function of frequency, and the simplicity of the mechanical structure. The tuning range of 755 to 985 MHz represents a 23.3% change in frequency, a value approaching the upper limit of any klystron tuning mechanism. Two tuner types which can achieve this large change in frequency are the capacitive tuner and the inductive sliding short tuner.

The cavity shape for each of these tuner types are very different; the capacitive tuner is almost always used in a cylindrical cavity, while the inductive sliding short tuner requires a rectangular cavity. In the frequency range of interest, the cylindrical cavity can be made compact and light weight, but the rectangular cavity becomes large and heavy since the cavity walls must be made thick to avoid distortion at brazing and bake-out temperatures.

Cold-testing was performed on each cavity type to determine its R/Q vs. frequency characteristics. The cylindrical cavity with the capacitive tuner had by far the highest R/Q in the frequency range of interest. A comparison of the R/Q vs. frequency for each of the tuner types is shown in Figure 2-12. Coupling its high R/Q with its compact size and tuning range made the capacitive tuner in a cylindrical cavity the best choice for this klystron.

The mechanical architecture of the capacitive tuning mechanism is shown in Figure 2-13. This design incorporate a special mechanism which eliminates the flow of rf currents through the walls of the tuner bellows. This eliminates the typical rf heating and arcing in the bellows, resulting in a more reliable tuning mechanism.

### 2.3.3 The Collector

The collector for this klystron was developed from an existing design and much use was made of the existing piece parts. Modifications were made in the collector beam entrance to ensure proper distribution of the energy in the spent electron beam and modifications were also made in the input and output water fittings because of space limitations within the transmitter. A water cooled collector was used for this tube. In a subsequent effort, the collector for another tube will be of the vapor-phase cooled variety. The water cooled collector will be redesigned to provide the necessary conditions to achieve vapor-phase cooling.

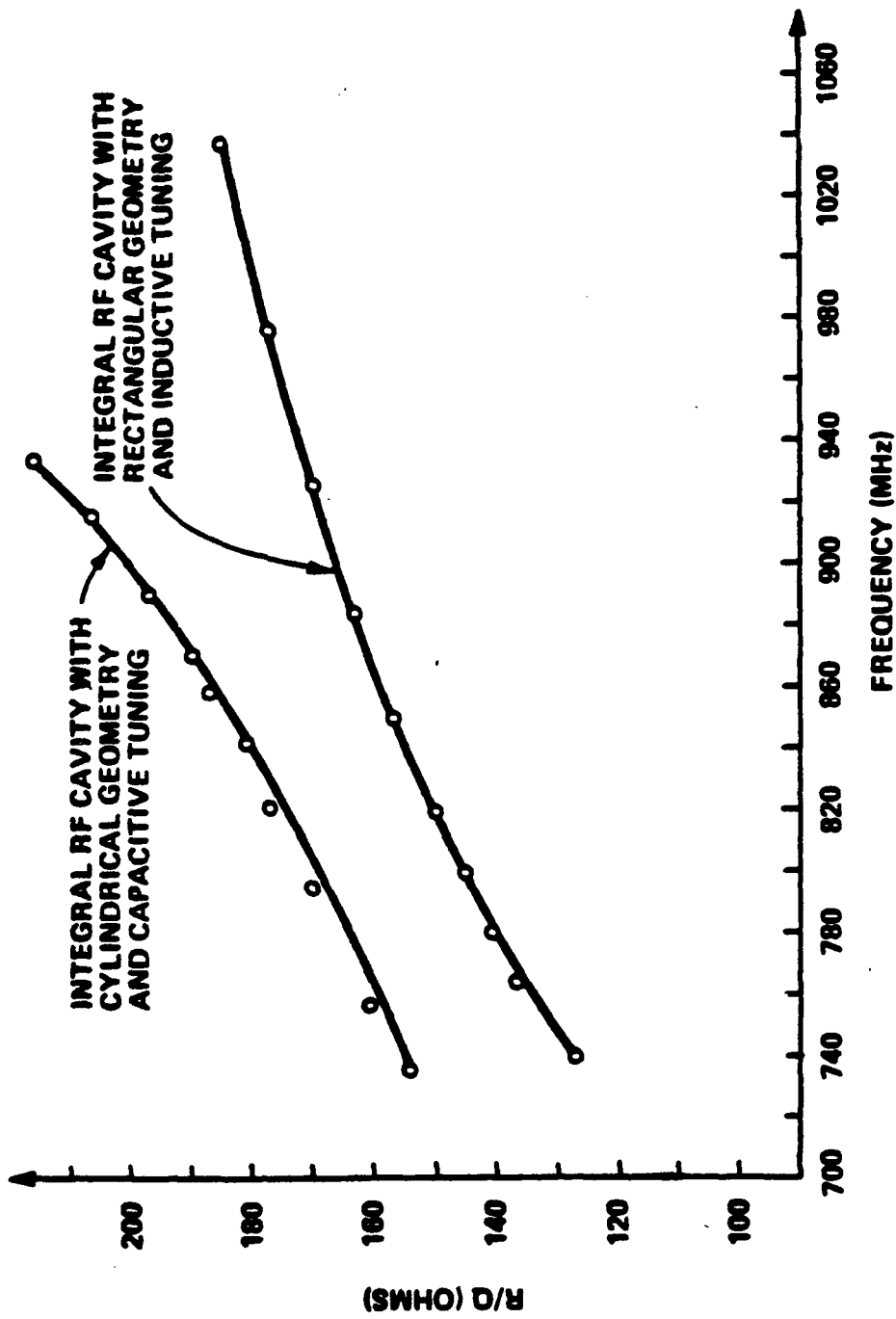


FIGURE 2-12. COMPARISON OF R/Q vs FREQUENCY FOR TWO DIFFERENT CAVITY GEOMETRIES AND TUNER TYPES

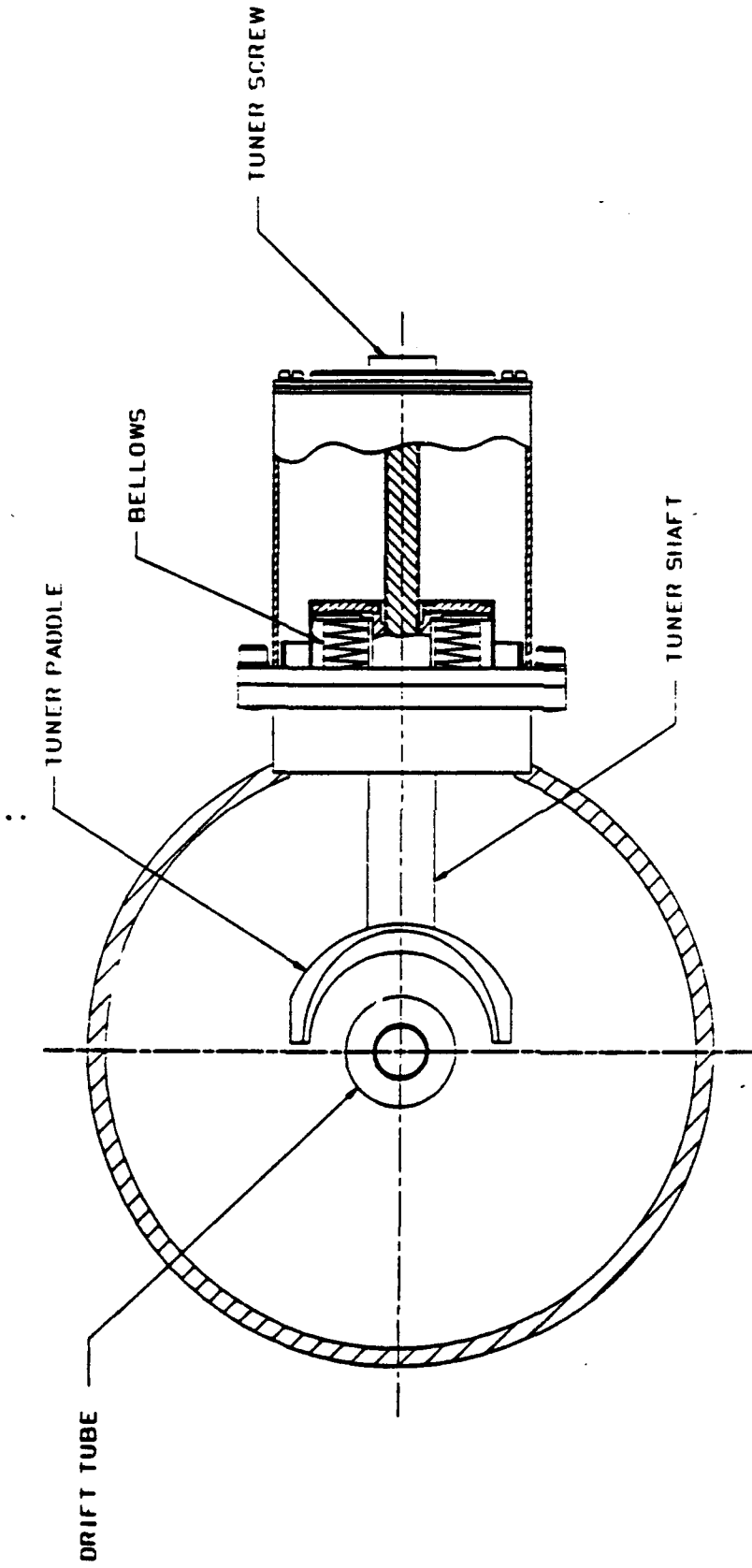


FIGURE 2-13. LAYOUT OF THE CAPACITIVE TUNER IN THE CYLINDRICAL RF CAVITY

#### 2.3.4 The Electromagnet

The electromagnet, for electron beam focusing, was developed using the magnetic field goal curve shown in Figure 2-14. The field distribution was chosen to minimize interception of the electron beam with the klystron drift tubes. The increasing field strength towards the output compensates for the increasing space charge in the electron beam caused by the increasing rf modulation on the beam. The mechanical architecture for the electromagnet is similar to existing designs. Special tuner counter mechanisms were developed and installed on the outside of the electromagnet. These counters provide a means to reference the tuner position for any operating frequency. Six of these tuner counters were installed, one for each rf cavity tuner mechanism. Figure 2-15 shows the electromagnet with the VKP-7865 klystron installed and the tuner counters engaged.

#### 2.3.5 The Electrical Design

The electrical design of the klystron involved the determination of the electron beam/rf cavity interaction circuit. This circuit consisted of the electron beam, the drift tubes, the electron beam/rf cavity interaction gaps, and the rf cavities. Using small and large signal computer programs to simulate tube performance, and much iteration, an electron beam/rf cavity interaction circuit was evolved.

#### 2.3.6 The Mechanical Design

The goal of the mechanical design was to develop a tube with high reliability. Because of its high conductivity, OFHC copper was used extensively in areas of potentially high temperatures, such as drift tubes, rf cavities, and the collector body. Where high strength rather than high conductivity was needed 304 stainless steel was used. 304L Stainless steel was also used wherever the stainless steel was exposed to water or other corrosive mediums. All critical tube parts subject to high temperatures were water cooled. This included all drift tubes, the 4th through the 6th cavity end plates and tuner support plates, the output cavity walls, and the output coupling loop. All vacuum joints were designed for maximum strength, ease of brazing, and ease of repair if necessary. Figures 2-16 and 2-17 show two views of the klystron's outer mechanical structure.

CURVE	COIL #1	COIL #2	COIL #3	COIL #4	COIL #5
A	18 A	18 A	18 A	18 A	18 A
B	17 A	17 A	17 A	15 A	15 A

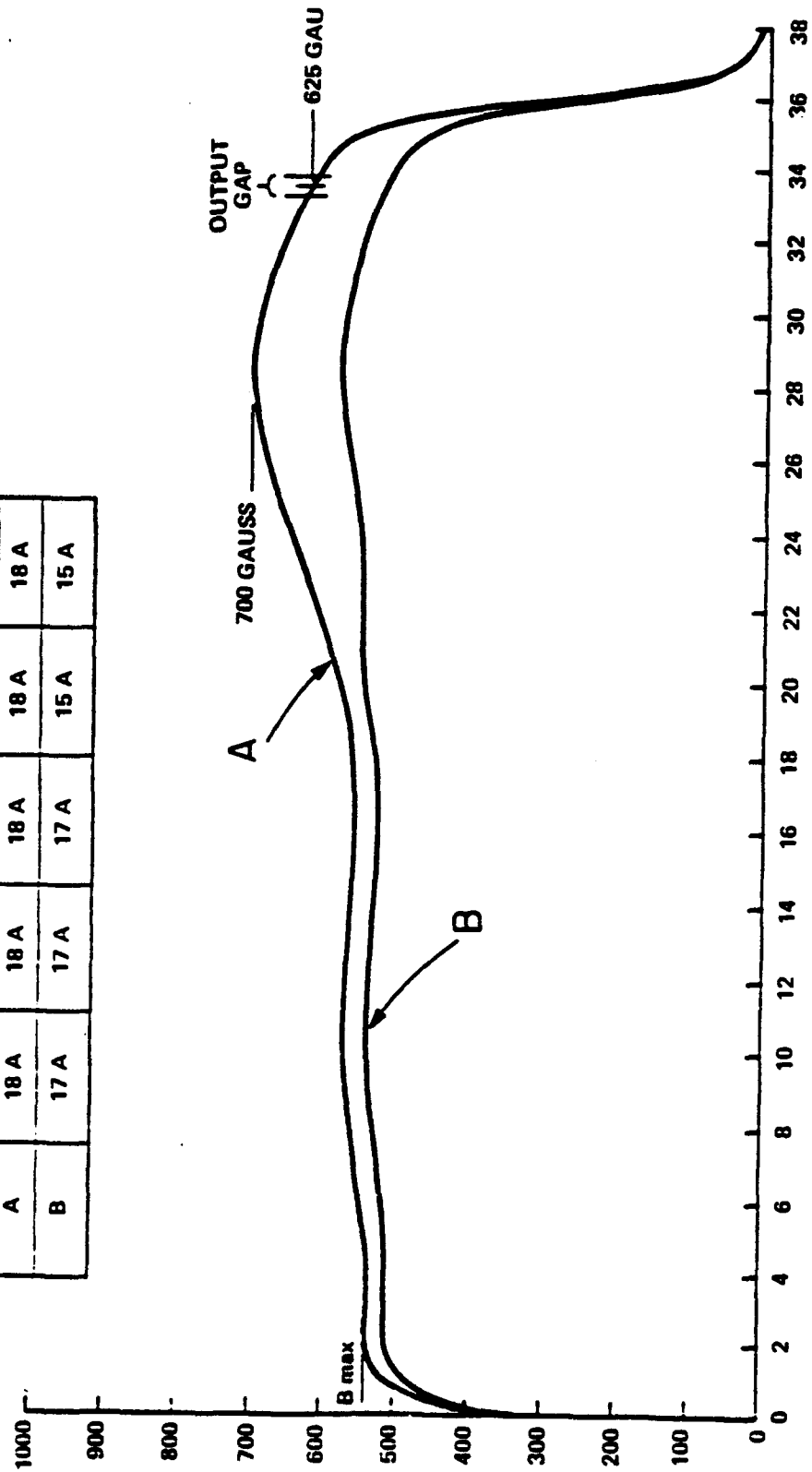
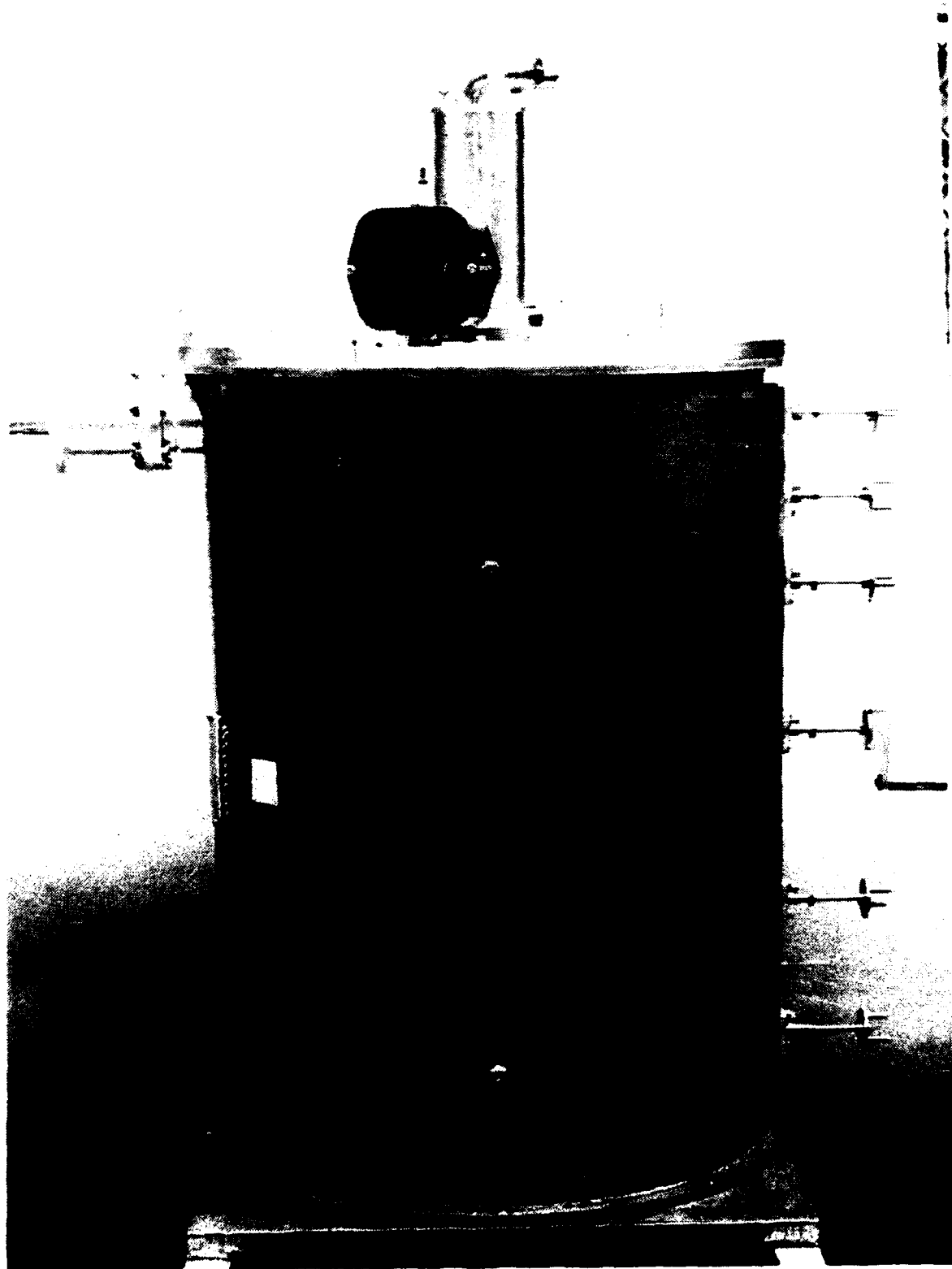
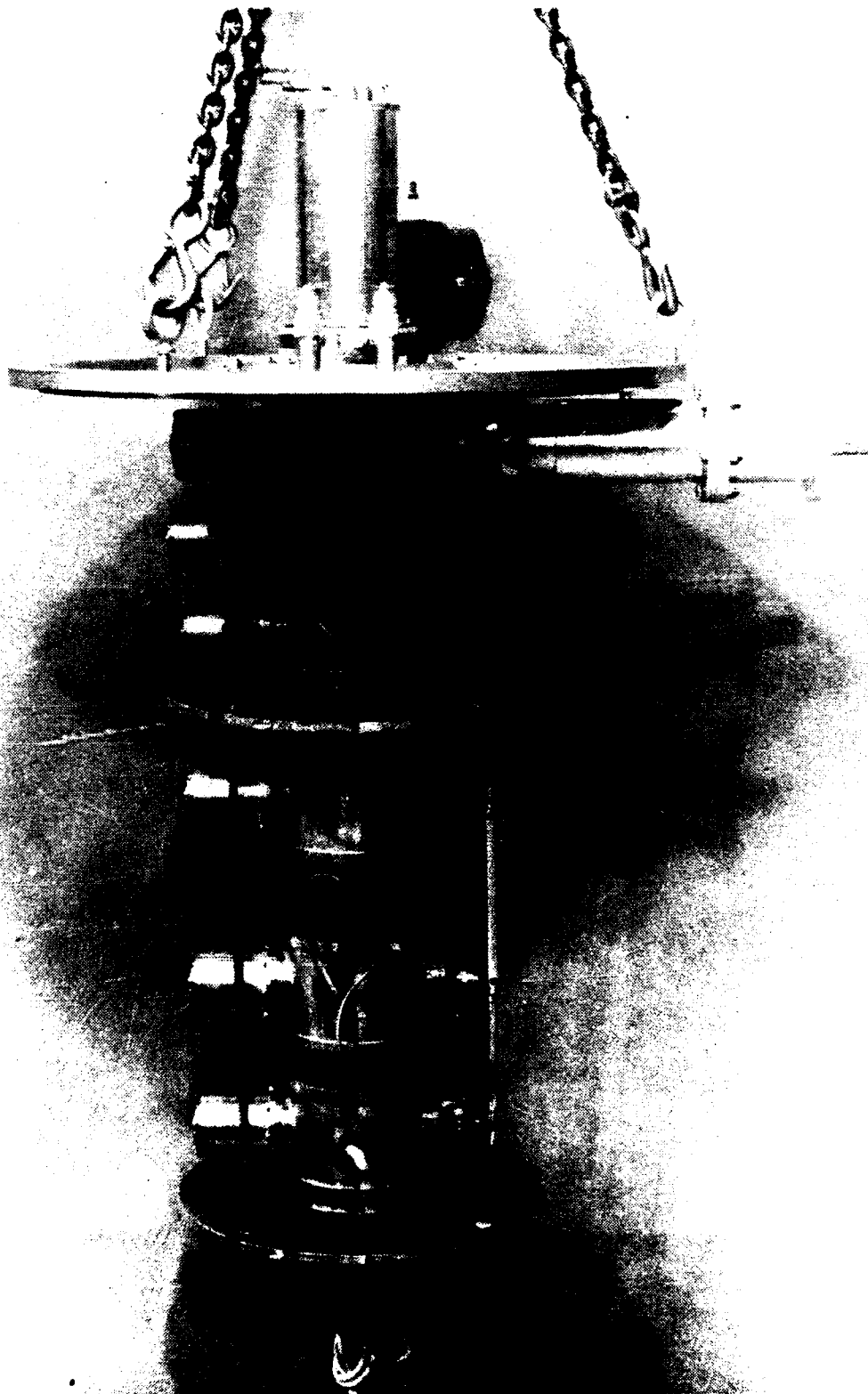


FIGURE 2-14. VYW-7865 MAGNETIC FIELD GOAL CURVE



**FIGURE 2-15. THE VYW-7865 ELECTROMAGNET WITH THE VKP-7865 KLYSTRON INSTALLED**



**FIGURE 2-16. THE VKP-7865 KLYSTRON AMPLIFIER**

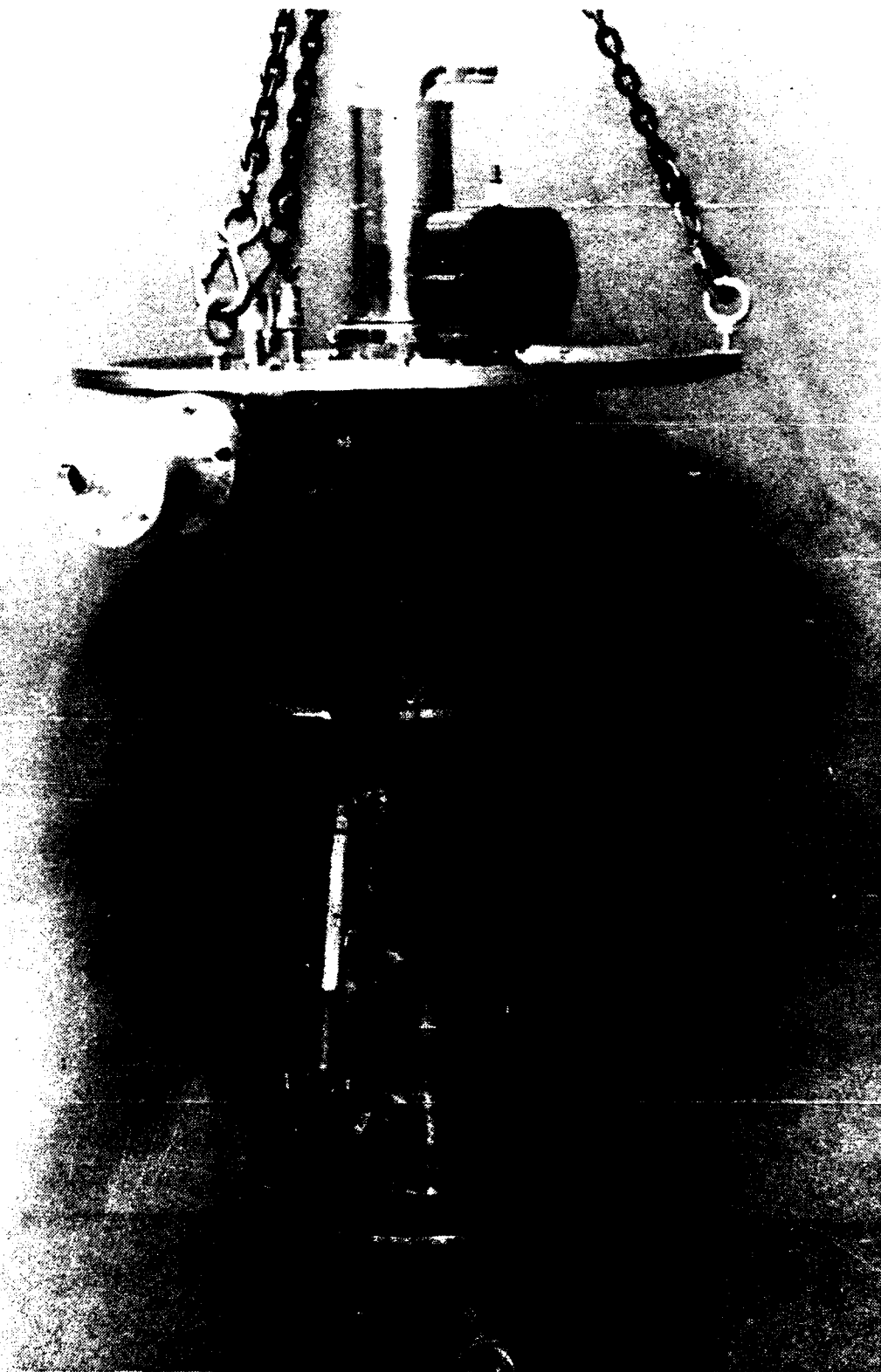


**FIGURE 2-17. THE VKP-7865 KLYSTRON AMPLIFIER ROTATED**

## 2.4 Performance Tests

### 2.4.1 The Electron Gun Performance

The electron gun was initially tested in the electron beam analyzer and the results of those tests are presented in Section 2.3.1 of this report. The results predicted optimum performance for the gun when installed in the klystron under development. The actual performance was as predicted. The dc beam transmission was an excellent 99.5 percent and the rf beam transmission was also excellent with a typical value of 98.9 percent. These values of beam transmission represent beam interception currents of approximately 10 and 20 mA respectively. The beam showed excellent stability under extreme conditions of magnetic field and rf input drive power. No signs of abnormal beam ripple were detected. The beam micro-perveance was a nominal  $1.11 \text{ A}/(\text{V})^{1.5}$  and the heater voltage and current were 6.1 Vac and 16.2 Aac respectively. The overall performance of the electron gun was excellent and well within the requirements specified by the contract.

### 2.4.2 Klystron RF Amplification Performance

Prior to the taking of the final data presented in this report, extensive testing was performed to empirically determine the appropriate beam voltages, rf input drive powers, magnetic field strengths, and rf cavity tunings necessary to insure compliance with the customer's specification requirements. It was found during this preliminary testing, that in order to meet the efficiency and instantaneous bandwidth requirements simultaneously, the rf input drive power had to be reduced approximately 2dB from that required for full saturated power output. This rf output power level has been designated as  $P_o(\text{sat-})$ . Some of the data presented was not required under the negotiated contract. After discussions with cognizant RADC and Mitre Corp. engineering personnel, it was established that the klystron would almost never be operated at full saturated power output, but rather at a level 0.9dB below the full saturated power output. Therefore, the saturated rf power output, designated as  $P_o(\text{sat})$ , and the desired customer operating rf power output level, designated as  $P_o(\text{sat-.9dB})$ , are presented as part of the final data.

The final test data was collected by using the following procedures. The klystron was tuned for operation at  $F_o = 755 \text{ MHz}$  and a minimum BW of 9 MHz, with the rf input drive power,  $P_d$ , set equal to a few mW. The beam voltage,  $E_b$ , and  $P_d$  were then adjusted until  $P_o(\text{sat})@F_o$  was at least 16.0 KW.  $E_b$ ,  $I_b$ ,  $P_d$ ,  $P_o(\text{sat})$ , and BW were measured and recorded. A power output vs. frequency plot was then drawn. This plot has been designated with an (A).

$P_d$  was then reduced until  $P_o$  was 13.0 KW which represented at least a 0.9dB drop from  $P_o(\text{sat})$ . This new operating condition has been

designated as  $P_o(\text{sat}-.9\text{dB})$ .  $P_d$  and BW were measured and recorded and then a power output vs. frequency plot was drawn. This plot has been designated with a (B). Plots (A) and (B) are presented in Figure 2-18 for comparison.

$P_d$  was then increased until  $P_o$  was sufficient to meet or exceed the minimum 50 percent dc to rf conversion efficiency while still maintaining a BW of at least 9.0 MHz. This new operating condition has been designated as  $P_o(\text{sat}-)$ .  $P_d$ , BW, and  $P_o(\text{sat}-)$  were measured and recorded. A power output vs. frequency plot was then drawn and this plot has been designated with a (C).  $P_d$  was then decreased in 2dB steps and power output vs. frequency plots were drawn at each new  $P_d$ . All of these plots are presented in Figure 19, so that performance of the power output response at various rf input drive levels can be seen.

The above tests were repeated for  $F_o = 780, 810, 845, 870, 900, 930, 960,$  and  $985$  MHz. A summary of the measured and calculated test results are tabulated in Table 2 and are presented in the test data section of this report along with the power output vs. frequency plots, Figures 2-20 through 2-35.

Special mention must be made of the existence of a 2nd harmonic cavity mode associated with the 4th rf cavity. When the klystron was tuned for operation at  $F_o = 840$  MHz, a very large notch in the rf power output bandpass was observed at a frequency of approximately 838 MHz. The notch could be moved lower in frequency by tuning the 4th cavity higher in frequency and vice versa. The amplitude of the notch was nil at very small  $P_d$  and was maximum at saturation which verifies its harmonic nature. Harmonic modes tend to disappear upon reduction of the rf input drive power because of the reduced harmonic content in the electron beam. A power output vs. frequency plot was drawn to show the mode existence and the plot appears in the test data section as Figure 2-36. It must be emphasized that the klystron must not be operated CW when this mode is present in the power output bandpass. To insure this operating condition will never occur, the klystron should not be tuned for operation at center frequencies between 830 and 850 MHz. Elimination of this mode would be an objective of any subsequent tube construction program.

Further testing was performed to check the sensitivity of the klystron efficiency to lower power output levels due to reductions in the dc beam power. The tests were performed at  $F_o = 755, 870,$  and  $985$  MHz and the dc beam powers were 25.760, 24.386, and 25.760 KW respectively. The klystron was tuned for a balanced small signal response and a BW of at least 9.0 MHz.  $P_d$  was then increased to maximize  $P_o(\text{sat}-)$  while still maintaining a BW of at least 9.0 MHz. The rf power output at each frequency was then measured as 13.464, 12.012, and 12.540 KW respectively and these values resulted in efficiencies of 52.3, 49.3, and 48.7 percent.



**KLYSTRON AMPLIFIER**

TUBE TYPE NO. **VKP-7805**

SERIAL NO. **16-001**

**TEST PERFORMANCE SHEET**

TESTED BY: EL Eisen DATE: 2/20/86 VARIAN QA

POWER OUTPUT vs FREQUENCY

EI 6.1 (Vac)  
II 16.2 (Aac)  
Imag 7AB.1.1 (Aadc)  
BW TAB. 1. MHz

Eb 14.5 (kVdc)  
Ib 1.935 (Aadc)  
Ibv 1.0 (mAadc)  
Fo 755 (MHz)

Po TAB. 1. (kW)  
Pd TAB. 1. (W)  
GAIN TAB. 1. (dB)  
EFF TAB. 1 (%)

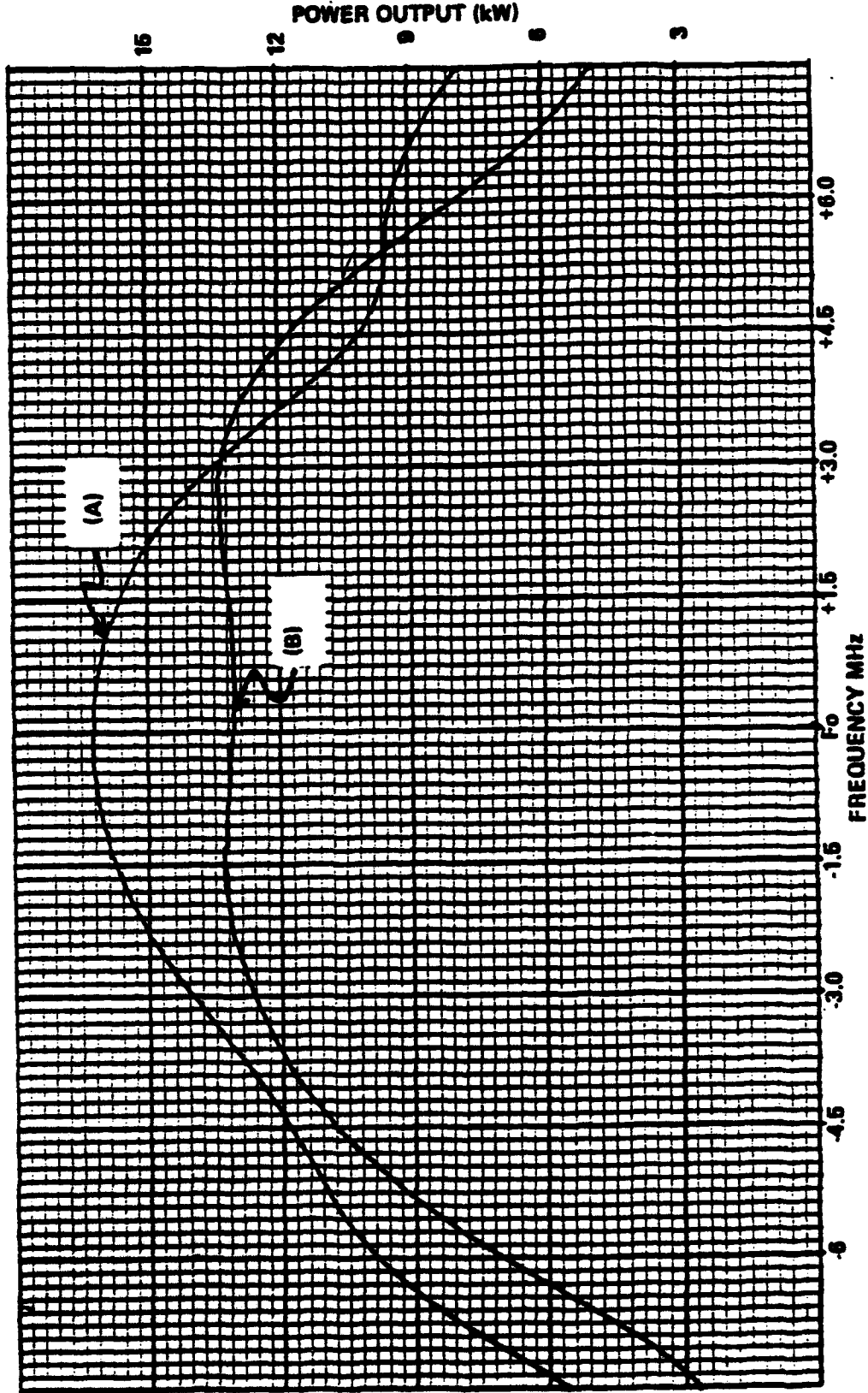


FIGURE 2-18. POWER OUTPUT vs FREQUENCY CURVES (A) AND (B) AT Fo=755MHz



**KLYSTRON AMPLIFIER**  
 TUBE TYPE NO. VKP-7885  
 SERIAL NO. 216-001

TESTED BY Ed Eisen TEST PERFORMANCE SHEET  
 DATE 03/05/86 VARIAN QA  
 POWER OUTPUT vs FREQUENCY  
 E1 6.1 (Vac)  
 I1 16.7 (Aac)  
 Imax TAB. 1.1 (Aac)  
 BW TAB. 1.1 MHz  
 Eb 14.5 (kVdc)  
 Ib 1.935 (Aac)  
 Iby 1.0 (mAac)  
 Fo 755 (MHz)

Po TAB. 1.1 (kW)  
 Pd TAB. 1.1 (W)  
 GAIN TAB. 1.1 (dB)  
 EFF TAB. 1.1 (%)

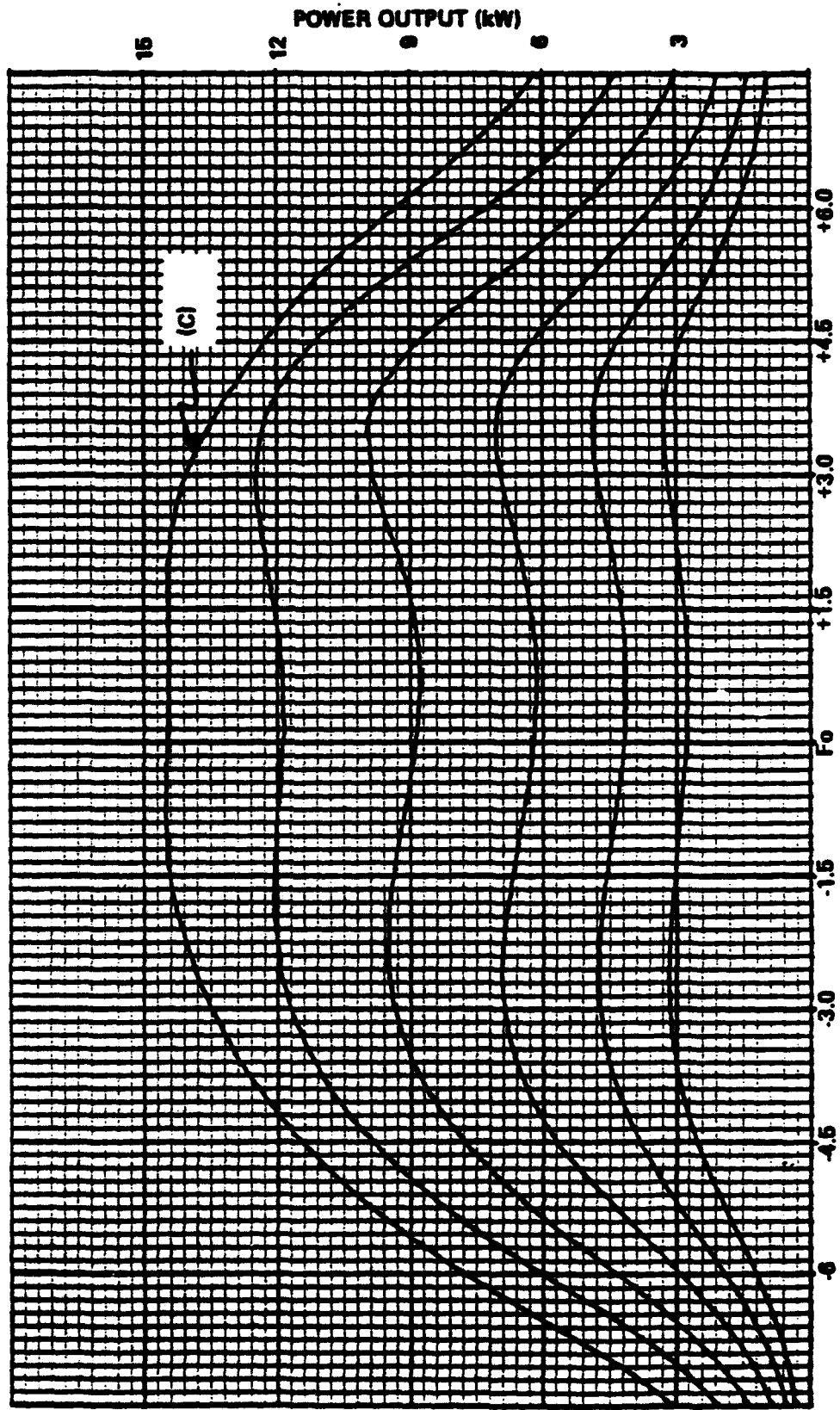


FIGURE 2-19 POWER OUTPUT vs FREQUENCY CURVE (C) AT Fo = 755 MHz

**TABLE 2**  
**SUMMARY OF THE VKP-7865 KLYSTRON AMPLIFIER RF PERFORMANCE**

PARAMETER	VALUE										UNITS
	755	780	810	845	870	900	930	960	985		
$F_o$	755	780	810	845	870	900	930	960	985		MHz
$E_b$	14.5	14.6	14.8	14.6	14.6	14.5	14.4	14.6	14.7		kVdc
$I_b$	1.935	1.95	1.99	1.95	1.95	1.935	1.92	1.95	1.97		Adc
$P_o$ (Sat)	16.12	16.26	16.26	16.41	16.26	16.26	16.12	16.12	16.26		kW
$P_d$	365	196	205	105	103	83	67	65	48		mW
Gain	46.5	49.2	49.0	51.9	52.0	52.9	53.8	53.9	55.3		dB
Eff.	57.4	57.1	55.2	57.6	57.1	58.0	58.3	56.6	56.1		%
BW	6.86	8.12	8.44	8.27	8.57	8.51	8.54	9.80	10.7		MHz
$P_o$ (Sat - 0.9 dB)	13.0	13.0	13.0	13.0	13.0	13.0	13.0	13.0	13.0		KW
$P_d$	130	78	66	38	36	23	19	22	16		mW
Gain	50.0	52.2	52.9	55.3	55.6	57.5	58.4	57.7	59.1		dB
Eff.	46.3	45.7	44.1	45.7	45.7	46.3	47.0	45.7	44.9		%
BW	9.53	10.08	9.73	9.82	10.00	10.07	10.55	10.64	11.24		MHz
$P_o$ (Sat-)	14.5	15.0	15.0	15.0	15.0	14.75	14.5	15.0	15.0		kW
$P_d$	175	120	110	53	59	35	26	35	24		mW
Gain	49.2	51.0	51.3	54.5	54.1	56.2	57.5	56.3	58.0		dB
Eff.	51.7	52.7	50.9	52.7	52.7	52.6	52.4	52.7	51.8		%
BW	9.42	9.36	9.30	9.66	10.07	10.38	10.75	11.13	11.81		MHz



**KLYSTRON AMPLIFIER**  
 TUBE TYPE NO. VKP-7005  
 SERIAL NO. A6-001

**TEST PERFORMANCE SHEET**

TESTED BY Ed Eisen

DATE 23/05/85 VARIAN QA

POWER OUTPUT vs FREQUENCY

Ef 6.1 (Vac)  
 If 16.2 (Aac)  
 Imag TAB. I. (Aac)  
 BW TAB. I. MHz

Eb 14.6 (kVdc)  
 Ib 1.95 (Aac)  
 Iby 1.5 (mAac)  
 Fo 780 (MHz)

Po TAB. I. (kW)  
 Pd TAB. I. (W)  
 GAIN TAB. I. (dB)  
 EFF TAB. I. (%)

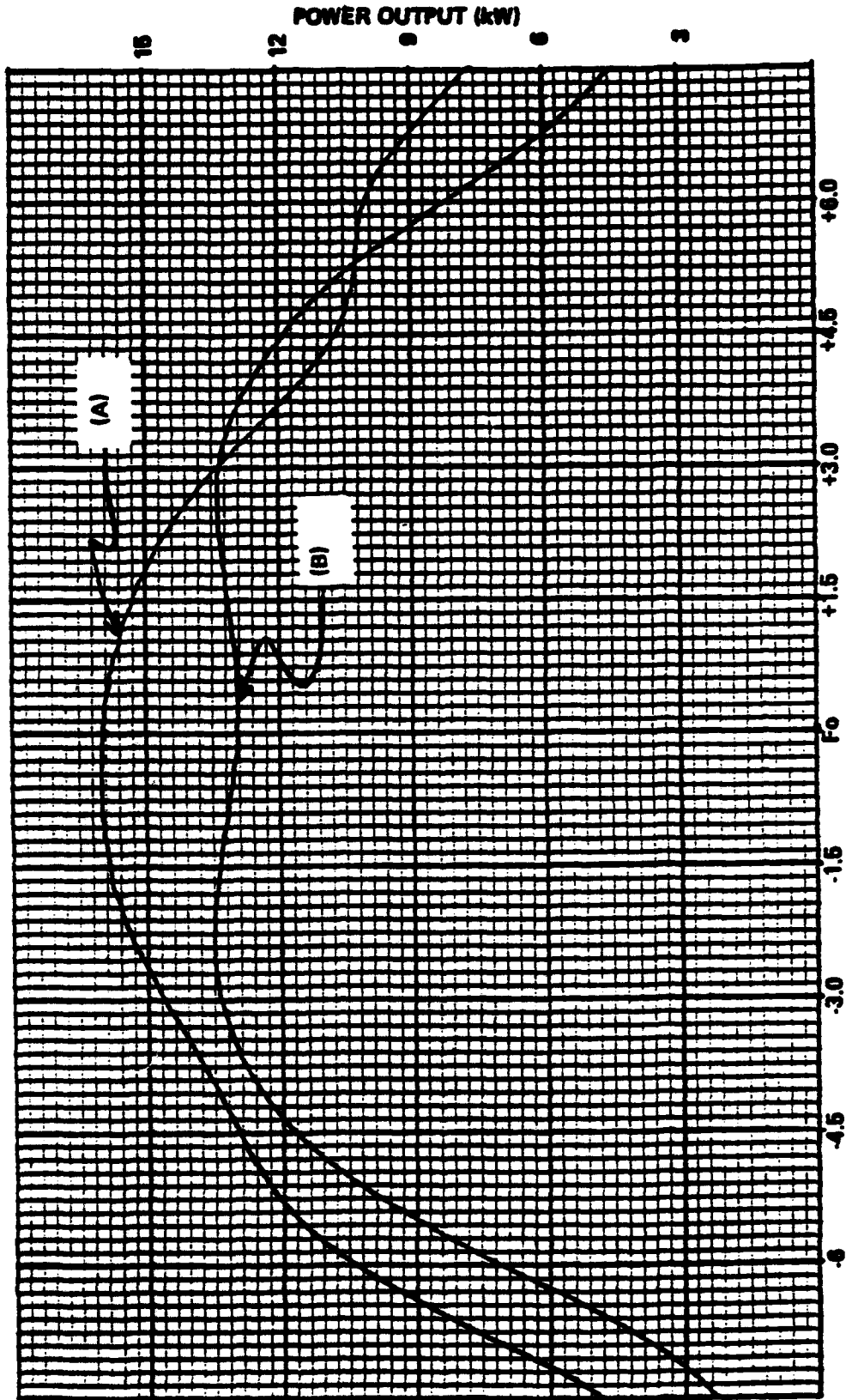


FIGURE 2-20 POWER OUTPUT vs FREQUENCY CURVES (A) AND (B) AT  $F_o = 780$  MHz

188 000 7/8



**KLYSTRON AMPLIFIER**

TUBE TYPE NO. **VKP-7005**  
SERIAL NO. **A6-001**

**TEST PERFORMANCE SHEET**

TESTED BY *Ed Eisen* DATE 03/05/86 VARIAN QA

**POWER OUTPUT vs FREQUENCY**

EI 6.1 (Vac) Eb 4.6 (kVdc) Po TAB. I. (kW)  
Ii 16.2 (Aac) Ib 1.5 (Adc) Pd TAB. I. (W)  
Imag TAB. I. (Aac) Iby 1.5 (mAac) GAIN TAB. I. (dB)  
BW TAB. I. MHz Fo 780 (MHz) EFF TAB. I. (%)

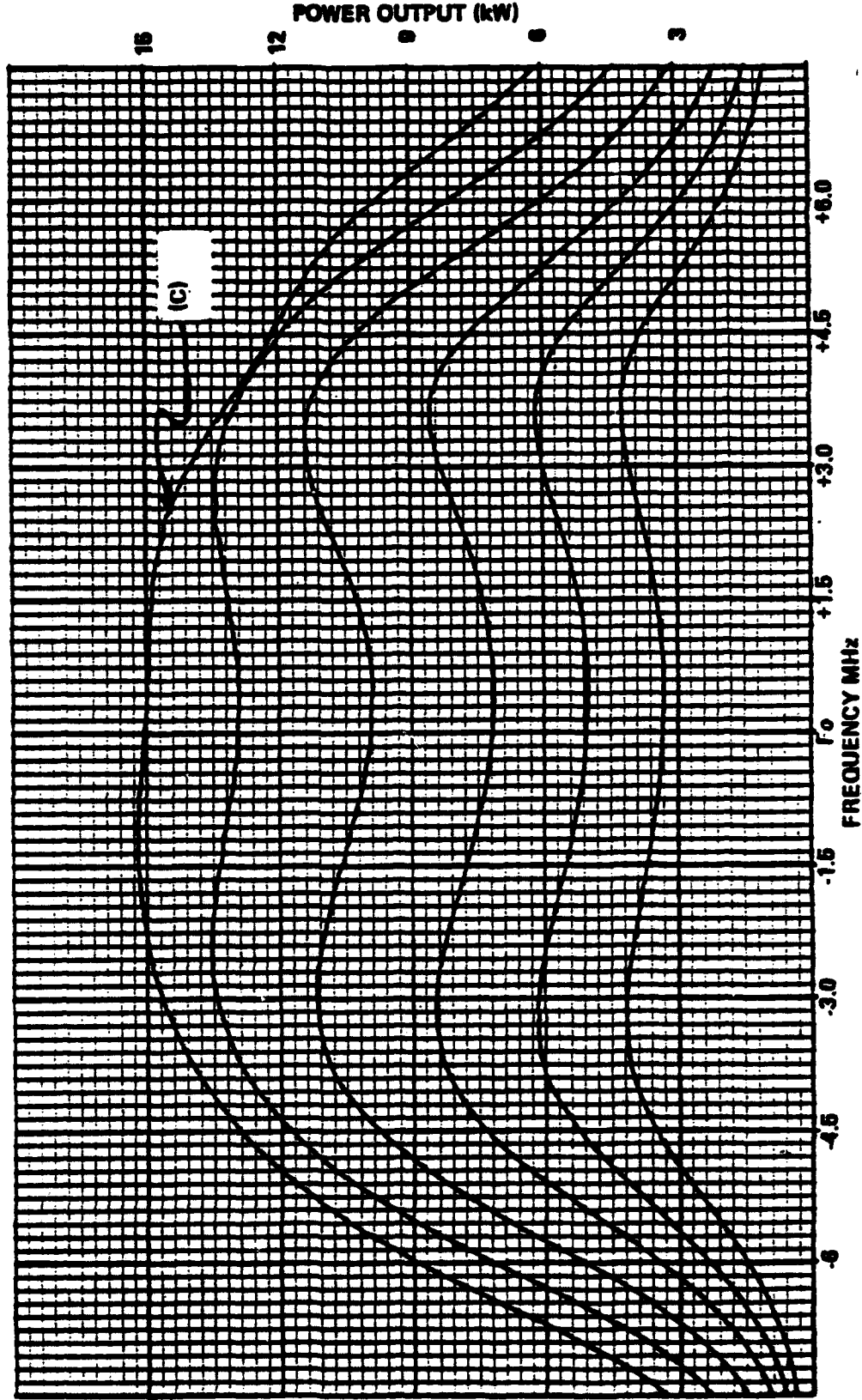


FIGURE 2-21. POWER OUTPUT vs FREQUENCY CURVE (C) AT  $F_0 = 780\text{MHz}$

87-000 001



**KLYSTRON AMPLIFIER**

TUBE TYPE NO. VKP-7865  
SERIAL NO. 26-001

**TEST PERFORMANCE SHEET**

TESTED BY E. J. Eisen DATE 03/05/86 VARIAN QA

**POWER OUTPUT vs FREQUENCY**

E1 <u>6.1</u> (Vac)	Eb <u>4.8</u> (kVdc)	Po TAB. 1. (kW)
I1 <u>16.2</u> (Aac)	Ib <u>1.99</u> (Adc)	Pd TAB. 1. (W)
Imag TAB. 1. (Adc)	Iby <u>2.0</u> (mAac)	GAIN TAB. 1. (dB)
BW TAB. 1. MHz	Fo <u>810</u> (MHz)	EFF TAB. 1. (%)

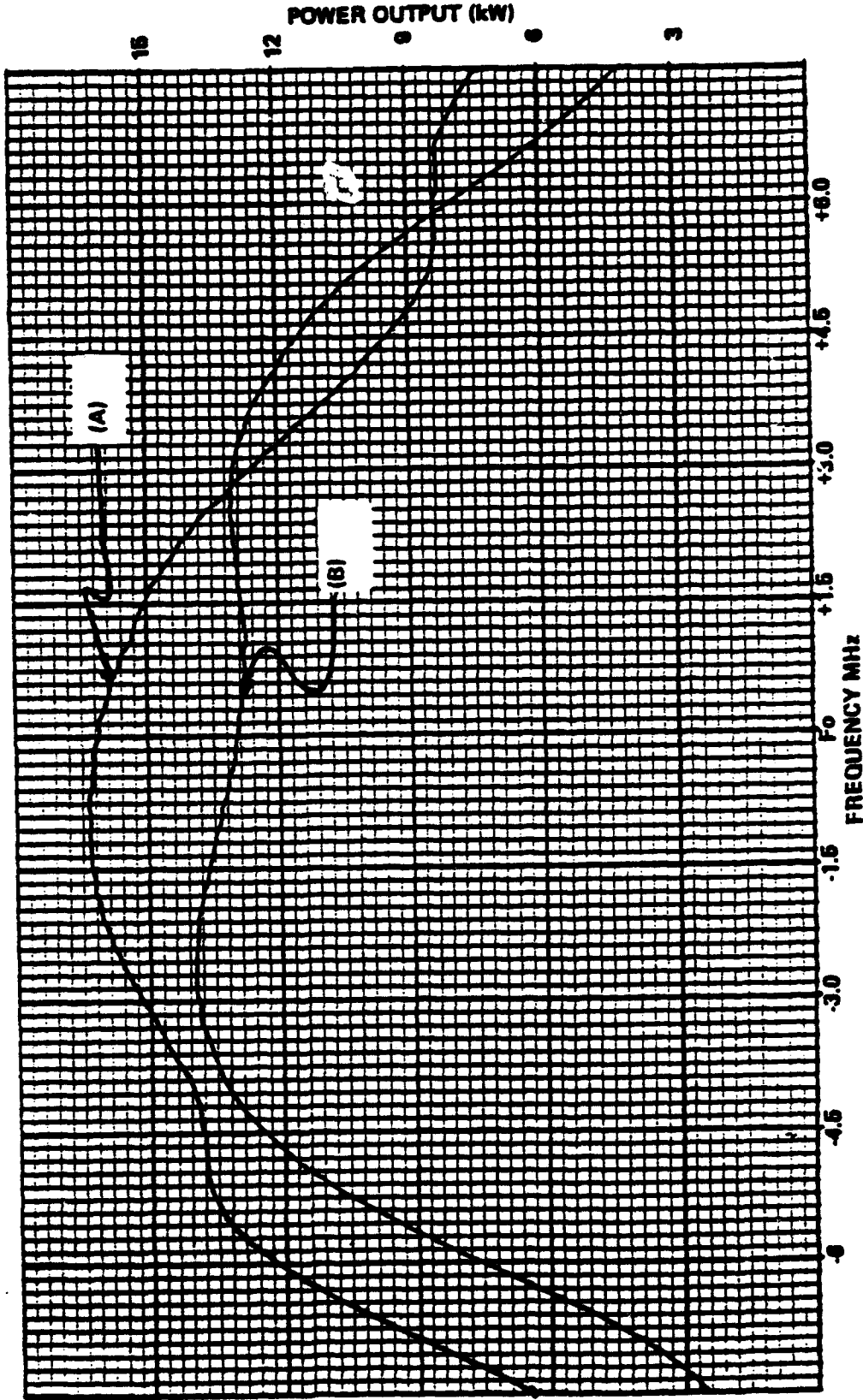


FIGURE 2-22 POWER OUTPUT vs FREQUENCY CURVES (A) AND (B) AT  $F_0 = 810$  MHz



**KLYSTRON AMPLIFIER**  
 TUBE TYPE NO. VKP-7865  
 SERIAL NO. A6-0d1

**TEST PERFORMANCE SHEET**

TESTED BY E.L. Ciarra DATE 03/05/86 VARIAN O.A. \_\_\_\_\_

POWER OUTPUT vs FREQUENCY  
 Eb 6.1 (V<sub>ac</sub>) Po TAB. I. (kW)  
 Ib 1.2 (A<sub>ac</sub>) Pd TAB. I. (W)  
 Imag TAB. I. (A<sub>dc</sub>) GAIN TAB. I. (dB)  
 BW TAB. I. (MHz) Fo 810 (MHz) EFF TAB. I. (%)

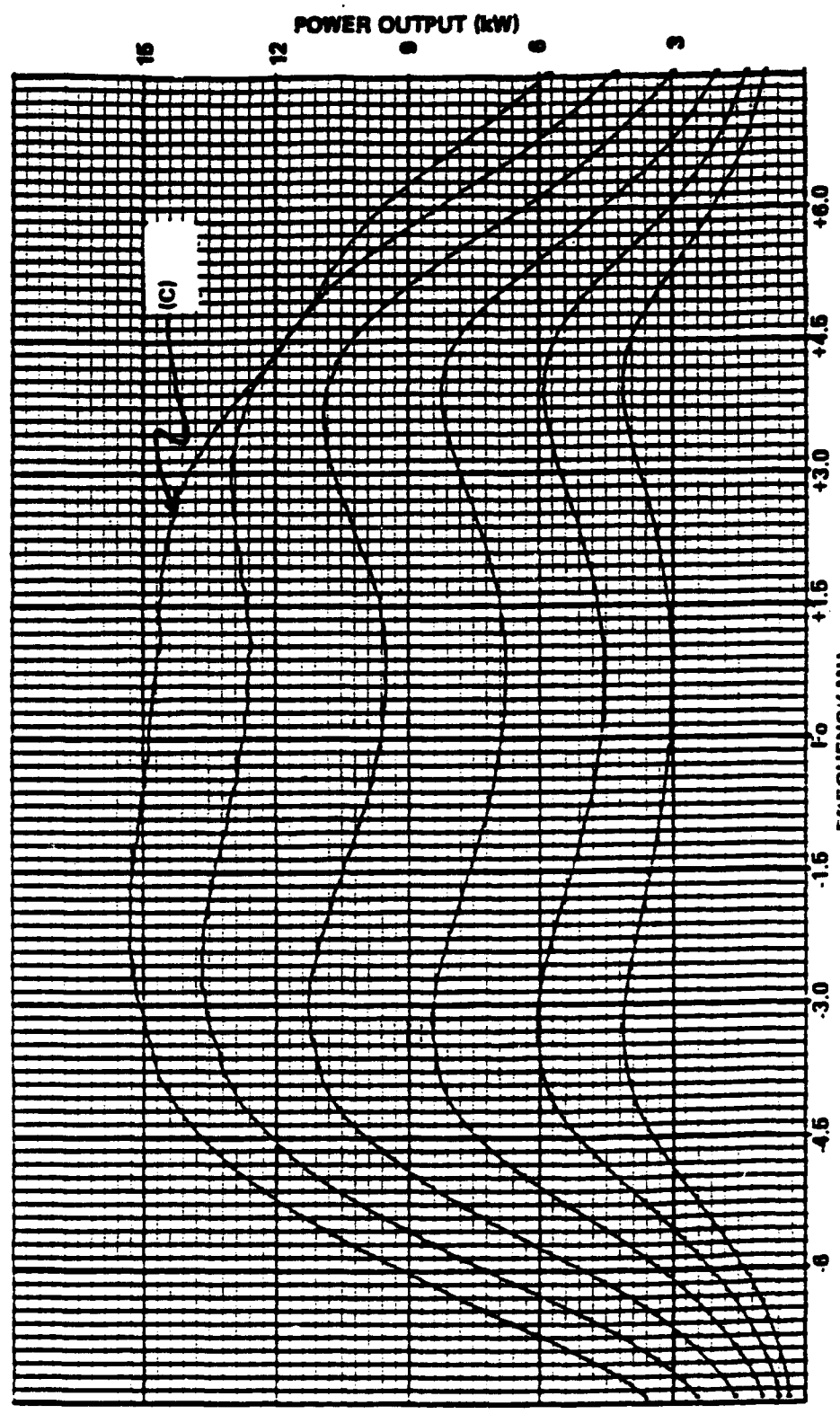


FIGURE 2-23. POWER OUTPUT vs FREQUENCY CURVE (C) AT F<sub>0</sub>=810MHZ

67-000 25



**KLYSTRON AMPLIFIER**  
 TUBE TYPE NO. **VKP-7885**  
 SERIAL NO. **16-901**

**TEST PERFORMANCE SHEET**

TESTED BY RL Egan DATE 03/05/86 VARIAN QA

**POWER OUTPUT vs FREQUENCY**

E1 6.1 (Vac)

I1 16.2 (Aac)

Iavg 7.6 (Aac)

BW 7.1 (MHz)

Eb 14.6 (kVdc)

Ib 1.25 (Aac)

Iby 30 (mAac)

Fo 845 (MHz)

PO TAB. I. (kW)

Pd TAB. I. (W)

GAIN TAB. I. (dB)

EFF TAB. I. (%)

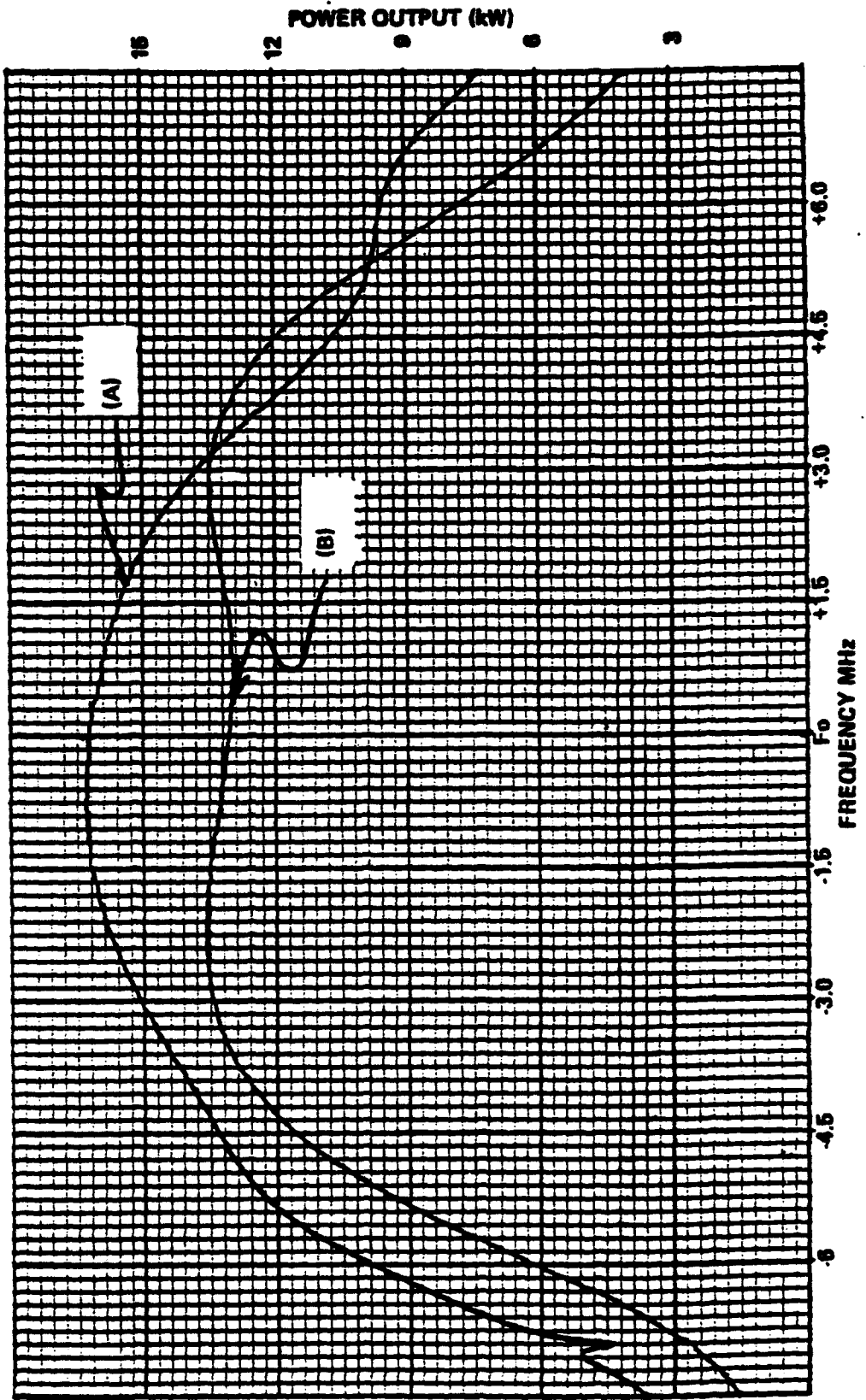


FIGURE 2-24. POWER OUTPUT vs FREQUENCY CURVES (A) AND (B) AT Fo=845MHz

158 009-18



**KLYSTRON AMPLIFIER**  
 TUBE TYPE NO. VKP-7885  
 SERIAL NO. A6-001

**TEST PERFORMANCE SHEET**

TESTED BY Ed Eisen DATE 03/05/86 VARIAN QA \_\_\_\_\_

**POWER OUTPUT vs FREQUENCY**

Ef 6.1 (Vac)      Eb 14.6 (kVdc)      Po TAB. I. (kW)  
 If 16.2 (Aac)      Ib 1.55 (Adc)      Pd TAB. I. (W)  
 Imag TAB. I. (Adc)      Iby 30 (mAac)      GAIN TAB. I. (dB)  
 BW TAB. I. MHz      Fo 845 (MHz)      EFF TAB. I. (%)

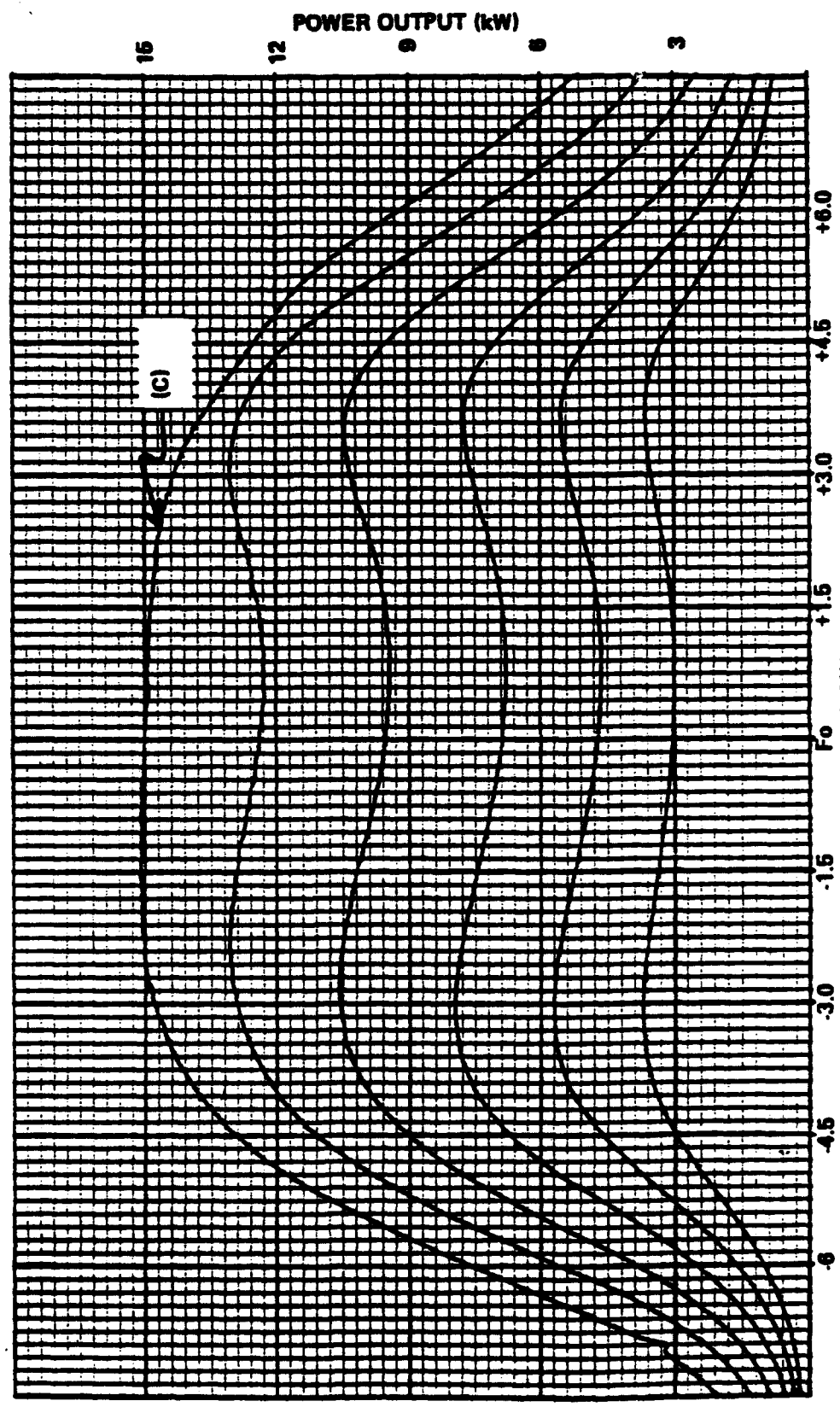


FIGURE 2-25 POWER OUTPUT vs FREQUENCY CURVE (C) AT F<sub>o</sub> = 845MHz



KLYSTRON AMPLIFIER

TUBE TYPE NO. VKP-7865  
SERIAL NO. 26-001

TEST PERFORMANCE SHEET

TESTED BY R. Eisen DATE 03/05/86 VARIAN QA

POWER OUTPUT VS FREQUENCY

E1 <u>6.7</u> (Vac)	Eb <u>4.6</u> (kVdc)	Po TAB. I. (kW)
If <u>26.2</u> (Aac)	Ib <u>1.55</u> (Adc)	Pd TAB. I. (W)
I <sub>mag</sub> TAB. I. (Adc)	I <sub>by</sub> <u>3.5</u> (mAac)	GAIN TAB. I. (dB)
BW TAB. I. MHz	Fo <u>870</u> (MHz)	EFF TAB. I. (%)

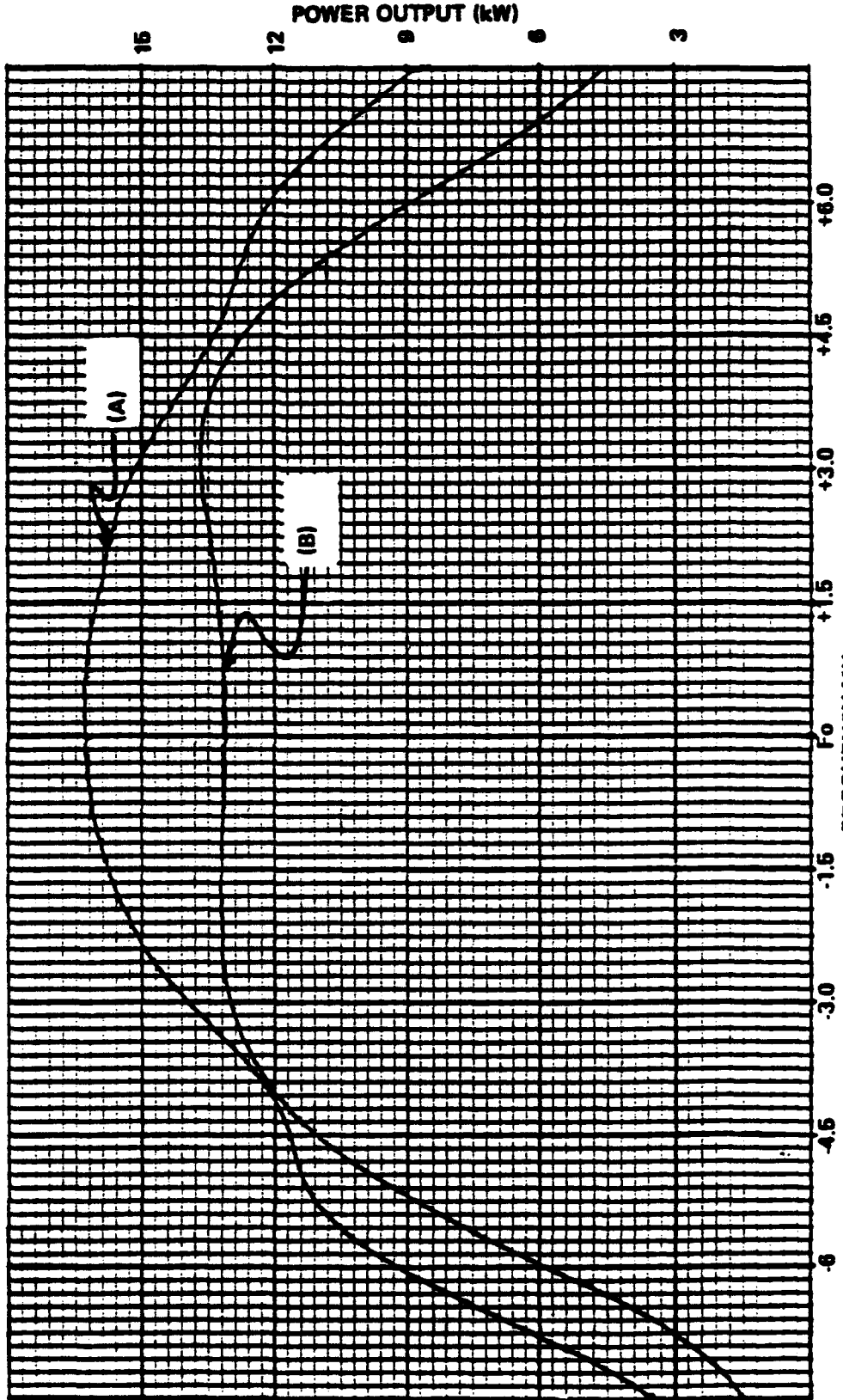


FIGURE 2-26 POWER OUTPUT VS FREQUENCY CURVES (A) AND (B) AT F<sub>0</sub> = 870MHz



**KLYSTRON AMPLIFIER**  
 TUBE TYPE NO. VKP-7885  
 SERIAL NO. A6-001

**TEST PERFORMANCE SHEET**

TESTED BY Ed Eisen DATE 03/05/86 VARIAN QA

POWER OUTPUT vs FREQUENCY  
 Ef 6.1 (Vac) Eb 4.6 (kVdc)  
 If 16.2 (Aac) Ib 1.95 (Adc)  
 Imag TAB. I. 1. (Adc) Iby 35 (mAac)  
 BW TAB. I. 1. MHz Fo 870 (MHz)

Po TAB. I. (kW)  
 Pd TAB. I. 1. (W)  
 GAIN TAB. I. 1. (dB)  
 EFF TAB. I. 1. (%)

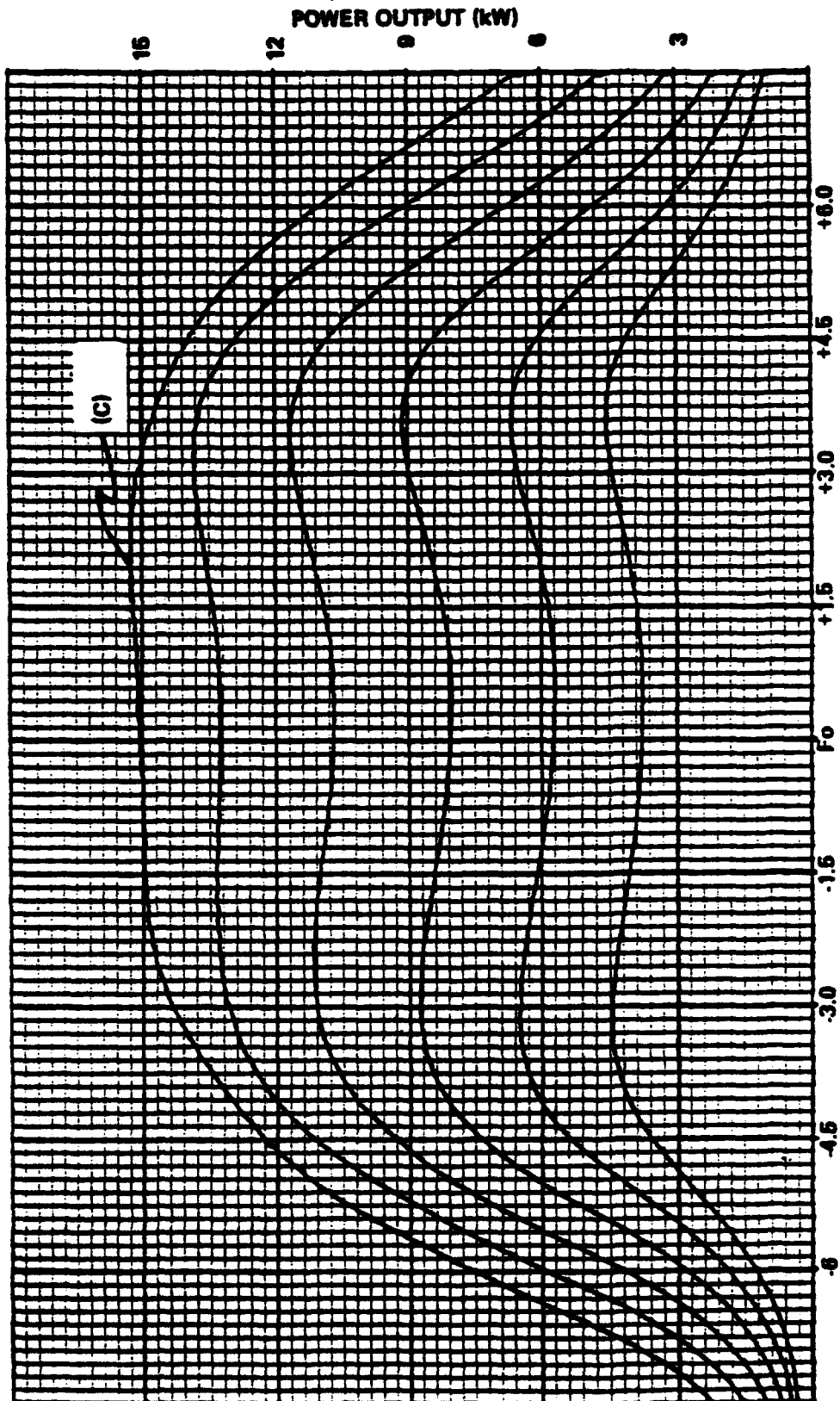


FIGURE 2-27 POWER OUTPUT vs FREQUENCY CURVE (C) AT F<sub>0</sub> = 870MHz



**KLYSTRON AMPLIFIER**

TUBE TYPE NO. **VKP-7885**  
SERIAL NO. **A6-001**

**TEST PERFORMANCE SHEET**

TESTED BY *Ed Eisen* DATE 03/04/86 VARIAN QA

**POWER OUTPUT vs FREQUENCY**

E1 <u>6.1</u> (Vac)	Eb <u>14.5</u> (kVdc)	Po TAB. I. (kW)
I1 <u>16.2</u> (Aac)	Ib <u>1.735</u> (Aac)	Pd TAB. I. (W)
Iavg TAB. I. (Aac)	Iby <u>3.7</u> (mAac)	GAIN TAB. I. (dB)
BW-TAB. I. (MHz)	Fo <u>900</u> (MHz)	EFF TAB. I. (%)

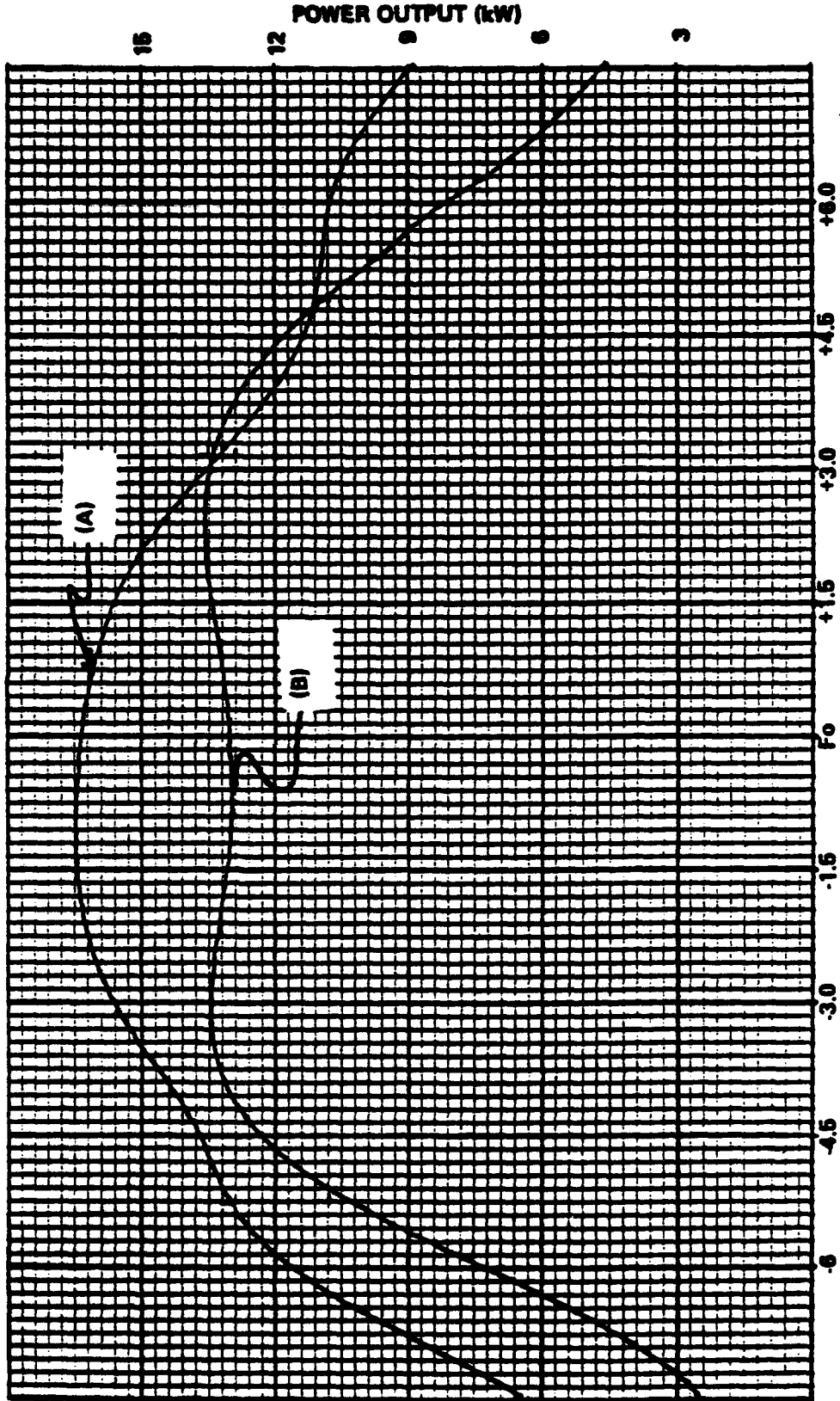


FIGURE 2-28 POWER OUTPUT vs FREQUENCY CURVES (A) AND (B) AT F<sub>0</sub> = 900MHZ



**KLYSTRON AMPLIFIER**

TUBE TYPE NO. **VKP-7005**  
SERIAL NO. **A6-001**

**TEST PERFORMANCE SHEET**

TESTED BY **P. L. Egan** DATE **03/04/86** VARIATION

**POWER OUTPUT vs FREQUENCY**

E1 **6.1** (Vac)  
I1 **16.2** (Asc)  
Imag **7AB.1.** (Adc)  
BW **7AB.1.** MHz

Po **7AB.1.** (kW)  
Pd **7AB.1.** (W)  
GAIN **7AB.1.** (dB)  
EFF **7AB.1.** (%)

Eb **17.5** (kVdc)  
Ib **1.335** (Adc)  
Iby **3.7** (mAdc)  
Fo **900** (MHz)

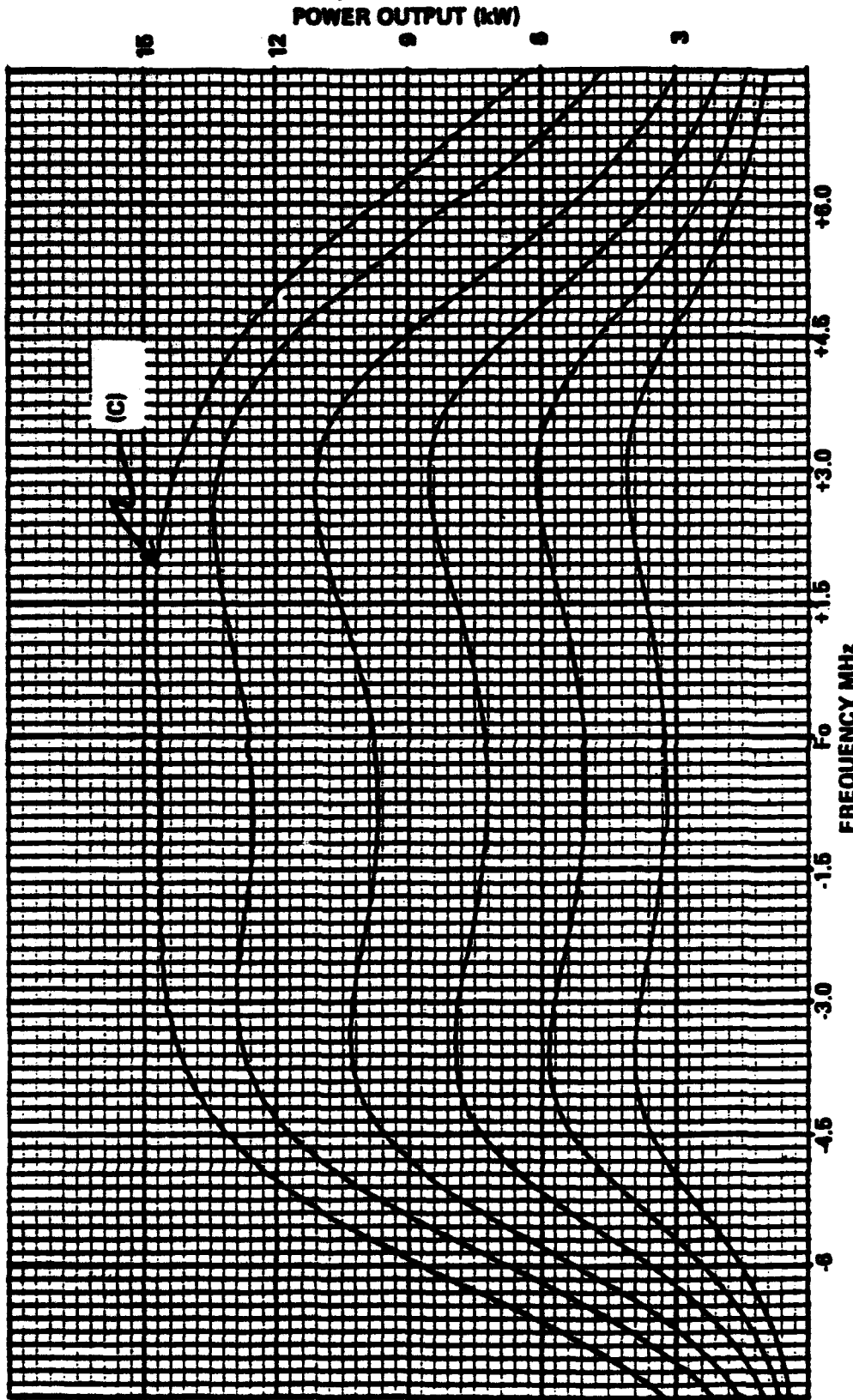


FIGURE 2-29. POWER OUTPUT vs FREQUENCY CURVE (C) AT  $F_0=900\text{MHz}$



**KLYSTRON AMPLIFIER**

TUBE TYPE NO. **VKP-7865**  
SERIAL NO. **A6-001**

**TEST PERFORMANCE SHEET**

TESTED BY *Ed Eisen* DATE 03/04/86 VARIAN QA

**POWER OUTPUT vs FREQUENCY**

EI <u>6.1</u> (Vac)	Eb <u>14.4</u> (kVdc)	Po <u>TAB. 1.1</u> (kW)
II <u>16.2</u> (Aac)	Ib <u>1.92</u> (Adc)	Pd <u>TAB. 1.1</u> (W)
Ireq <u>TAB. 1.1</u> (Adc)	Iby <u>1.5</u> (mAac)	GAIN <u>TAB. 1.1</u> (dB)
BW <u>TAB. 1.1</u> MHz	Fo <u>930</u> (MHz)	EFF <u>TAB. 1.1</u> (%)

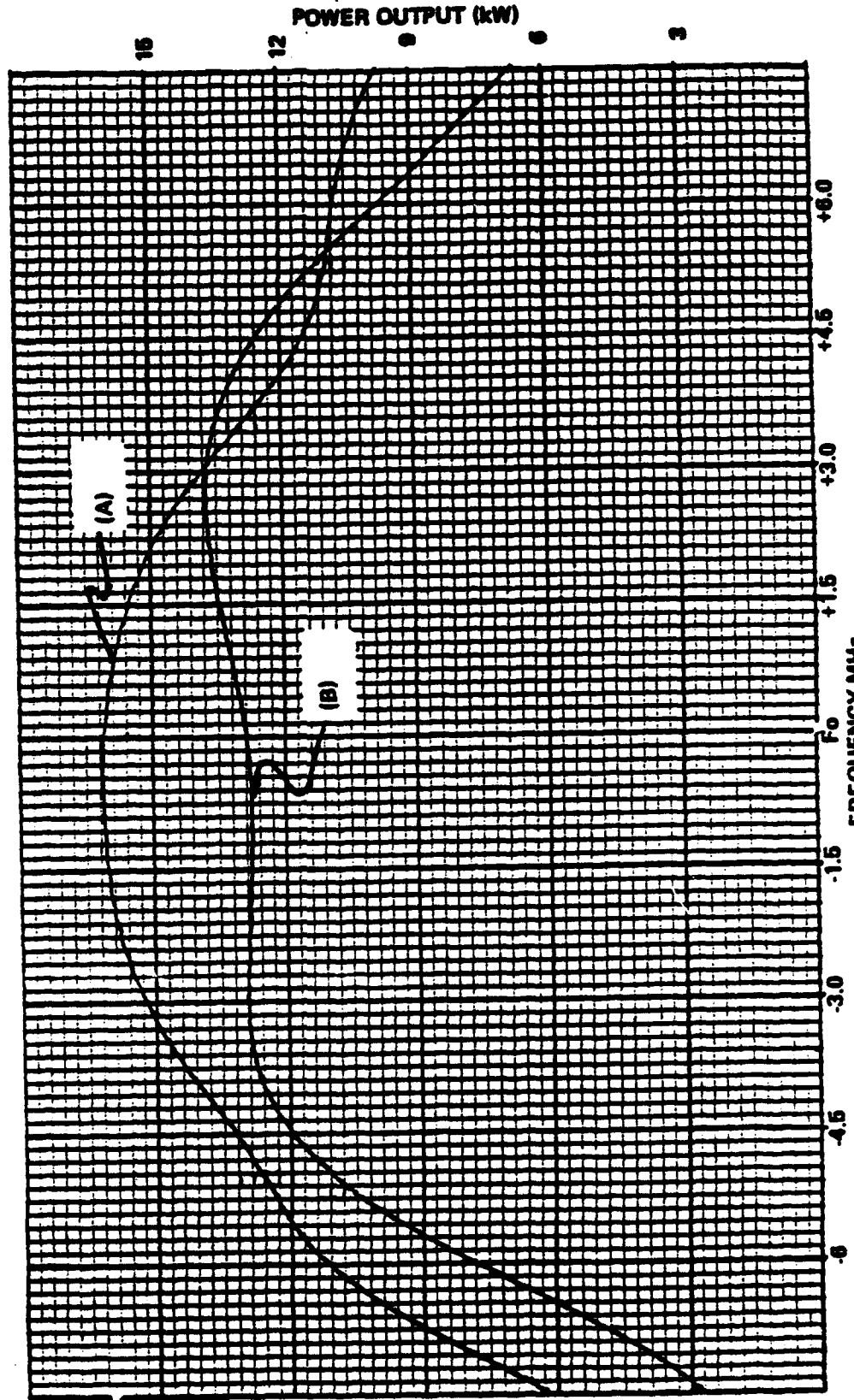


FIGURE 2-30 POWER OUTPUT vs FREQUENCY CURVES (A) AND (B) AT  $F_0 = 930$  MHz



**KLYSTRON AMPLIFIER**

TUBE TYPE NO. VKP-7885  
SERIAL NO. 46-001

**TEST PERFORMANCE SHEET**

TESTED BY Ed E. ... DATE 2/30/1966 VARIAN QA

**POWER OUTPUT vs FREQUENCY**

E1 <u>6.1</u> (Vac)	Eb <u>14.4</u> (kVdc)	Po <u>TAB. 1</u> (kW)
I1 <u>16.7</u> (Aac)	Ib <u>1.92</u> (Adc)	Pd <u>TAB. 1</u> (W)
I <sub>mag</sub> <u>TAB. 1</u> (Adc)	I <sub>by</sub> <u>15</u> (mAac)	GAIN <u>TAB. 1</u> (dB)
BW <u>TAB. 1</u> MHz	Fo <u>930</u> (MHz)	EFF <u>TAB. 1</u> (%)

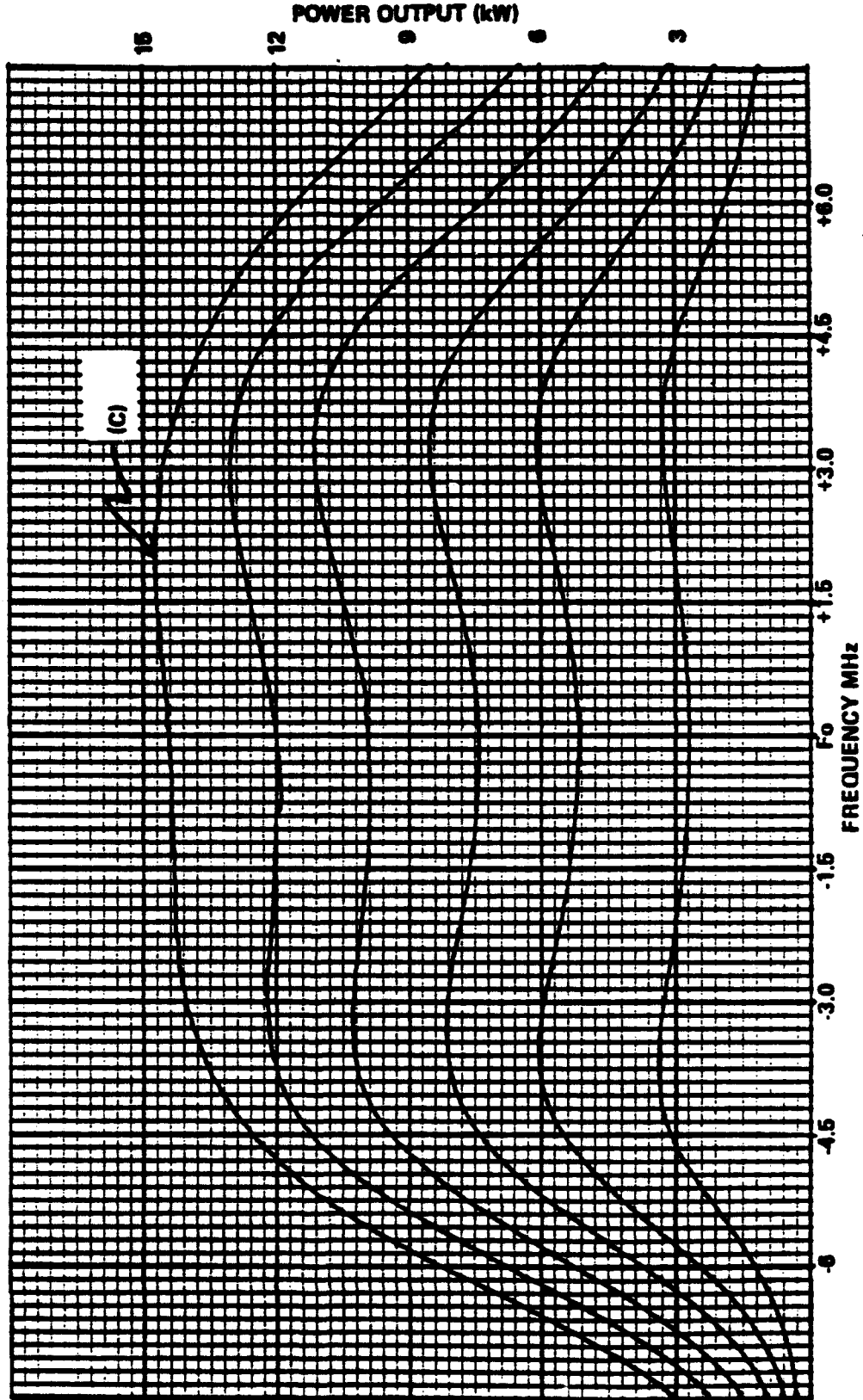


FIGURE 2-31 POWER OUTPUT vs FREQUENCY CURVE (C) AT F<sub>o</sub> = 930 MHz



**KLYSTRON AMPLIFIER**

TUBE TYPE NO. **VKP-7885**  
SERIAL NO. **A6-001**

**TEST PERFORMANCE SHEET**

TESTED BY Ch. E. E. E. DATE 03/04/86 VARIAN QA

**POWER OUTPUT vs FREQUENCY**

Ef <u>6.1</u> (V <sub>ac</sub> )	Eb <u>14.6</u> (kV <sub>dc</sub> )	Po <u>TABLE</u> (kW)
If <u>16.2</u> (A <sub>ac</sub> )	Ib <u>1.95</u> (A <sub>dc</sub> )	Pd <u>TABLE</u> (W)
I <sub>max</sub> <u>TABLE</u> (A <sub>dc</sub> )	I <sub>by</sub> <u>15</u> (mA <sub>dc</sub> )	GAIN <u>TABLE</u> (dB)
BW <u>TABLE</u> (MHz)	Fo <u>960</u> (MHz)	EFF <u>TABLE</u> (%)

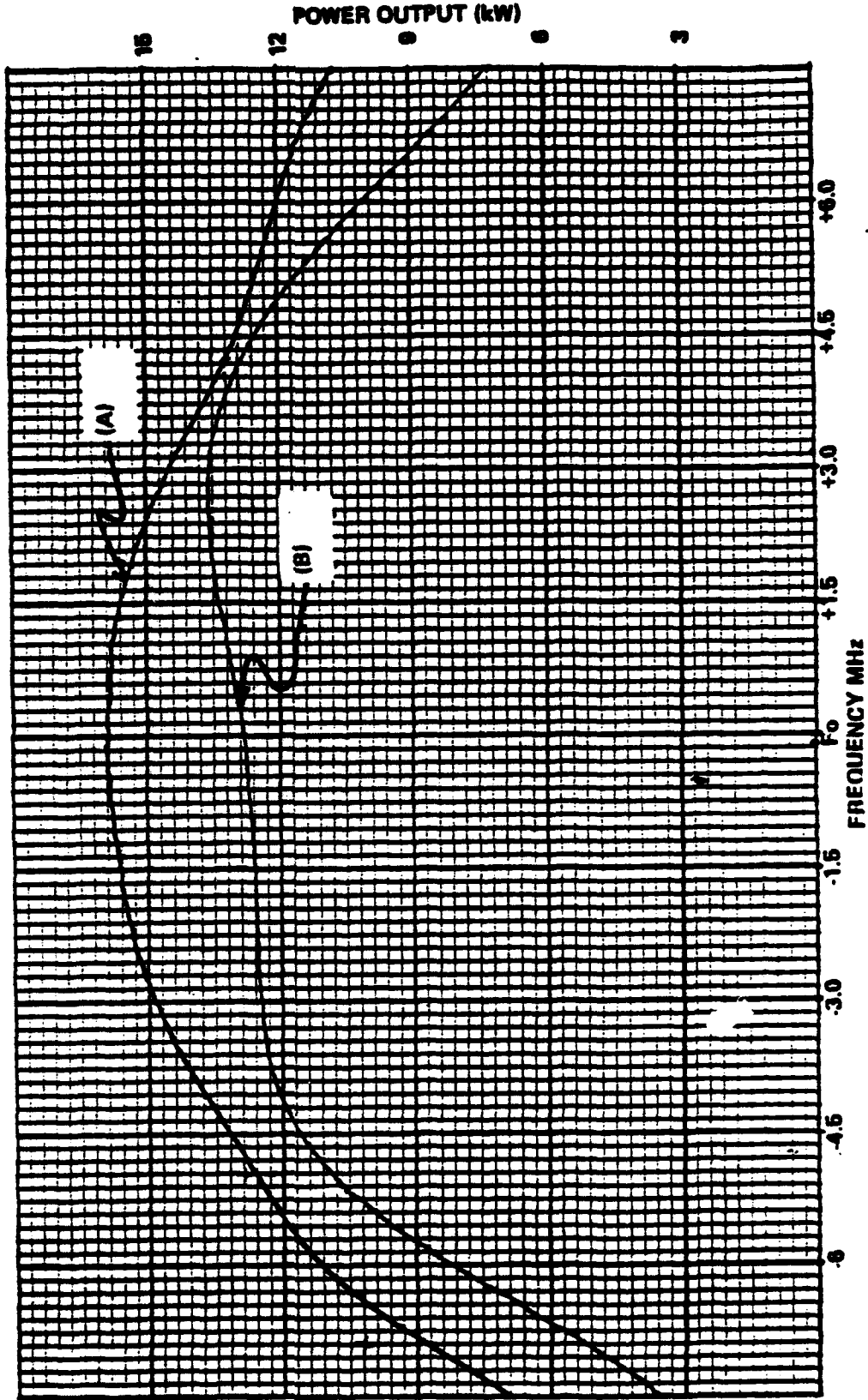


FIGURE 2-32 POWER OUTPUT vs FREQUENCY CURVES (A) AND (B) AT  $F_0 = 960$  MHz



**KLYSTRON AMPLIFIER**  
 TUBE TYPE NO. **VKP-7865**  
 SERIAL NO. **A6-001**

**TEST PERFORMANCE SHEET**

TESTED BY: Ed Eisen DATE: 03/04/86 VARIAN QA

**POWER OUTPUT vs FREQUENCY**

EI 16.1 (Vac)      Eb 11.6 (KVdc)      Po TAB. 1 (kW)  
 II 16.2 (Aac)      Ibv 1.55 (Aac)      Pd TAB. 1 (W)  
 Imag TAB. 1 (Aac)      Fo 960 (MHz)      GAIN TAB. 1 (dB)  
 BW TAB. 1 (MHz)                EFF TAB. 1 (%)

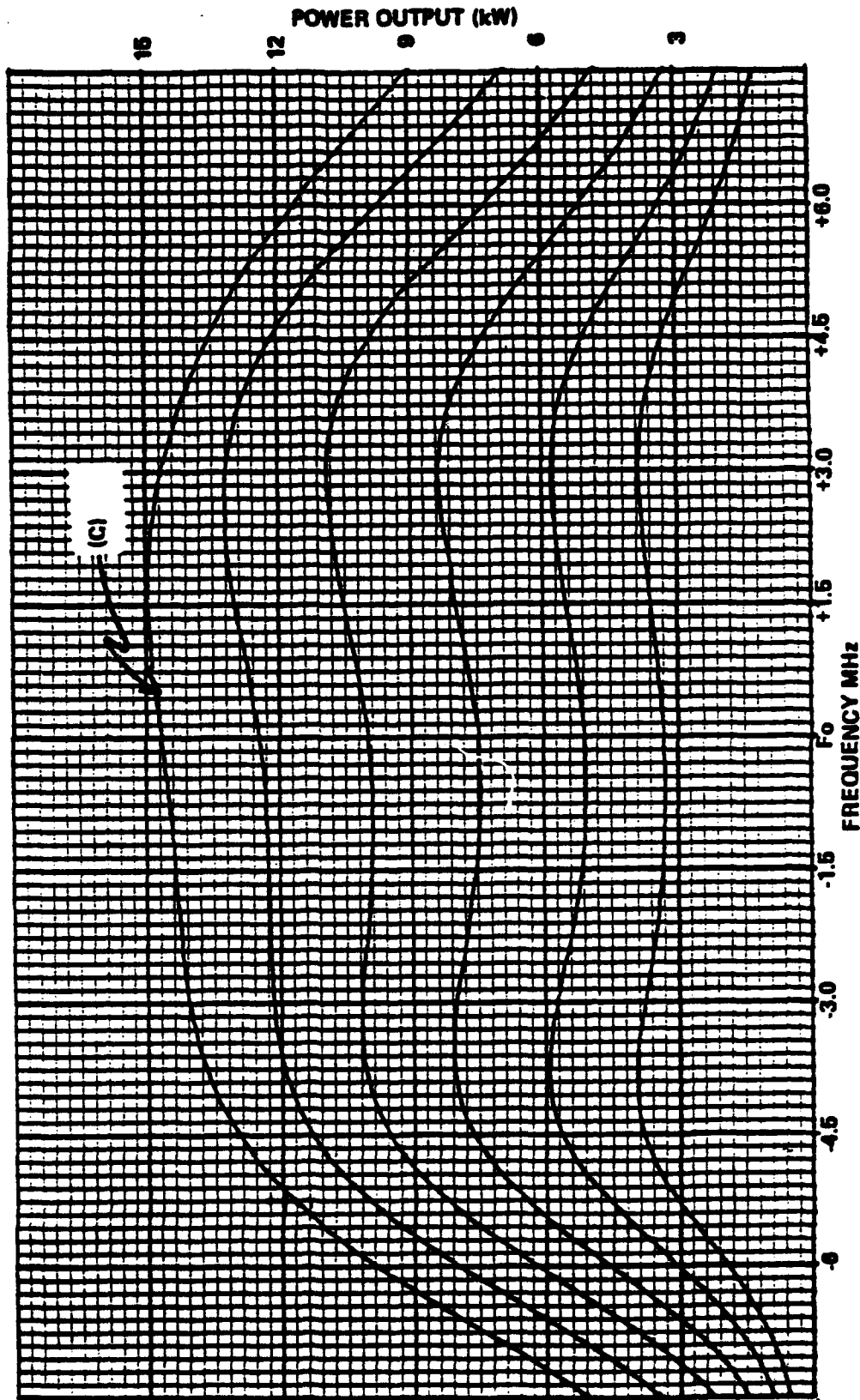


FIGURE 2-33 POWER OUTPUT vs FREQUENCY CURVE (C) AT F<sub>0</sub> = 960MHz



KLYSTRON AMPLIFIER  
 TUBE TYPE NO. VKP-7006  
 SERIAL NO. A6-001

TEST PERFORMANCE SHEET

TESTED BY Ed Eisen DATE 03/04/86 VARIAN DA \_\_\_\_\_  
 POWER OUTPUT VS FREQUENCY  
 E1 6.1 (Vac) Eb 14.7 (kVdc) Po TAB. I. (kW)  
 I1 16.2 (Aac) Ib 1.97 (Aac) Pd TAB. I. (W)  
 Imag TAB. I. (Aac) Iby 70 (mAac) GAIN TAB. I. (dB)  
 BW TAB. I. MHz Fo 985 (MHz) EFF TAB. I. (%)

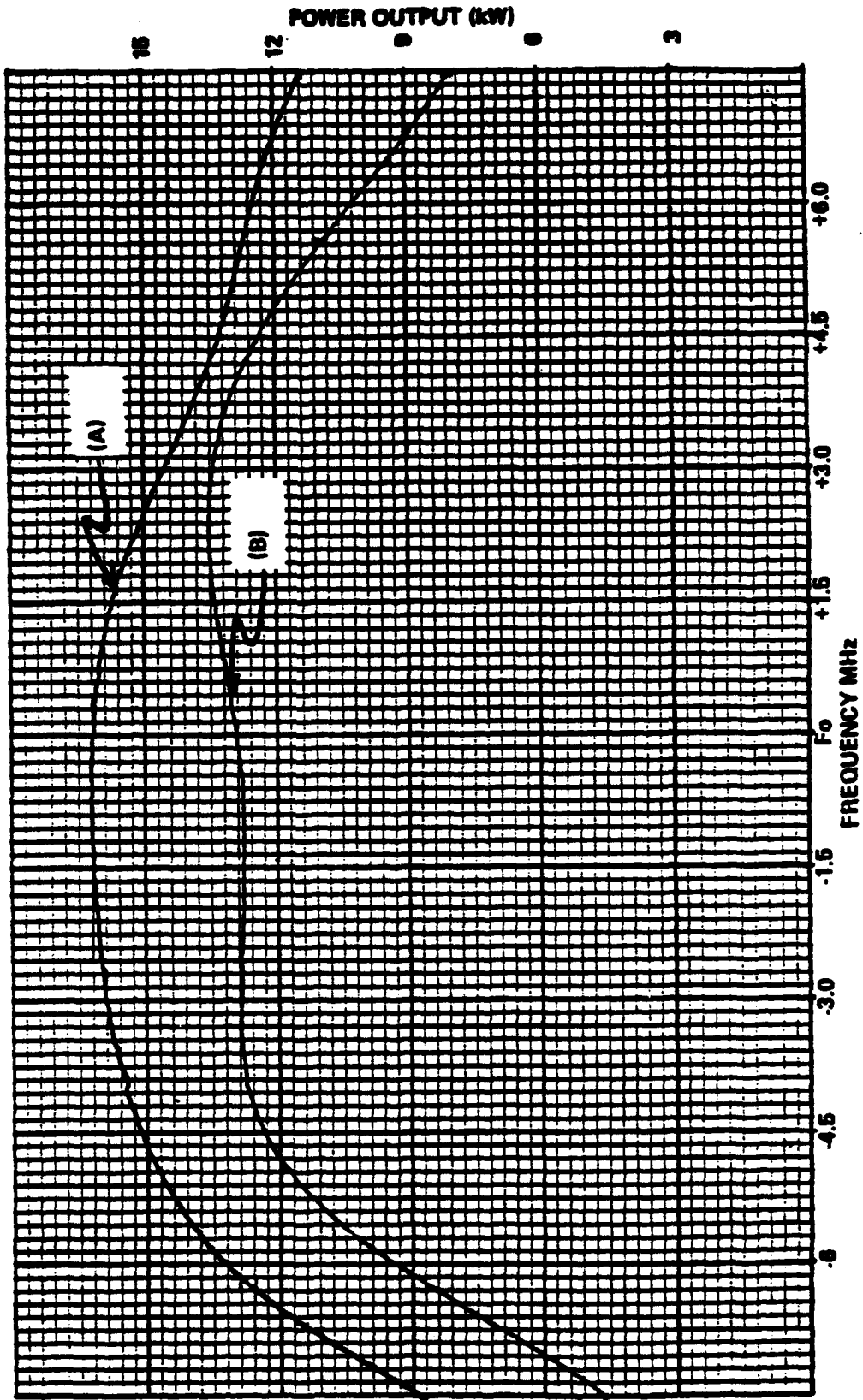


FIGURE 2-34 POWER OUTPUT VS FREQUENCY CURVES (A) AND (B) AT F<sub>o</sub> = 985 MHz



**KLYSTRON AMPLIFIER**

TUBE TYPE NO. **VKP-7005**  
SERIAL NO. **Ab-001**

**TEST PERFORMANCE SHEET**

TESTED BY Ed Eisen

DATE 03/04/86 VARIAN QA

**POWER OUTPUT VS FREQUENCY**

E1 6.1 (Vac)      Eb 14.7 (kVdc)  
I1 16.2 (Aac)      Ib 1.97 (Adc)  
Imag 18.7 (Adc)      Iby 1.0 (mAac)  
BW 18.1 MHz      Fo 985 (MHz)

Po 18.1 (kW)  
Pd 18.1 (W)  
GAIN 18.1 (dB)  
EFF 18.1 (%)

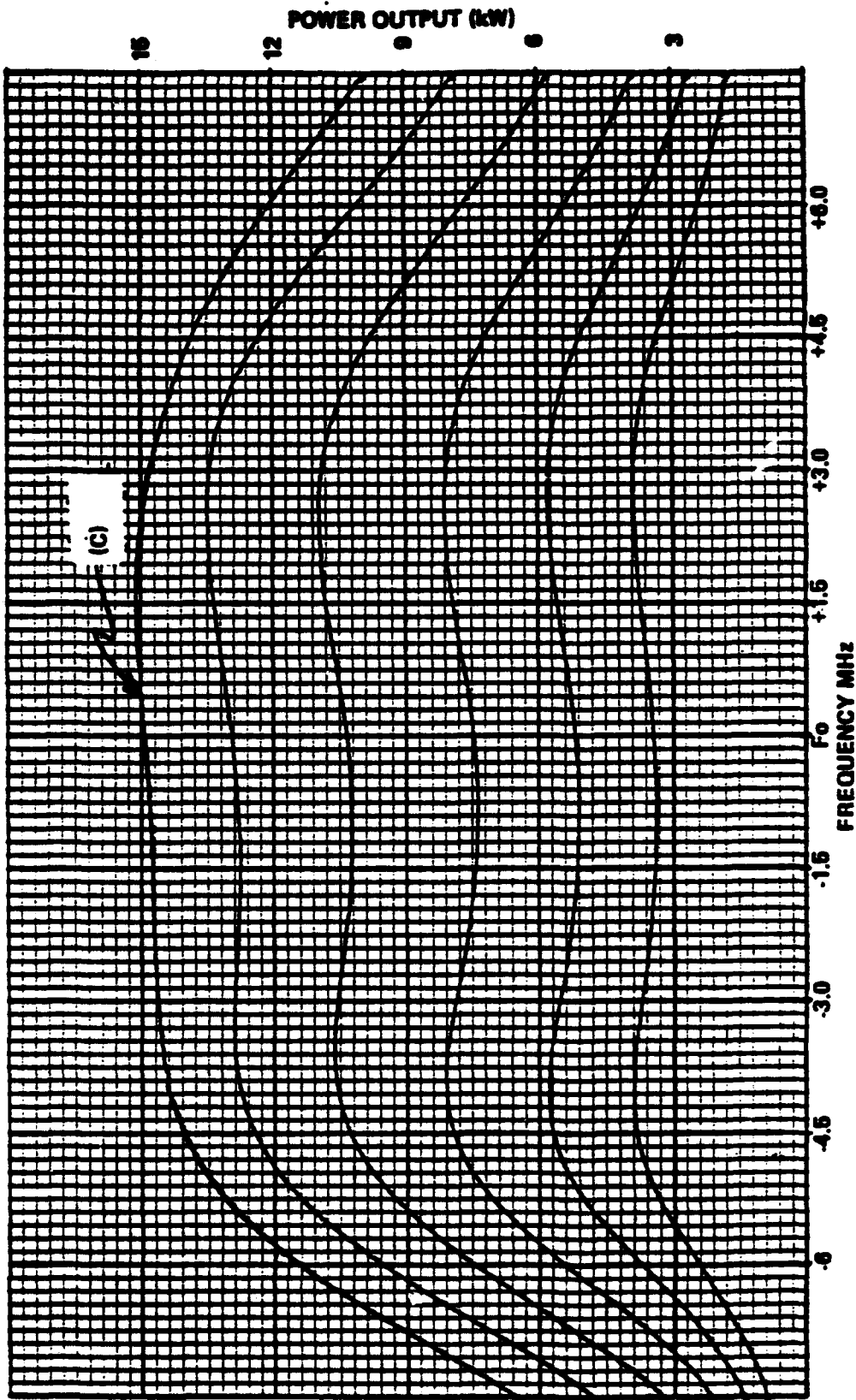


FIGURE 2-35 POWER OUTPUT VS FREQUENCY CURVE (C) AT F<sub>0</sub> = 985 MHz



KLYSTRON AMPLIFIER  
 TUBE TYPE NO. VKP-7865  
 SERIAL NO. 16-001

TEST PERFORMANCE SHEET

TESTED BY: Ed Eisen DATE: 3/11/86 VARIAN QA

POWER OUTPUT vs FREQUENCY  
 Eb 14.6 (kVdc)  
 Ib 1.95 (Adc)  
 Iby 20 (mAadc)  
 Fo 840 (MHz)

Po N/A (kW)  
 Pd N/A (W)  
 GAIN N/A (dB)  
 EFF N/A (%)

Ef 6.1 (Vac)  
 If 16.7 (Aac)  
 Imag N/A (Adc)  
 BW N/A (MHz)

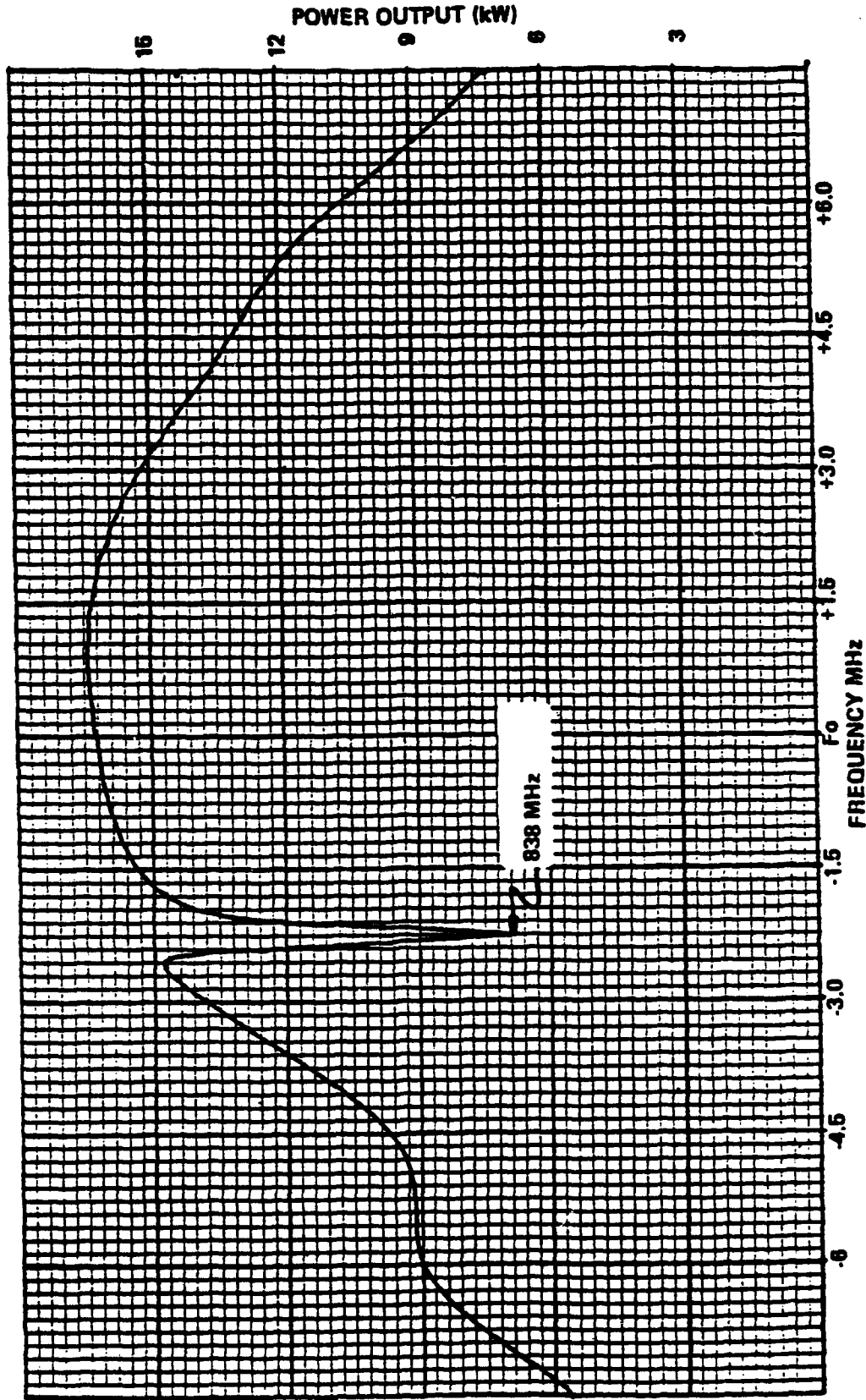


FIGURE 2-36. POWER OUTPUT vs FREQUENCY AT  $F_0 = 840$  MHz 4th CAVITY HARMONIC MODE SHOWN

Curves were made which show rf power output as a function of the rf input drive power. The curves were made at  $F_o = 755, 870, \text{ and } 985$  MHz and are presented in the test data section of this report as Figures 2-37 through 2-39.

Tuning curves were drawn for each cavity for setting the tuner counters for a desired  $F_o$ . These curves are presented as Figures 2-40 through 2-45. As an alternative to the tuning curves, Table 3 provides counter readings for each cavity for  $F_o$ 's in 5 MHz steps. The counter readings provide an approximate method for tuning to the desired  $F_o$ .

Further testing was performed to determine, whether or not, the optimum output coupling had been achieved for maximum efficiency at  $F_o = 755, 870, \text{ and } 985$  MHz. The coupling of the output cavity to the load was varied in steps by changing the position of a special Teflon slug located in the output coax line. At each new position of the Teflon slug, the klystron was optimized for maximum  $P_o(\text{sat})$  and the efficiency was calculated. The maximum efficiencies were 67.7, 63.5, and 62.8 percent respectively while the output cavity  $Q_e$ 's were 66.8, 63.3, and 71.9 respectively. These results lead to some interesting possibilities for increasing the efficiency in the  $P_o(\text{sat}-.9\text{dB})$  mode of operation. These possibilities are discussed later in Section 2.5.2 of this report.

#### 2.4.3 Overall Klystron Performance

The discussions, so far, have mainly dealt with the electrical performance of the klystron. The mechanical and thermal characteristics are also of importance to the overall performance of the tube. The klystron tuning mechanisms are the only dynamic structures in the tube/electromagnet system. These mechanisms consist of two parts, the rf cavity tuner mechanism and the tuner counter mechanism. The performance of the rf cavity tuner mechanism was of special interest because its mechanical design, though based on sound mechanical and electrical concepts, was new and untried. The overall performance was excellent, the tuner mechanism operated smoothly over the entire frequency range and no evidence of arcing could be found. The tuning rate was well within acceptable limits even at the low end of the frequency range where the rate increases exponentially. Some small amount of tuner back-lash could be detected and was most noticeable at the low end of the frequency range due to the higher tuning rate, but only minor tuner adjustments were necessary to achieve the desired bandpass. The only negative performance of the tuner mechanism occurred during the optimum efficiency tests where power outputs in excess of 19 KW were obtained. At these high power levels minor thermal detuning was noticed in the output cavity. Since 19 KW is nearly 1.5 times higher than the expected operating power level and

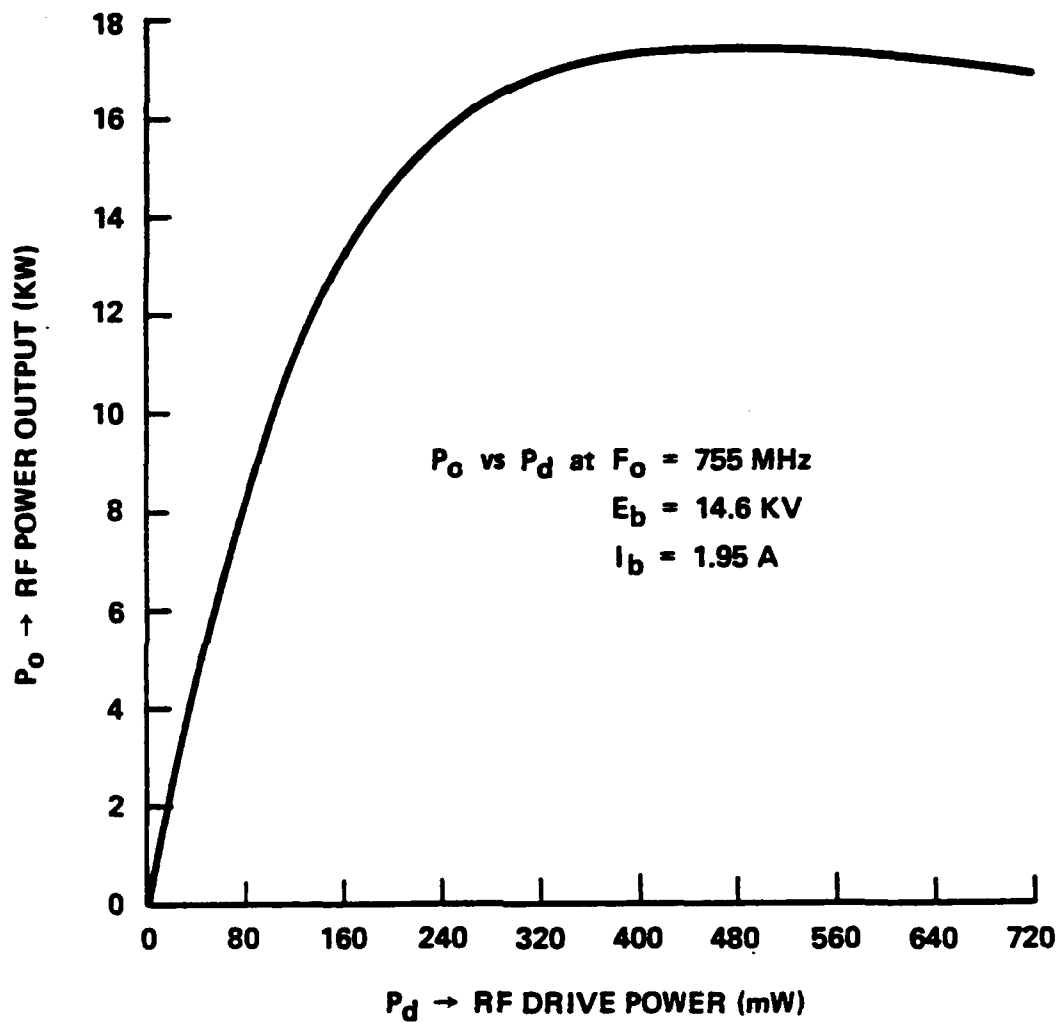


FIGURE 2-37. POWER OUTPUT vs DRIVE POWER AT  $F_o = 755$  MHz

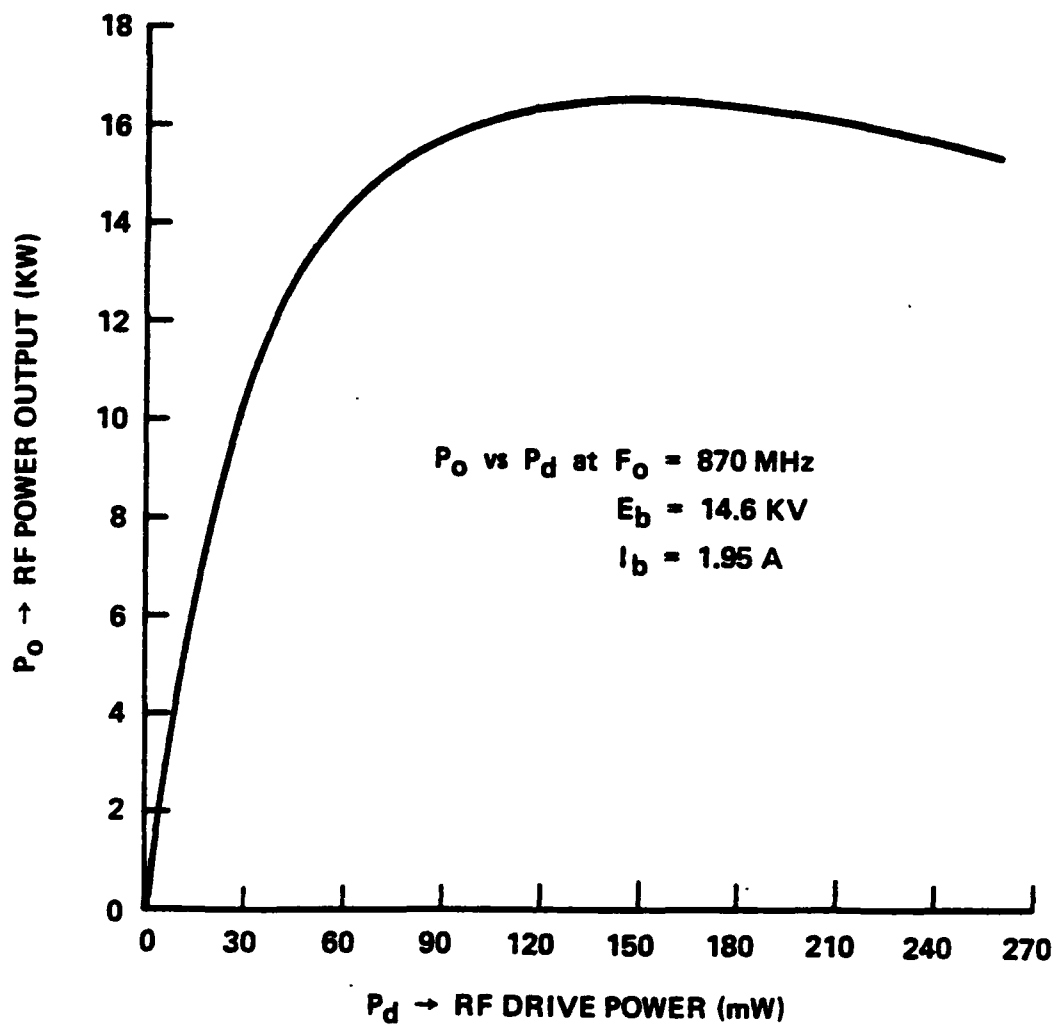


FIGURE 2-38. POWER OUTPUT vs DRIVE POWER AT  $F_o = 870$  MHz

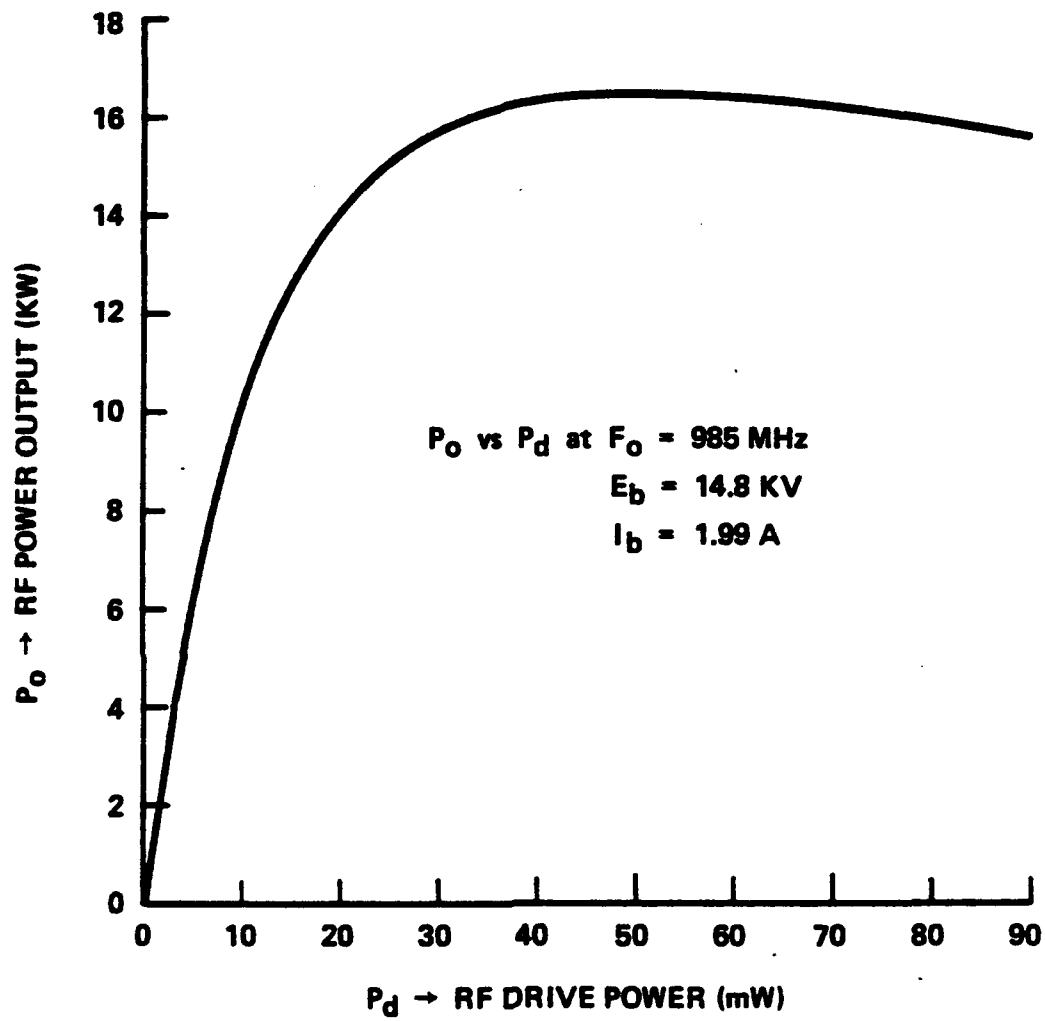


FIGURE 2-39. POWER OUTPUT vs DRIVE POWER AT  $F_o = 985$  MHz

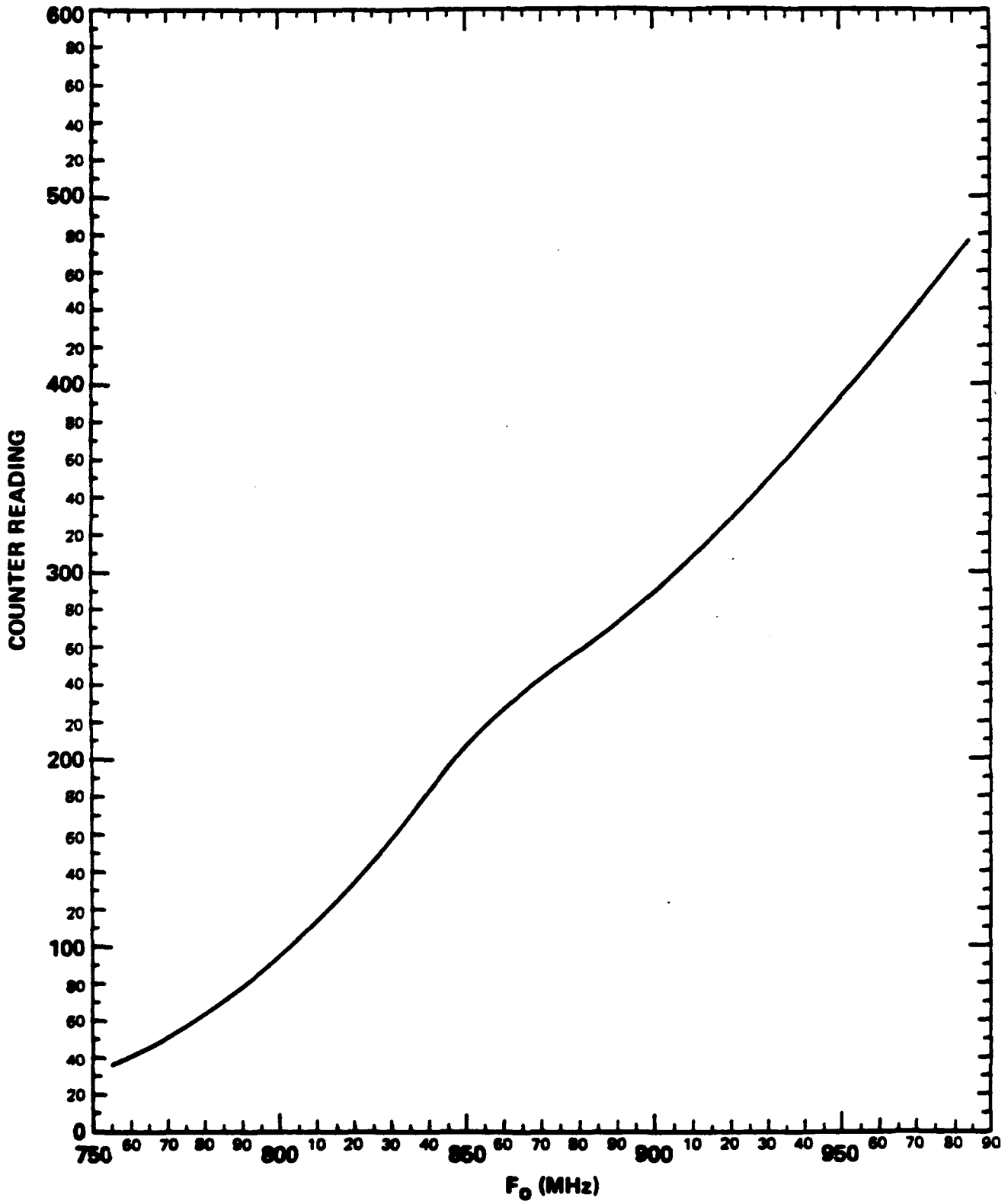


FIGURE 2-40. TUNING CURVE FOR CAVITY #1

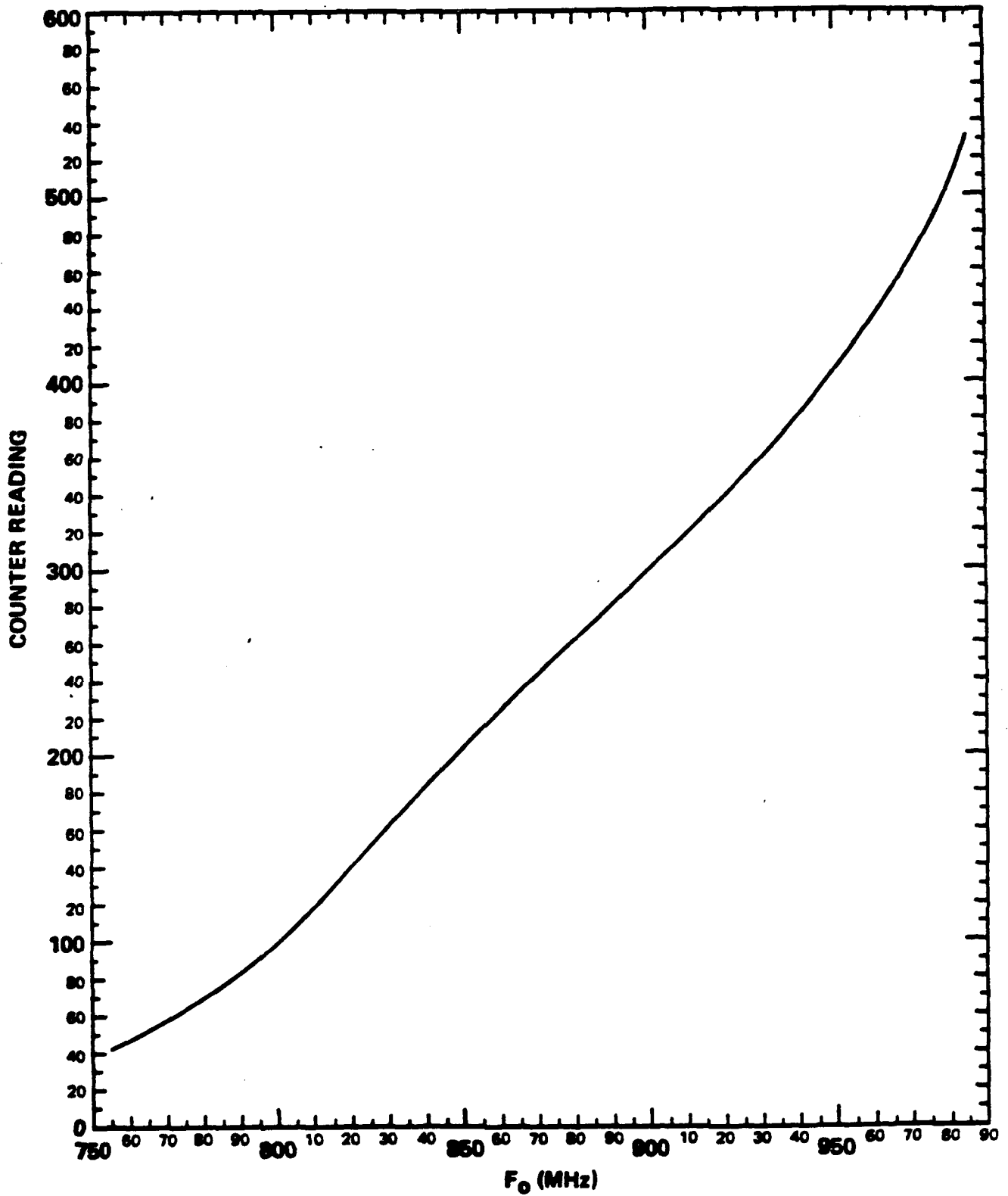


FIGURE 2-41. TUNING CURVE FOR CAVITY #2

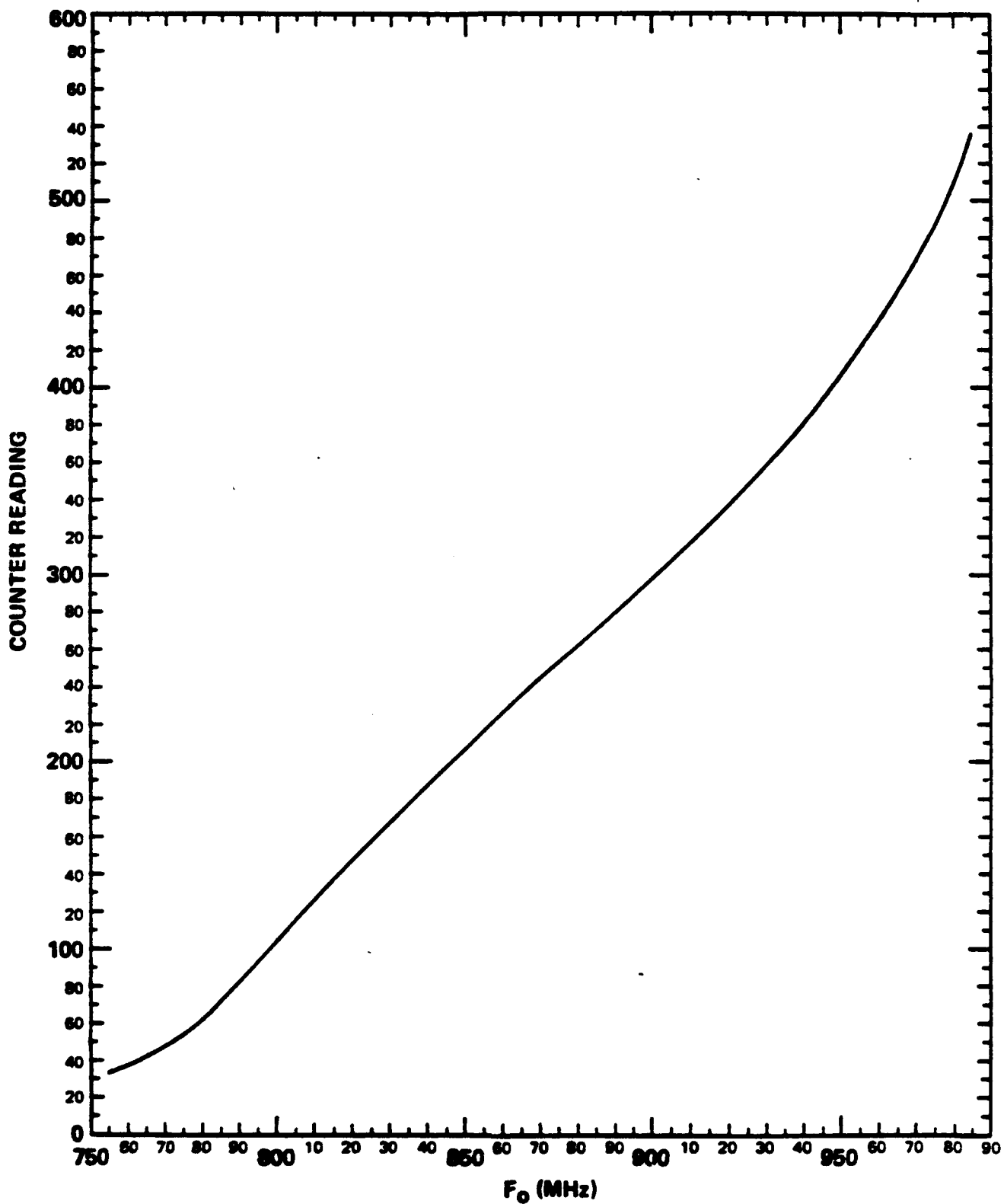


FIGURE 2-42. TUNING CURVE FOR CAVITY #3

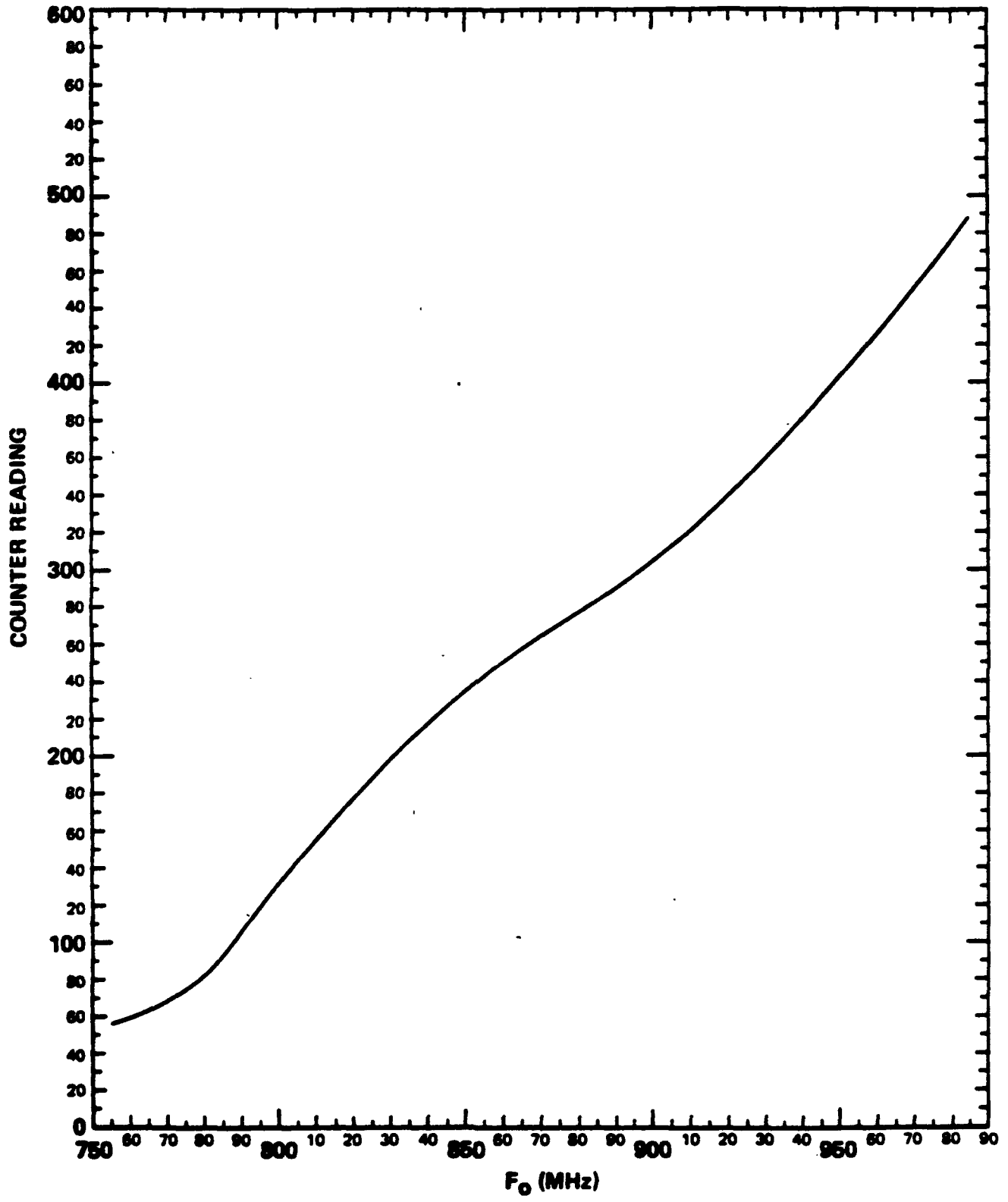


FIGURE 2-43. TUNING CURVE FOR CAVITY #4

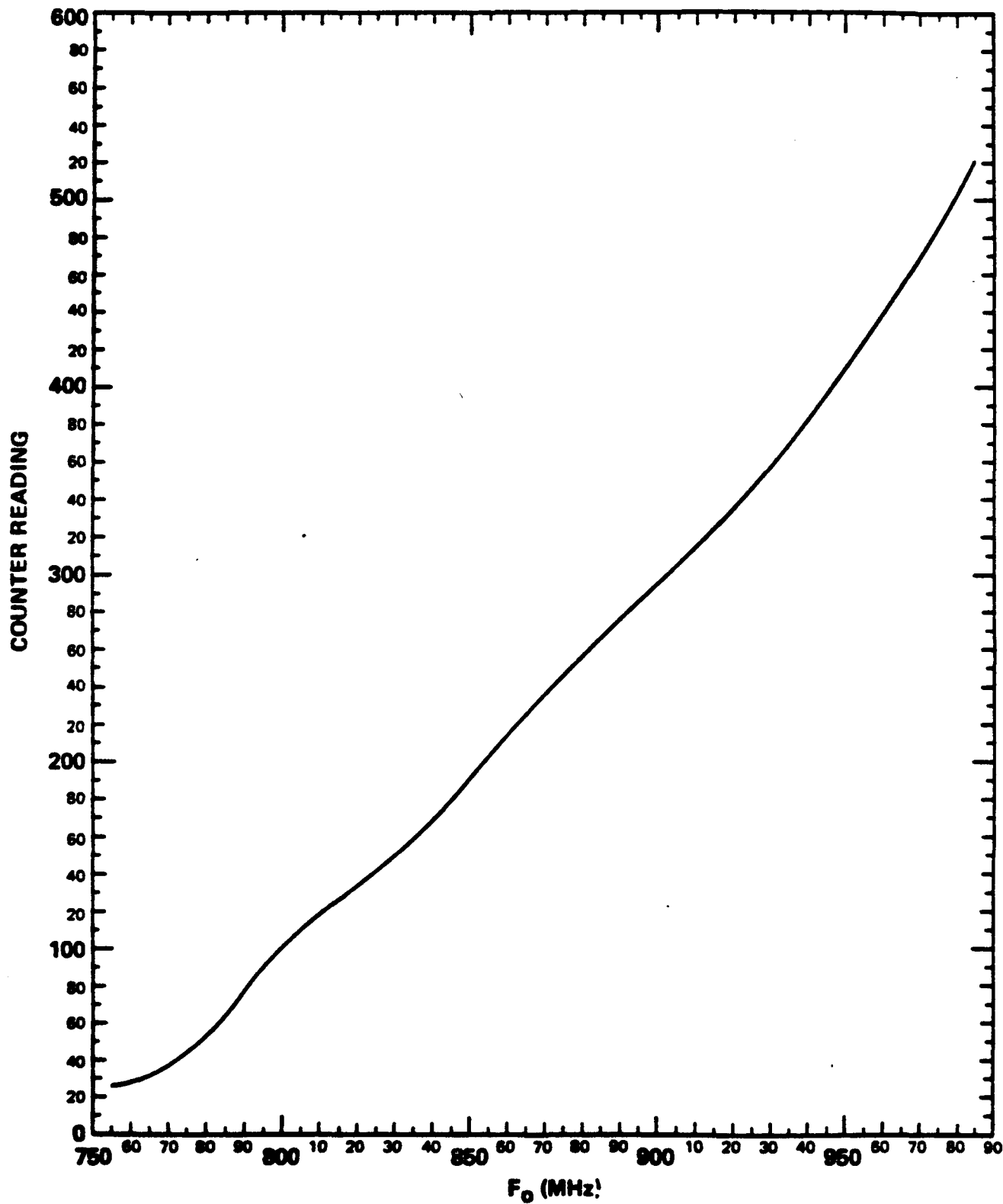


FIGURE 2-44. TUNING CURVE FOR CAVITY #5

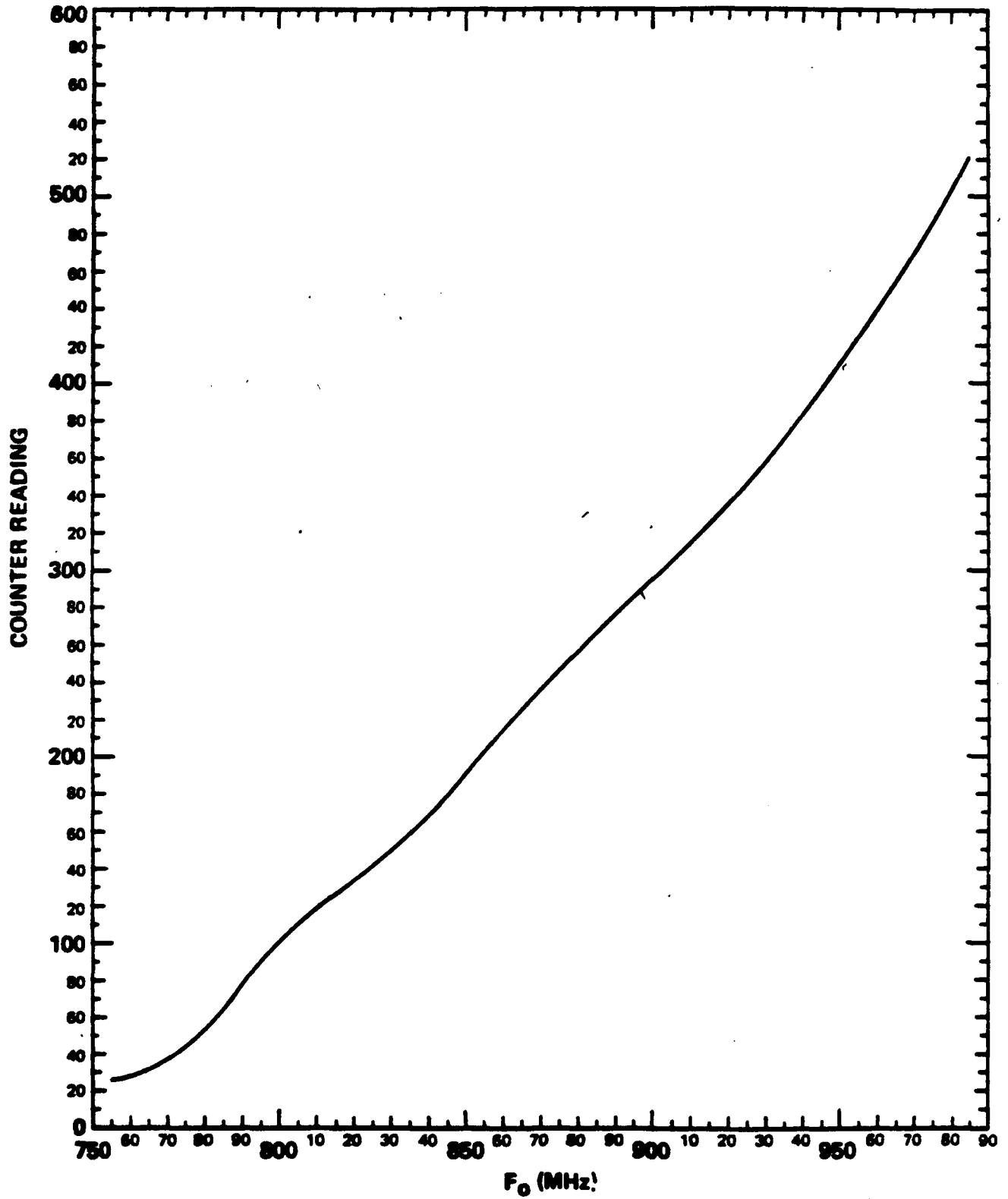


FIGURE 2-45. TUNING CURVE FOR CAVITY #6

**Table 3**  
**Counter Readings for Each Cavity to Set Fo in 5 MHz Steps.**

Fo	CAVITY #1	CAVITY #2	CAVITY #3	CAVITY #4	CAVITY #5	CAVITY #6
755	36	42	33	56	26	43
760	41	47	38	59	28	47
765	46	52	42	63	32	51
770	51	58	48	68	37	56
775	57	63	54	75	45	62
780	63	70	62	82	53	69
785	71	76	72	94	64	77
790	78	83	83	107	77	87
795	86	91	93	120	91	96
800	95	99	104	132	101	105
805	104	109	115	144	111	115
810	113	119	126	155	119	125
815	124	131	136	166	127	134
820	134	141	147	177	134	144
825	145	152	157	188	141	154
830	157	163	167	197	150	164
835	169	174	177	207	159	175
840	181	184	187	217	169	185
845	195	194	197	225	179	196
850	206	205	207	233	191	206
855	217	215	217	241	203	217
860	227	225	226	249	215	227
865	236	235	236	257	226	237
870	244	244	245	264	237	248
875	251	253	253	270	247	256
880	257	262	262	276	257	265
885	265	272	271	283	267	274
890	273	281	280	289	277	283
895	281	290	289	296	287	293
900	289	299	298	304	296	302
905	298	309	307	312	305	312
910	307	318	317	320	315	322
915	317	328	326	329	325	333
920	327	338	336	338	335	343
925	337	348	346	347	346	354
930	348	359	357	357	357	365
935	359	370	369	367	371	376
940	370	381	380	379	384	387
945	381	394	392	390	398	399
950	392	406	405	401	411	411
955	404	420	419	413	425	425
960	416	434	435	425	440	438
965	427	449	450	437	455	453
970	439	465	466	449	470	469
975	452	483	485	461	486	486
980	464	505	507	474	503	505
985	477	532	536	487	522	530

only minor drifting was noticed, it appears that a more than adequate safety factor is inherent in this design.

The tuner counter mechanism used for this tube was similar to those used on previous tubes requiring this function. It performed its function as designed, but, in future systems, the moving parts (gears, bearings, and the engaging shafts) will be made larger and stronger to reduce some of the flexing experienced with the present design.

The thermal characteristics of the tube were also excellent. No thermal detuning was detected under normal operating conditions. The tube was operated with a collector flow of approximately 20 gpm of water and the body and the electromagnet were operated in series with approximately 2 gpm of water during the taking of all the performance data. The collector showed no signs of boiling until the flow had been reduced to approximately 15 gpm. Operation with 18 gpm of water should be adequate to insure proper cooling of the collector. The body and the electromagnet should be operated with no less than 1.5 gpm of water to insure proper cooling.

## 2.5 Design Refinements for a Future Engineering Development Model

### 2.5.1 Introduction

This report has described in detail the design and test of an Advanced Development Model 10 KW L-Band Klystron. A follow-on effort to construct an Engineering Development Model should include certain design refinements.

Recommended improvements are discussed in this section.

### 2.5.2 RF Output Circuit Loading for Improved Efficiency

As stated previously in Section 2.4.2, the maximum efficiency achieved for this klystron was well above 60 percent. This efficiency was achieved by adjusting the rf output circuit loading,  $Q(\text{external})$ , to a value somewhat in excess of 60 and this resulted in the maximum transfer of energy from the electron beam (the generator) to the output coax line (the load). Prior to the adjustment, the  $Q(\text{external})$  had a value of 40 at 755 MHz and this resulted in a (-1dB) instantaneous bandwidth in excess of 9.0 MHz at full saturated power output. A  $Q(\text{external})$  of 60 only provides a (-1dB) instantaneous bandwidth of 6.4 MHz at full saturated power output, but will support a (-1dB) instantaneous bandwidth in excess of 9.0 MHz from 0.9dB below saturated power output to the lowest extremes of the small signal region.

If in fact, typical field operation of the klystron is to be conducted at power output levels of  $P_o(\text{sat}-.9\text{dB})$  or less and the bandwidth at power outputs greater than  $P_o(\text{sat}-.9\text{dB})$  are not of importance, then the higher Q (external) will be used to maximize the klystron dc to rf conversion efficiency.

### 2.5.3 Loading of the Driver Cavities for the Desired Bandwidth

Continuing on the assumption that the rf power output will be limited to  $P_o(\text{sat}-.9\text{dB})$ , then the (-1dB) instantaneous bandwidth, within limits, will be determined almost solely by the response of the driver cavities and the loading in the rf output circuit would be adjusted to achieve optimum efficiency. The response of the driver cavities will be controlled by the loading of each individual driver cavity and its tuned frequency. The ripple in the bandpass can be minimized by properly loading the 1st, 2nd, and 3rd cavities resulting in a very flat bandpass. However, because of the across the band variability of the loading, extensive testing must be performed to achieve the desired performance. Tests already performed indicate that ripple in the bandpass can be limited to no greater than 1dB by reducing the loading in the 1st and 3rd cavities and completely eliminating the loading in the 2nd cavity. This would help reduce costs and complexity of future models.

### 2.5.4 The Vapor-Phase Collector

The collector used on the Advanced Development Model was of the water cooled type. The desired vapor-phase collector will be incorporated on the Engineering Development Model. The present collector will be modified to vapor-phase operation using existing design criteria for vapor-phase collectors. The new vapor-phase collector will be compatible with the existing C. H. Bull heat exchanger.

### 2.5.5 Magnetic Field Refinements

During hot-test it was found that the efficiency could be increased significantly by reducing the magnetic field strength in the region of the output cavity. This reduction in field strength was accomplished by driving the 4th and 5th electromagnet coils with a separate power supply. The reduction in field strength caused the electron beam diameter to increase resulting in increased coupling between the beam and the rf output circuit. The field reduction was limited by the increase in the beam interception current which was held to values no greater than 50 mA under stable operating conditions. To eliminate the need for a separate power supply to

drive the 4th and 5th coils, future magnets will have the windings of these coils reduced to provide the desired magnetic field strength.

#### 2.5.6 Mechanical Refinements

The most significant mechanical refinement would be in the design of the output polepiece. The polepiece now in use was designed to be part of the klystron structure and because of the large diameter of the electromagnet, the polepiece diameter had to be made large. The very large size and weight of the polepiece caused some difficulty in its manufacture and handling by assembly personnel and made the klystron unnecessarily heavy. The next polepiece will be made as two concentric polepieces, the inner polepiece would be part of the klystron and the outer polepiece would be part of the electromagnet. This design change would result in a klystron polepiece diameter of approximately 17 inches compared with the 28 inch diameter polepiece now in use. The resulting klystron would be much easier to handle and could be shipped and stored in a much smaller container.

Some mechanical refinements will be necessary in connection with the modification of the collector from a water cooled type to a vapor-phase cooled type, but these changes would be confined mostly to the collector itself.

The counter mechanism will also be redesigned to reduce the flexing that was present in the engaging shaft and bearing assembly.

#### 2.5.7 Elimination of Interfering Harmonic Mode

An effort will be made to eliminate or reduce the interference caused by the 2nd harmonic mode associated with the 4th rf cavity. However, no guarantee of success for such an effort is implied due to the difficulty of the problem.

### 2.6 Conclusions

During this program, an Advanced Development Model of a high-power klystron amplifier was developed, built, and tested. The performance of the klystron met all customer specifications which included a tuning range from 755 to 985 MHz, a minimum (-1dB) instantaneous bandwidth of 9 MHz, a minimum rf gain of 35 dB, a minimum saturated rf power output of 12 KW CW within the specified tuning range, and a minimum dc to rf conversion efficiency of 50 percent. The Klystron met system compatibility requirements and should provide very stable and reliable performance in field operation.

During the next phase of this program an Engineering Development Model would be constructed to include certain design refinements which are as follows:

- (1) Increase the dc to rf conversion efficiency by optimizing the output cavity loading.
- (2) Simplify tube construction and test by reducing the loading in the driver cavities.
- (3) Redesign the collector to provide vapor-phase cooling.
- (4) Reduce the 4th and 5th coil windings of the electromagnet to achieve the desired magnetic field shape.
- (5) Redesign the output polepieces of the klystron and the electromagnet to reduce the weight of the klystron and make polepiece handling easier.
- (6) Redesign the tuner counters to eliminate the flexing of the engaging shaft and bearing assembly.
- (7) If possible, eliminate or reduce the effects of the 2nd harmonic mode associated with the 4th rf cavity.

## 3.0 10 KW KLYSTRODE

### 3.1 Introduction

#### 3.1.1 Program Objectives

The objective of this program was to develop a new 12KW Klystrode Amplifier for use in troposcatter communication systems. The amplifier must be tunable from 755 to 985 MHz with a 9 MHz 1 dB bandwidth at any given center frequency within this range. The energy conversion efficiency should exceed 50%. Collector cooling will be achieved using water. An electromagnet system is to be used for electron beam focusing. A convergent gun with an intercepting control grid will develop the electron beam. The output power gain of the device is to be measured. However, it is recognized that a solid state preamplifier will be required to drive the Klystrode to full power output. Excluding this requirement, the Klystrode amplifier should be closely compatible with existing troposcatter equipment.

#### 3.1.2 Work Completed During the First Half of the Program

The first half of the program was mainly engineering design work. A great deal of information was learned from EIMAC's UHF-television program. For a first approximation, the dimensions of the Troposcatter Klystrode device (X2255) and circuit were determined by applying known scaling rules to the dimensions of the 30KW television Klystrode. The output cavity, a double-tuned iris-coupled structure, was also scaled directly from that which is used on the television Klystrode.

The computer was used extensively in this design process. The television input circuit was modeled and the various modes of operation were explored. It was during this process that a high gain mode was discovered. This information was then applied directly to the design of the X2255 and its circuitry. The gun geometry and electron optics were modeled and optimized using Varian's gun optics program, HGUN. This was necessary to develop a convergent gun structure. Also, studies of the resonant frequency, R/Q and beam interactions with the output gap vs. circuit & tube geometry were made using the computer to determine the best circuit configuration.

Although experimentation was not the main emphasis of this phase, an EIMAC developed RF beam tester was used to aid in the design of the device's output gap and circuit geometry. Also, an attempt was made to characterize the amplifier's input impedance by way of slotted line measurements and reflected power measurements.

The gun design was time consuming and involved. One of the more significant achievements was the deposition of grid blanks of a precise radius of curvature. As laser cutting would determine the final grid structure, a special fixture to rotate the grid about 2 axis was required and developed. The generation of a program to cut a spherical structure completed the grid development process. Spherical cathodes were designed and ordered. Finally the ceramics and other gun parts were procured. To test the electron gun a beam test unit was developed and built.

### 3.1.3 Work Completed During the Second Half of the Program

Contrasting with the first half, the second half of the program was characterized by experimentation. The last of the computer work determined tailpipe geometry and allowed the use of an existing collector. It was decided that an internal conical anode pole piece would be used. An experimental structure was created and the axial magnetic field component of the proposed structure was measured. This data and previous trajectory calculations directed the anode design. The conical pole piece is clamped to the anode structure. This completed the device design as far as beam transmissibility was concerned.

The first spherical grid was cut and mounted in the beam test unit. Gun design progressed by experimentation using the new gun tester. This test unit was demountable and allowed experimentation to continue at a quickened pace and at a reduced cost. This became critical as it was found that the first gun had excessive grid current. After several theoretical and experimental changes, it was determined that the radius of curvature of the grid was incorrect. A change in grid curvature and a slight modification to the anode shape reduced the grid current to an acceptable level.

After a satisfactory gun was designed, the first tube was built and baked out. The first tests to be made were the beam transmission measurements and the triode measurements. Both proved the Klystrode device was acceptable. Magnetic focusing measurements showed the magnet power to be quite low. The Input and Output Circuits were assembled and cold tested. Hot tests using low duty cycle pulses indicated that the X2255 would have about 20 dB of gain.

The Output and Input Circuits were tuned to about 785 MHz and the power measurements began. However, before critical RF data could be taken, the output window cracked and the tube failed. Because the window was not coated with a film of low secondary emission material, it was believed that multipactor was the problem. A new tube was built with a titanium coated ceramic. Unfortunately this tube failed also. It was theorized that either the coating had

been destroyed or that excessive RF heating was occurring in the thin film because it was too thick. A BeO ceramic was ordered.

The third and final tube was built using a coated BeO ceramic. This tube performed correctly. All of the final data was taken using this tube. Figure 3-1 shows a photograph of the basic tube without any tuning cavities or focussing solenoids.

### 3.2 Design Review of Critical Subassemblies

The various subsections of a Klystrode Amplifier are: The input circuit, electron gun, output circuit, collector and focusing system. These subsections had interdependent design problems. Therefore a brief discussion of the various subsections and their design compromises relative to each other is due. A schematic of the klystrode device is shown in Figure 3-2.

#### 3.2.1 The Input Circuit

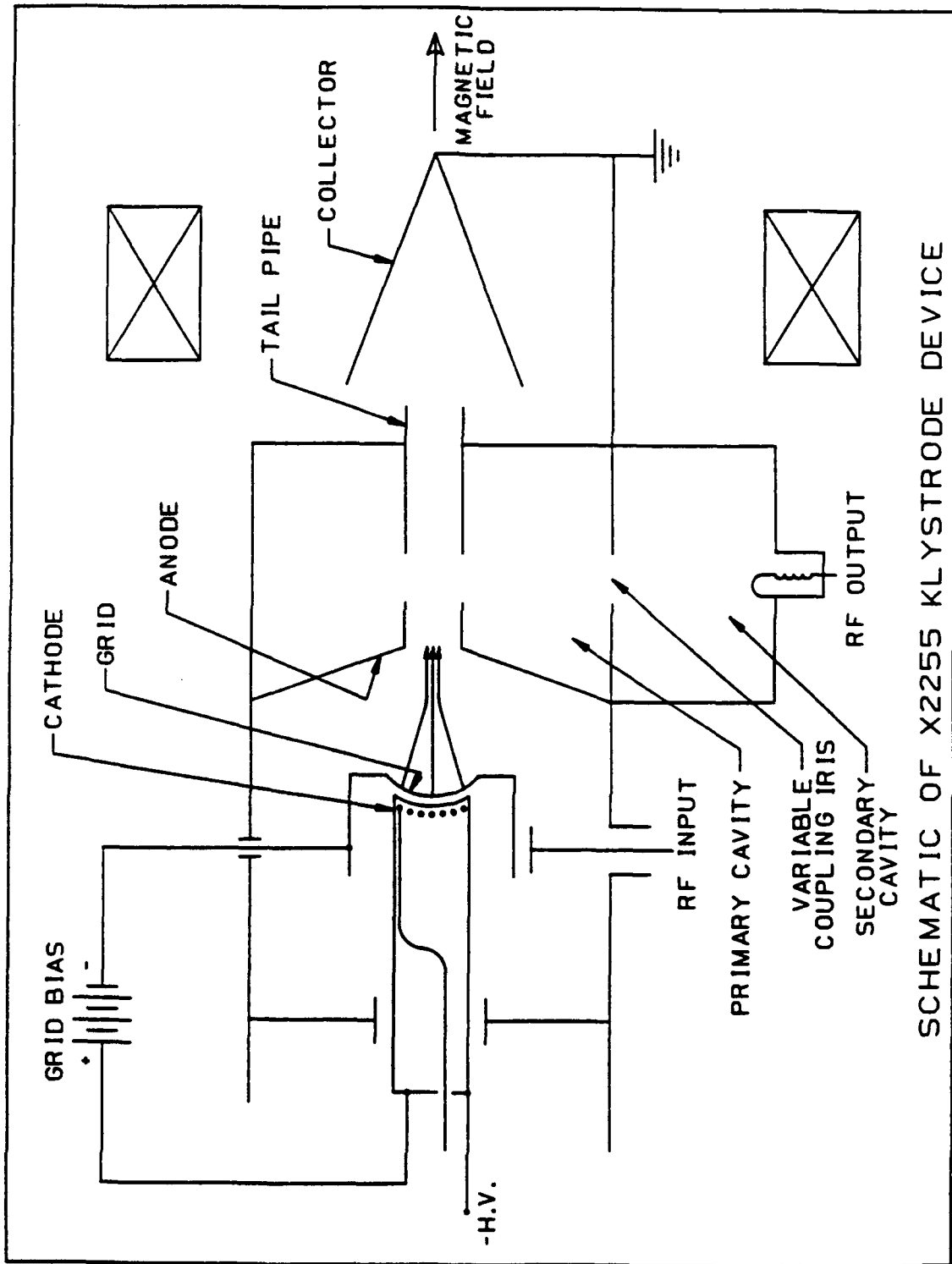
One of the major benefits of EIMAC's UHF television program was the development of the "bell" input circuit. The circuit for the Troposcatter klystrode amplifier was scaled directly from that of the television amplifier. The purpose of the grid bell is to RF bypass the anode of the Klystrode back to the cathode effectively. This is similar in function to the screen grid bypass capacitor of a tetrode. The length of the grid bell is a function of frequency and is set so that the path from cathode to anode is approximately one wave length long. The cathode is at B- and the anode is at ground potential. A 1/4 wave open line choke section is necessary to develop the RF short which completes the outer conductor of the feedback path from anode to cathode (see figure 3-2). The position of this short is moveable and its position effectively generates the necessary transformation between grid-anode and grid-cathode voltages.

#### 3.2.2 The Input Coupler

The RF drive energy is coupled to the grid bell by way of a capacitive probe. For experimental purposes the input coupling was adjusted with a multi-parallel-stub tuner. The combination of this circuit and the input cavity act similarly to a double tuned circuit and can be adjusted to give the required band width. Some experimentation was done to develop a coupling cavity similar to that used for television broadcast service. However, more design work would be necessary to complete such a coupler.



FIGURE 3-1. X2255 KLYSTRODE DEVICE



SCHMATIC OF X2255 KLYSTRODE DEVICE

FIGURE 3-2. SCHEMATIC OF KLYSTRODE DEVICE

### 3.2.3 The Electron Gun

The electron gun for this tube can be seen in Figure 3-3. The gun contains a pyrolitic graphite grid in close proximity to a cathode. This control grid density modulates the electron beam as opposed to velocity modulating it. A convergent structure is used for two reasons. First, a spherical cathode allows a larger surface area for a given diameter beam than a flat cathode. This means a decrease in cathode loading which leads to a lowered cathode temperature and an increase in tube life. Second, the convergent gun generates a smaller beam diameter for a given cathode current. This reduced diameter allows one to decrease the diameter of the output cavity drift tubes.

The output bandwidth and efficiency of the Klystrode tube depend heavily on the output gap dimensions. One would like to keep the electron transit angle across the gap as short as possible so that the electrons do not become de-bunched due to space charge or encountering a reversing field polarity at the resonant frequencies. This requires a decreasing gap length as we increase the output frequency of the device. The effect of decreasing the gap length is to increase its capacitance. We however, need to keep the R/Q high in order to obtain a large output bandwidth. If we increase the capacitance we will decrease the R/Q. Hence the only way to decrease the gap length without increasing its capacitance is to simultaneously decrease its diameter. This requires using a convergent gun structure.

### 3.2.4 The Output Circuit

In order to keep a large R/Q ratio, one would also like to keep the gap centered in the output cavity. However, one would also like the transit angle from cathode to gap to be as short as possible to keep the electrons from debunching. As one increases the output frequency, this means moving the gap closer to the cathode or off the central plane of the output cavity. As a compromise to this problem, the Klystrode tube has its gap only slightly off center, but has a conical anode which allows the gun to be moved up closer to the gap. The increase in capacitance due to the conical anode distorting the output cavity electric field is not as great as it would have been had the gap been moved down to the anode end of a conventional output cavity with flat end plates.

The output window has been an item of some concern. The first window used was AD-995, high purity alumina. The failure of this window was believed due to multipactor. Multipactor is an avalanche secondary emission effect where electrons do an oscillatory impact between two points on the ceramic guided by the RF electric and static magnetic fields. The cure is to reduce the secondary emission coefficient by coating the ceramic with a thin film of titanium. This was the process utilized on the first

# X2255 ELECTRON GUN OUTLINE

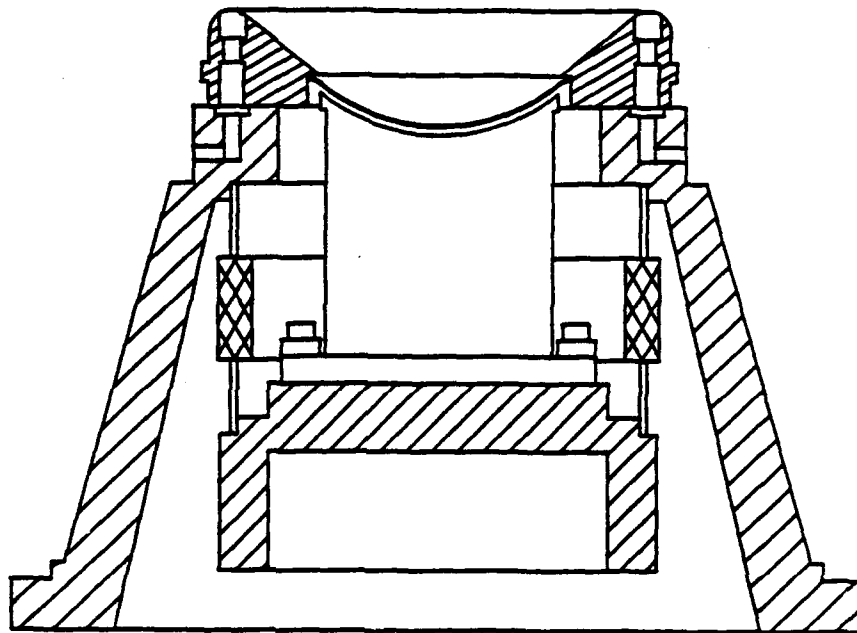


FIGURE 3-3. X2255 ELECTRON STRUCTURE

rebuild of the Klystrode. When this window also failed suspicion was cast in two directions. Either the coating disappeared or was overlaid during the bake out and tube processing, or the RF losses in the film generated enough heat to cause ceramic failure. It was the second possibility that lead to the choice of using BeO for the ceramic and coating it with titanium. BeO has a higher thermal conductivity. This combination solved the problem.

The failure of the second window was very suprising because great care was taken to insure that the coating thickness was well within the acceptable range. The tolerances of this thickness were discovered and well documented in the past. Rather than pursue a new program of coating development it was decided that BeO would be used. (Subsequently it was found that alumina cermic was perfectly satisfactory when coated with a Titanium film of the correct thickness which was considerably less than what had been established earlier. The inconsistency is suspected to involve the surface finish of the ceramic).

The external output cavity used on the Klystode is an iris coupled double tuned structure (see figure 3-4). It is important to keep the R/Q ratio high for a wide band output cavity. The R/Q ratio is really an expression of the characteristic impedance ( $Z_0$ ) of the output cavity. The purpose of this structure is to match the beam impedance and the load impedance. Therefore a large R/Q ( $Z_0$ ) is generally required. To increase the  $Z_0$  for proper Impedance matching, the cavity height was increased to 3.5 inches. However, the output window diameter was decreased to 3 inches to keep the cavity's tuning range from being shifted lower in frequency. Wide bandwidth is also achieved by using two resonant circuits (i.e., two cavities) coupled by an iris that looks like an inductor. By proper iris adjustment one can tune from a double humped over coupled state through the flat critically coupled state to the single peaked under coupled state. Bandwidth is then a function of both iris and load coupling.

### 3.2.5 The Focusing System and the Collector

The electron beam must be focused from cathode to collector. One of the objectives of the program was to minimize electromagnet power. The Klystrode tube being short in length is already efficient in that it requires only one focusing magnet. However, with proper design it is possible to reduce the power of even that magnet. It would be desirable to make the tail pipe conical in shape allowing the beam to spread rapidly into the collector by decreasing the magnetic field in this region. This, however, would once again reduce the R/Q ratio. It was decided this was not a good approach. However, with the gun pushed up into the conical anode, it was possible to place a conical pole piece in this region. The pole-piece is made of core iron and is in the vacuum.

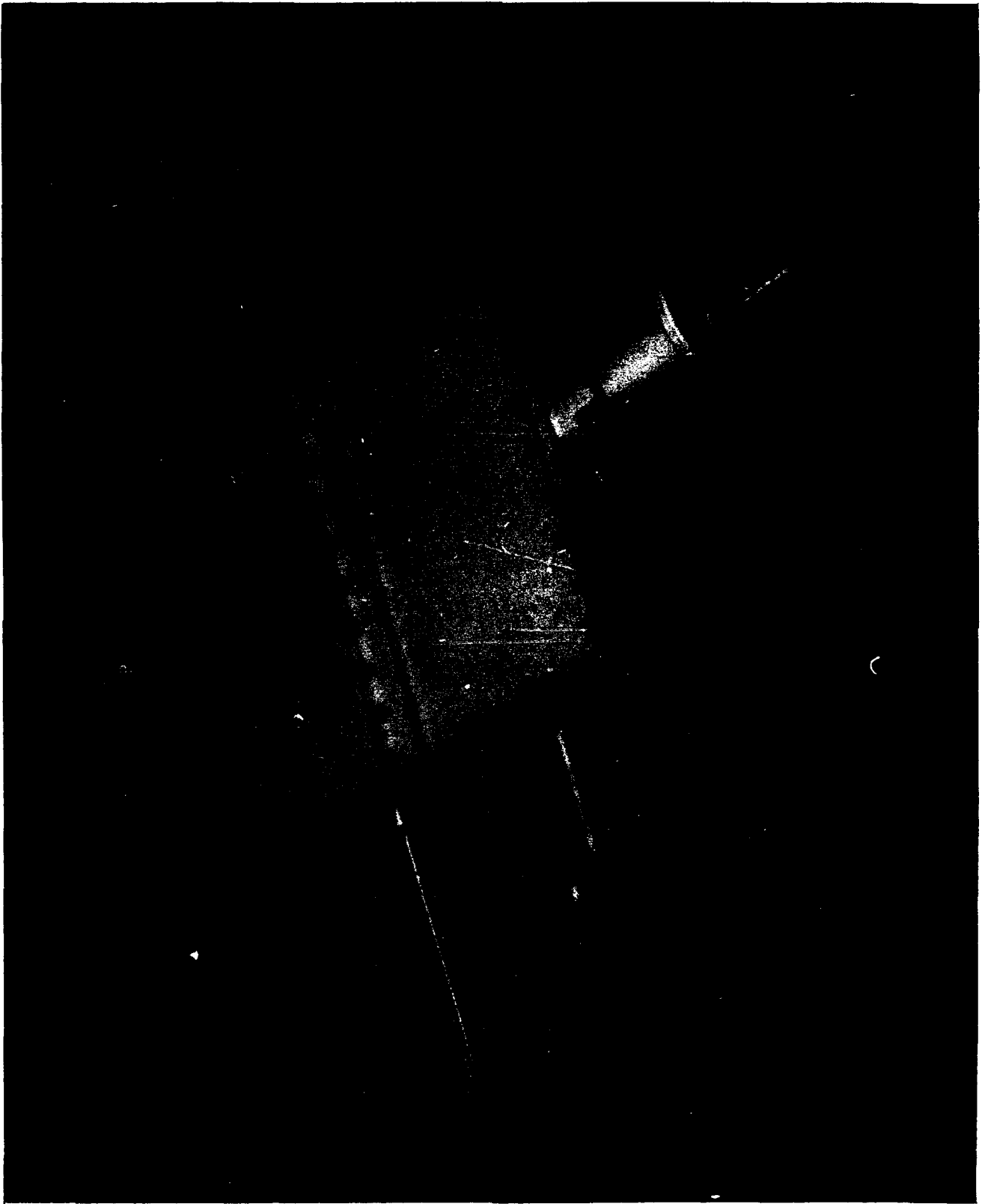


FIGURE 3-4 DOUBLE TUNED OUTPUT CIRCUIT

This meant a smaller aperture could be used and less power would be required to generate the magnetic field. Figure 3-5 shows a plot of the axial magnetic field required to focus the beam.

### 3.2.6 The Complete Klystrode Amplifier

Figure 3-6 shows the completed experimental troposcatter klystrode amplifier. The various detailed subsections are as follows, from top to bottom. The silver top canister contains the high voltage and bias voltage feed throughs as well as oscillation suppression circuitry. The red cylindrical structure is the input cavity which houses the grid bell and sliding cathode short. The silver box is the double tuned output cavity. The red object with wire leads connected to it is the single focusing magnet, and the blue structure is an iron flux path connecting the pole pieces. Below the amplifier the collector can be seen with its water connections. The output coupler and water load is visible on the right side. Air is required to cool both the input and the output cavities.

### 3.2.7 Subsystem Support

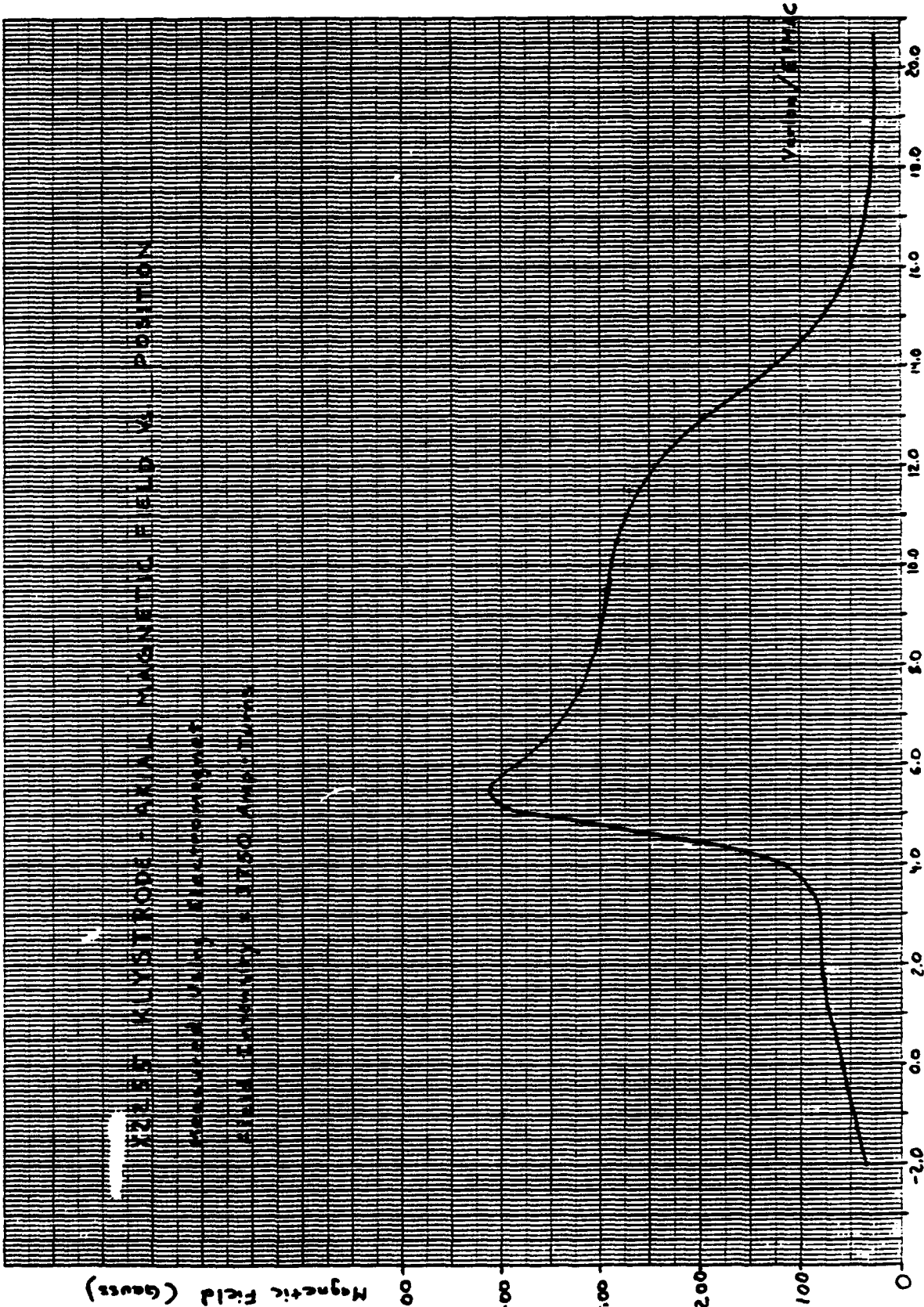
The complete amplifier system requires several external support subsystems. The required power sources are: B- supply, Bias supply, Magnet supply and Vac Ion pump supply (see figure 3-7). A crowbar protection circuit is necessary to protect the tube from damage by arcs. A solid state amplifier is necessary to drive the Klystrode; and the Klystrode amplifier should be decoupled from this solid state amplifier with a circulator. The cooling subsystems are shown schematically in figure 3-8. Water sources are necessary for both collector and body cooling. Air sources are required to cool the cavities. All of these subsystems should have proper interlocking to protect the tube.

The Klystrode device's operational specifications are listed in Table 4.

## 3.3 Performance Tests

### 3.3.1 DC Beam Performance

The first critical performance test for the Klystrode is measurement of the triode characteristics of the gun. Figure 3-9 shows a plot of beam and grid current versus grid voltage with an anode voltage of 17.5KV. Since grid current represents lost gain, it is important to keep its value as low as possible. The plot shows that grid current is never greater than 23% of beam current for grid voltages up to 30 volts positive. This is very acceptable. Also notable is that anode interception current is negligible even



3/11/85 MPC

FIGURE 3-5 AXIAL MAGNETIC FIELD (ELECTROMAGNET)

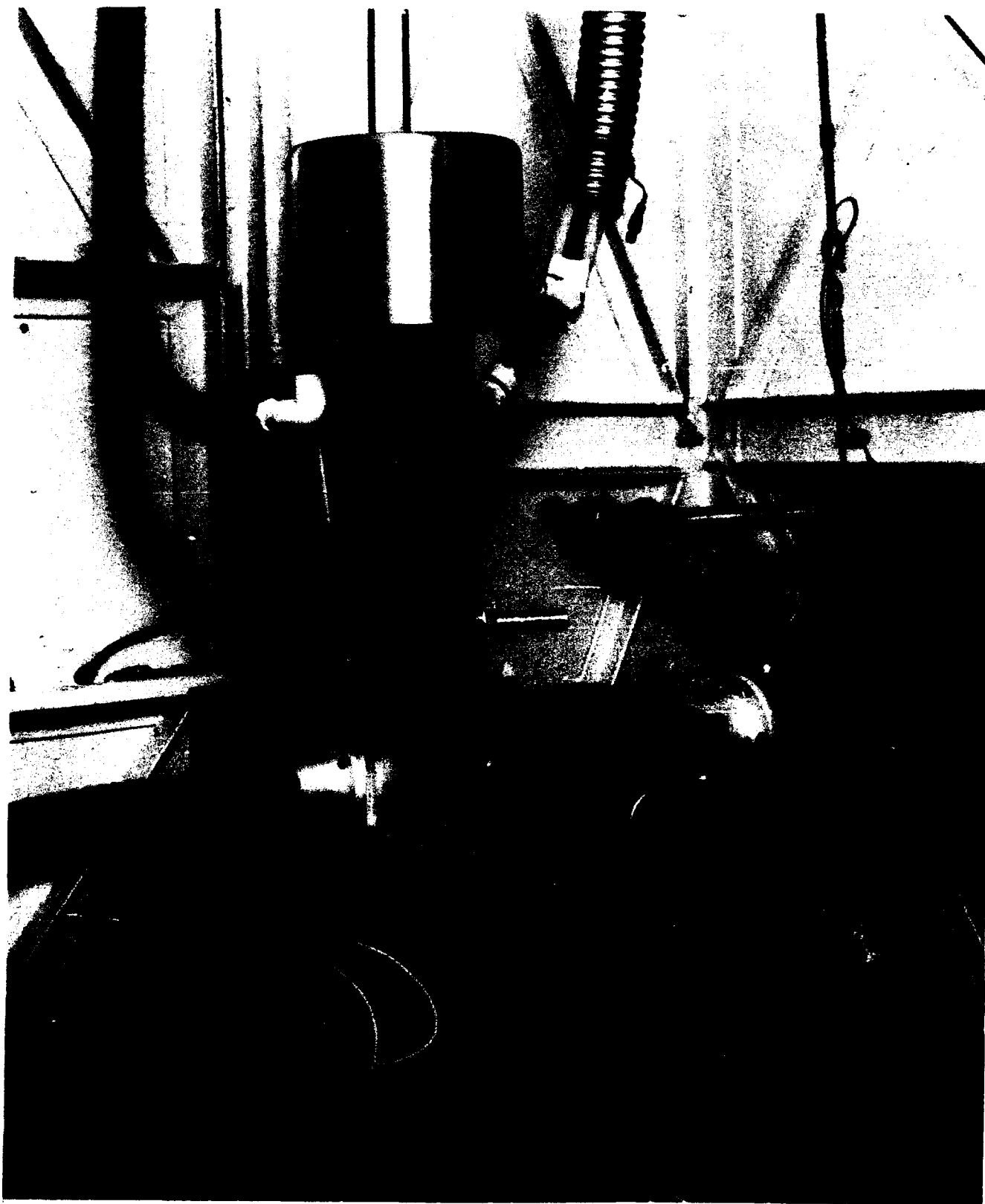


FIGURE 3-6 KLYSTRODE IN ITS EXPERIMENTAL CIRCUIT

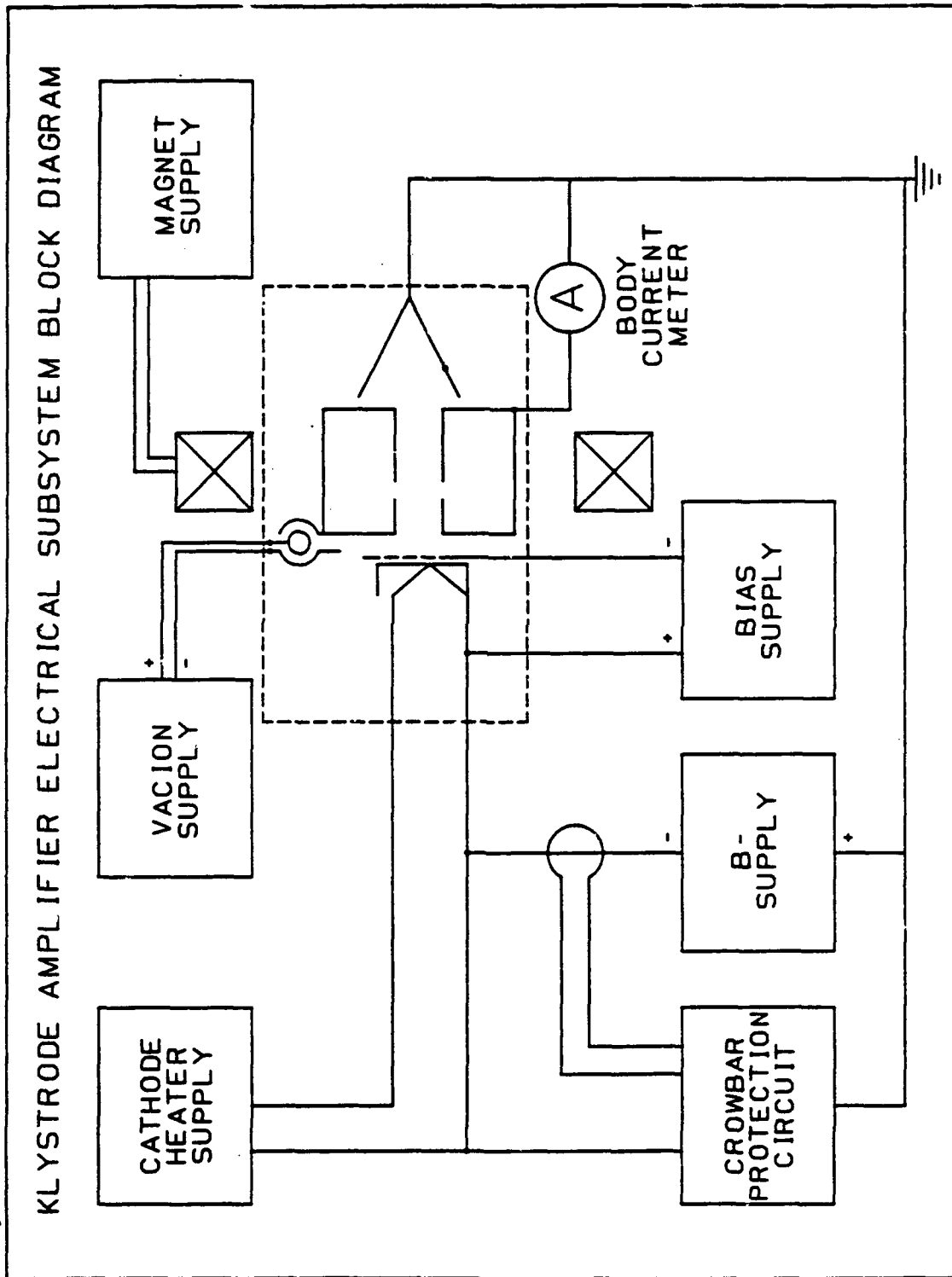


FIGURE 3-7 ELECTRICAL SUBSYSTEMS

# KLYSTRODE AMPLIFIER COOLING SUBSYSTEM BLOCK DIAGRAM

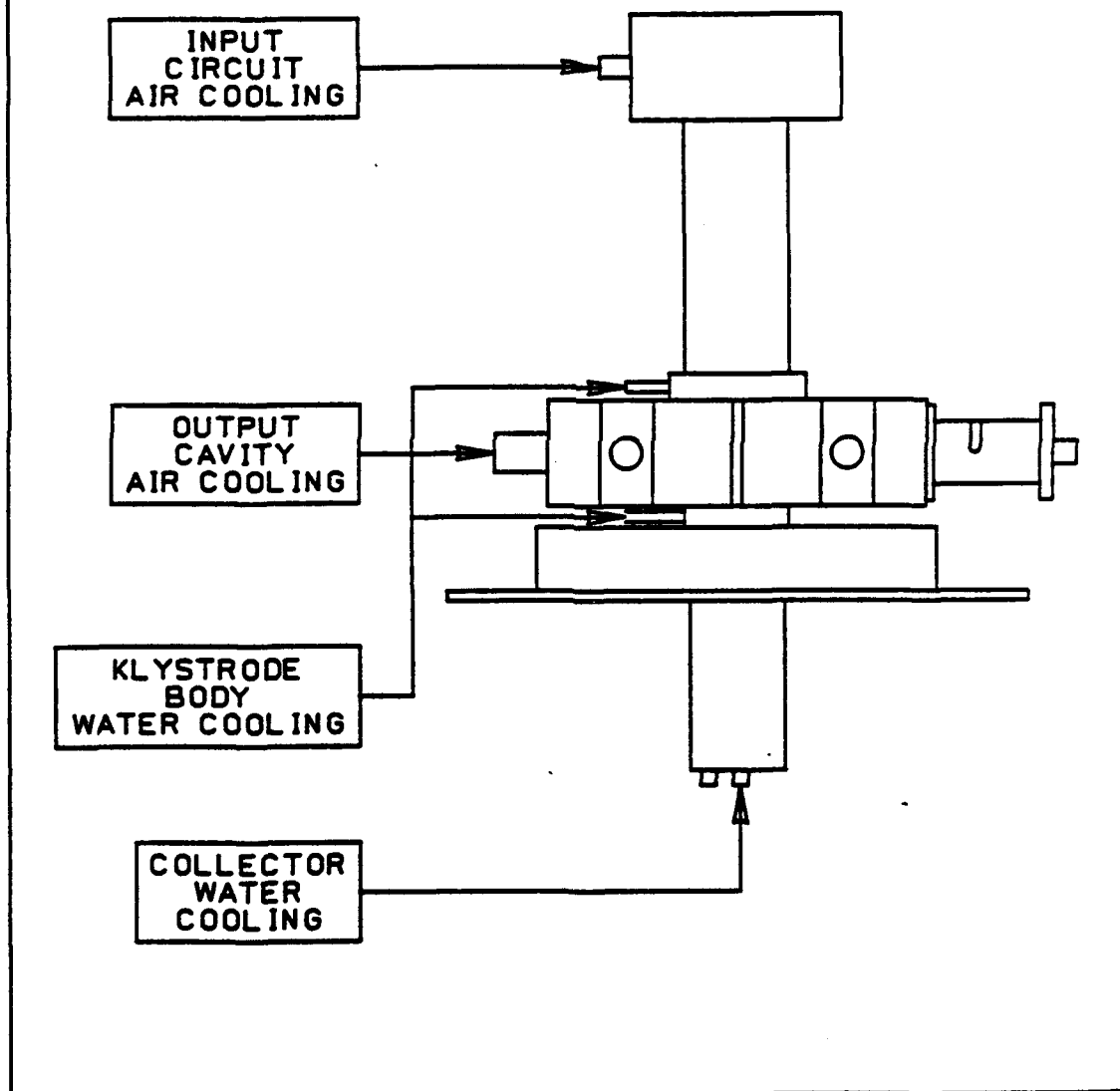


FIGURE 3-8 COOLING SUBSYSTEMS

**TABLE 1 X2255 GENERAL OPERATING SPECIFICATIONS**

<b>Beam Voltage</b>	<b>16 to 18 KV</b>
<b>Grid Bias Voltage Range</b>	<b>-30 to -80 Volts</b>
<b>Cathode Heater Voltage</b>	<b>7.0 Volts</b>
<b>Cathode Heater Current</b>	<b>10.8 Amps</b>
<b>Maximum Allowable Gas Current</b>	<b>100 uAmps</b>
<b>Magnet Voltage</b>	<b>35 Volts</b>
<b>Magnet Current</b>	<b>5 Amps</b>
<b>Collector Cooling Water Flow</b>	<b>25 gpm @ 25 psi</b>
<b>Body Cooling Water Flow</b>	<b>1.5 gpm @ 25 psi</b>
<b>Input Circuit and Cathode Cooling Air Flow</b>	<b>10 cfm @ 2 in of H2O</b>
<b>Output Circuit Cooling Air Flow</b>	<b>100 cfm @ 1 in of H2O</b>

4/28/87 MPC  
Varian/ELMAC

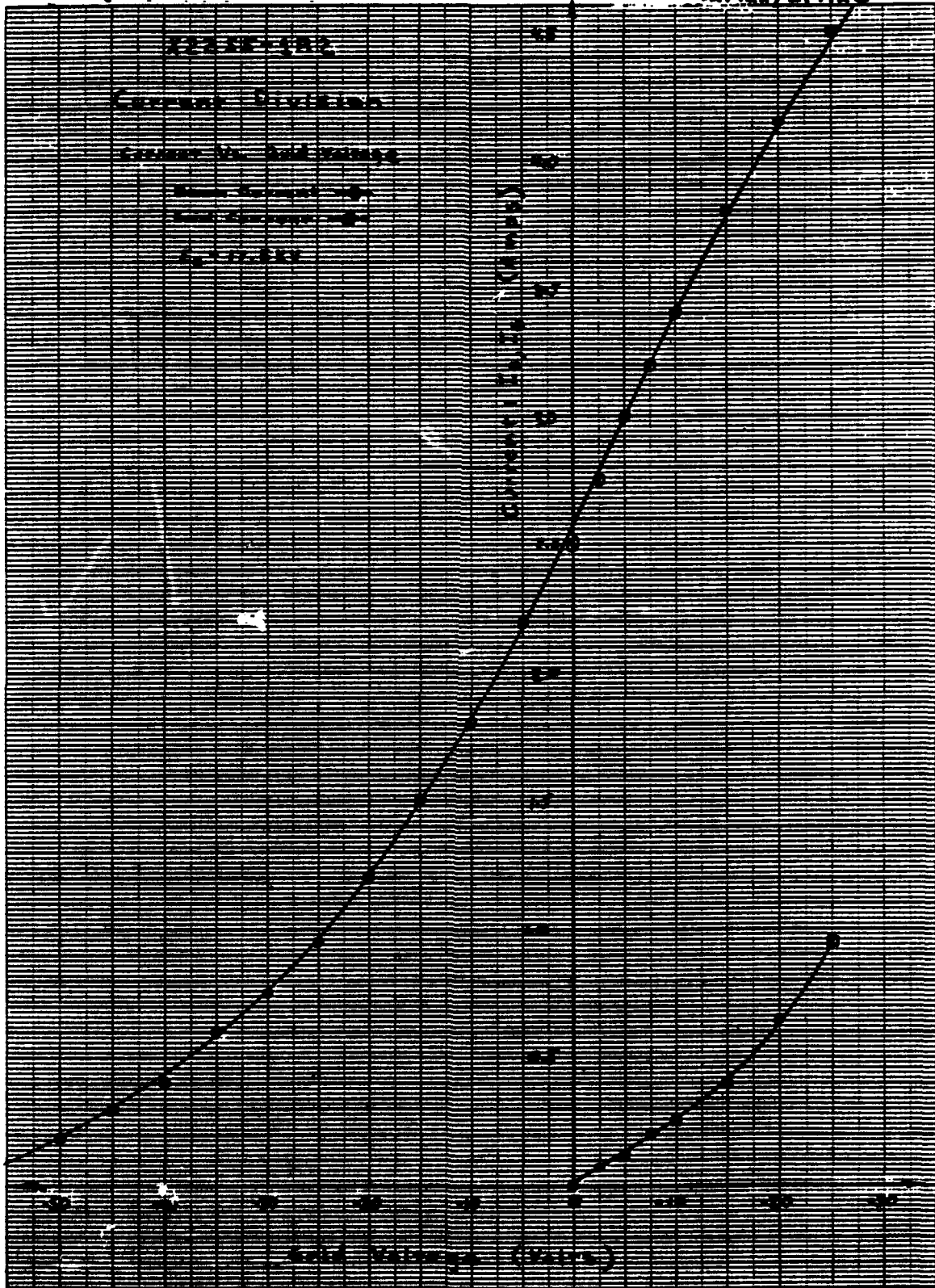


FIGURE 3-9 DC TRIODE CURVES

at beam current levels of 4.5 Amps. This shows that the electrostatic focusing is correct. Finally, the measured grid-cathode cut-off voltage is 75 volts negative.

### 3.3.2 Klystrode RF Amplification Performance

Figure 3-10 is a typical transfer curve for the X2255 Klystrode amplifier. This curve has its left ordinate indicating RF output power in kilowatts and its right ordinate showing average DC beam current both as a function of RF drive power. The data was measured at the center frequency of 920 MHz with the circuit adjusted for a 0.5 dB power roll-off with a 10 MHz bandwidth or 1.0db at 11 MHz. It appears that output saturation occurs at slightly greater than 12 KW. The 12 KW output power gain is shown to be about 19.6 dB and the 10 KW output power gain is 22 dB.

### 3.3.3 Efficiency Results

Device efficiency is of extreme importance. Figure 3-11 gives an indication of the change in energy conversion efficiency as a function of center frequency. Again the amplifier is set for a 0.5 dB 10 MHz response. Figure 3-12 shows how the energy conversion efficiency will vary as the bandwidth is changed. This data was measured at 780 MHz close to the lowest desirable operating frequency range for this device. As one would expect, efficiency decreases with both increasing frequency and bandwidth.

Due to time and test equipment limitations, the Klystrode's performance was measured at the upper edge of the band and at the mid-band frequency of 780 MHz. One can reasonably ask if device performance will degrade at 755 MHz, the lower edge of the band. The answer to this question is no. With Klystrodes, as with most power grid tubes, performance degrades with increasing frequency.

The major degradation in performance is caused by an increase in transit angle with an increase in frequency. Transit angle (or transit time) is the time it takes an electron to traverse from one point to another point expressed in radius of a cycle period of the given frequency. With the beam voltage fixed, the actual time of transit from point to point is fixed. However, an increase in frequency means a decrease in cycle period leading to a larger transit angle. The Klystrode's transit angle is from cathode to output gap. This distance is composed of three segments. First an increase in the grid to cathode transit angle means that with increasing frequency the grid is less effective at drawing current off the cathode. Second, an increase in the grid output gap will allow greater bunch spreading and a decrease in efficiency. Finally, an increase in the output gap transit angle decreases the output gap coupling coefficient resulting in a drop in efficiency.



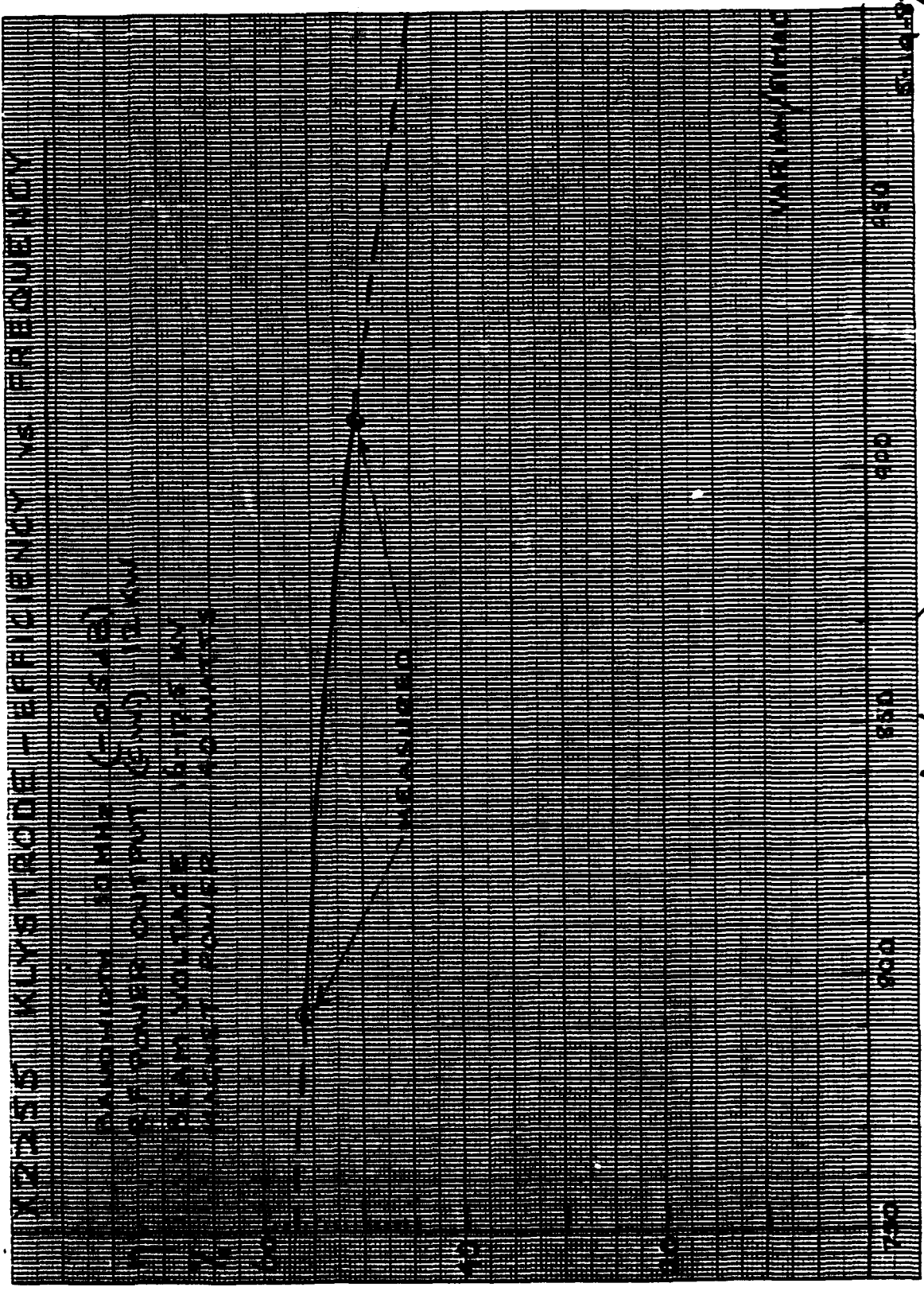


FIGURE 3-11 EFFICIENCY VS. CENTER FREQUENCY CURVE

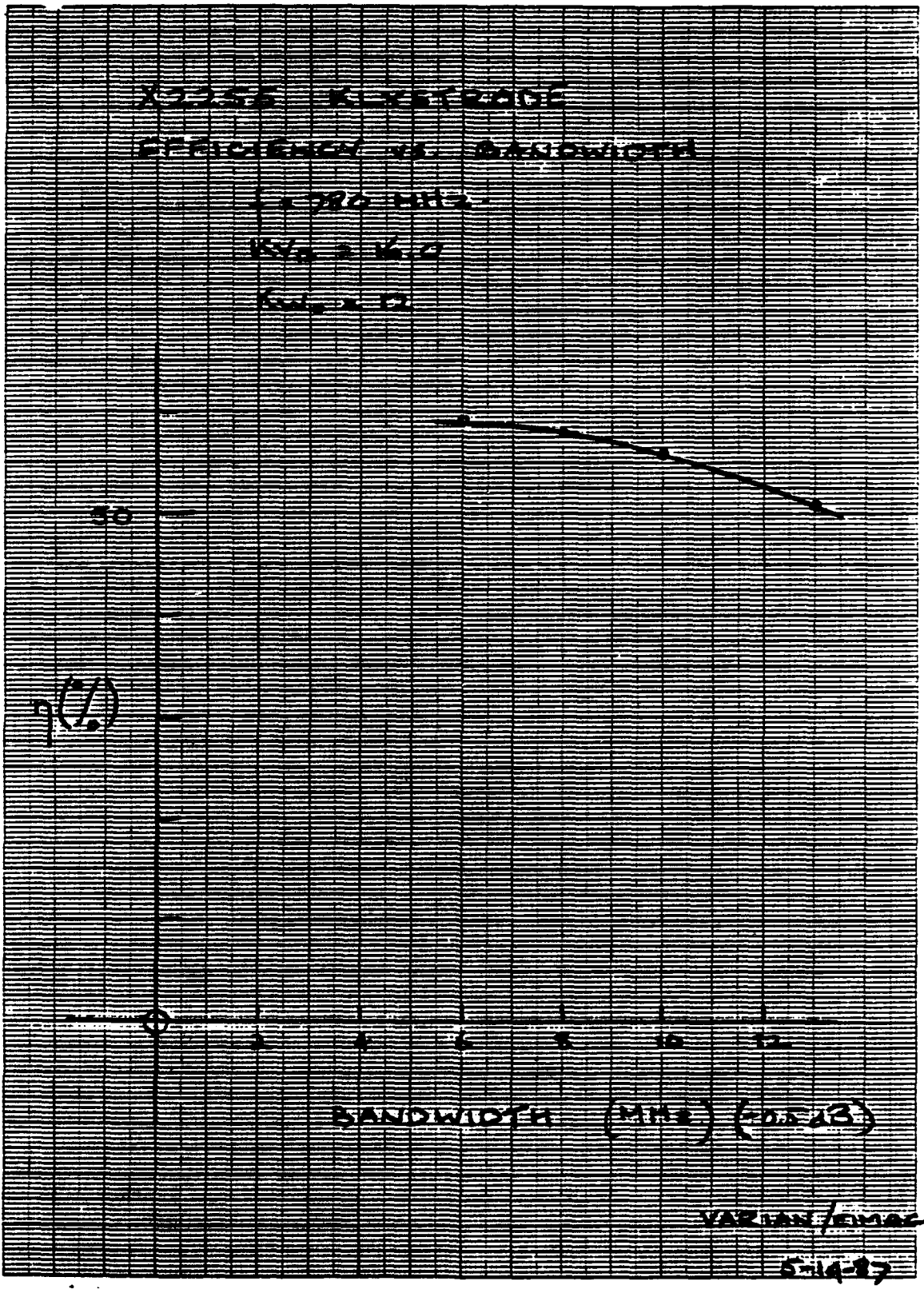


FIGURE 3-12 EFFICIENCY VS. BANDWIDTH CURVE

The result of this is that if performance can be achieved at the upper edge of the desired band, it can be achieved at the lower edge. The use of an external double tuned cavity allows one to obtain the full 10 MHz bandwidth at 755 MHz. In particular, a 15KW television Klystrode with a gun identical to this Klystrode is operating at 632 MHz (ch 41) in Charlottesville, Virginia.

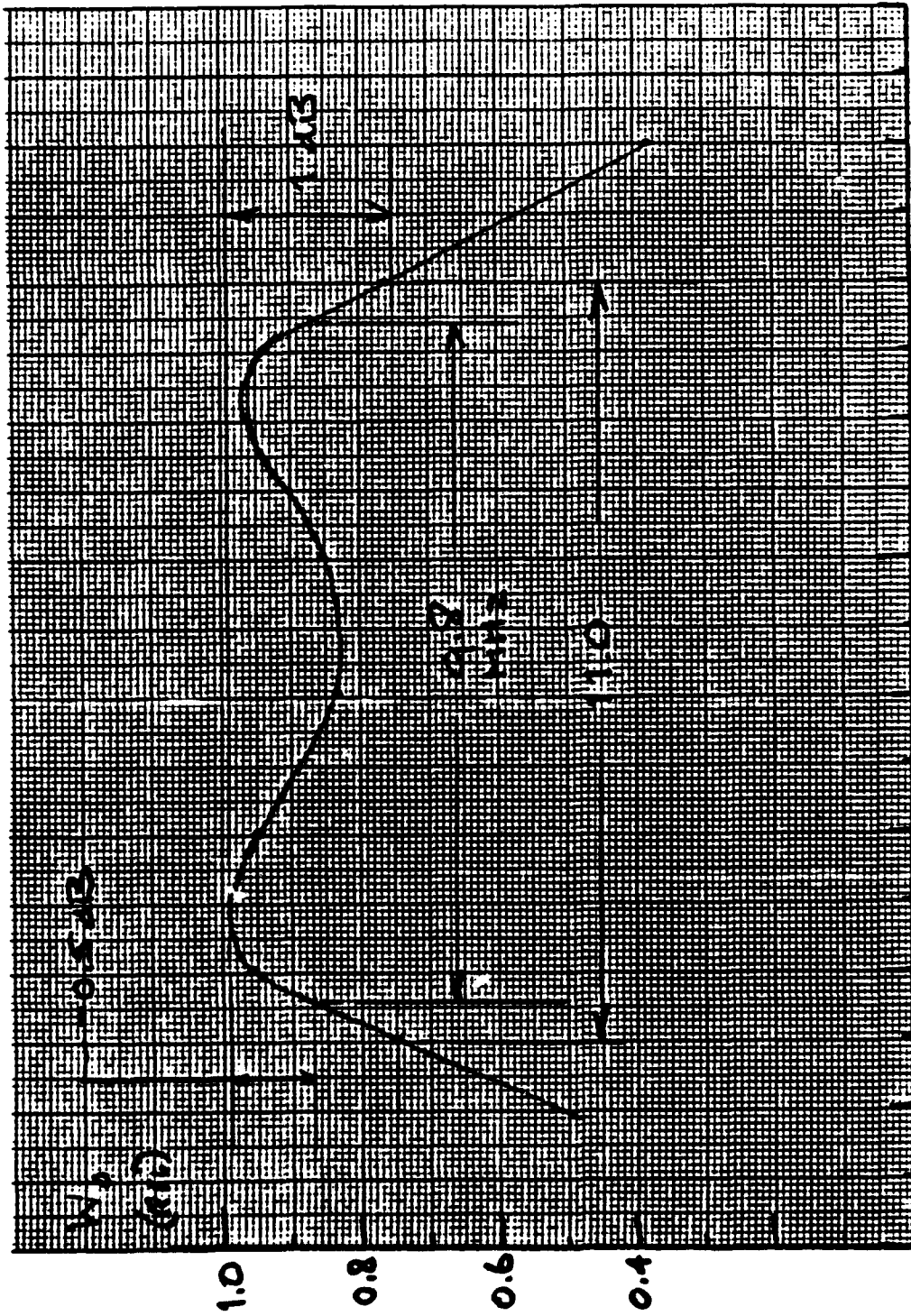
#### 3.3.4 Bandwidth Data

Most of the data measured for the X2255 Klystrode amplifier is around two frequencies 800 and 920 MHz. We at EIMAC were not able to measure the device's performance at higher frequencies due to the unavailability of RF drive above 930 MHz. The passband was measured at both of these frequencies. Figure 3-13 is a plot of the measured passband of the Klystrode amplifier when tuned for a center frequency of 920 MHz. The output power at the center frequency is 12 KW with a conversion efficiency of 50%. The measured passband is plotted in Figure 3-14 for a center frequency of 800 MHz with 12 KW of output power and a conversion efficiency of 56%. Although measurements were not taken at the highest frequency required of this device, cold cavity measurements indicate that both output and input circuits will indeed tune to 985 MHz. The 10 MHz of required bandwidth will be easier to obtain at this higher frequency. By extrapolating the above data one can deduce that 45% efficiency may be expected of this device in this frequency range.

#### 3.4 Problems Encountered During the Program

The program could not be completed without first overcoming some problems. Two major technological problems slowed the project down. First was the inability to create a grid with the correct radius of curvature. The result was excessive grid current. This problem was a process control problem and was eventually solved. The second technological problem was the ceramic failures discussed earlier. This problem had to be experimentally solved. The solution of using BeO is not a very good solution. BeO ceramics are expensive because materials containing Beryllia require special handling techniques. However, more research into coating processes is required before returning to the use of Alumina ceramics.

From the beginning of the contract it was realized that the grid of the klystrode would have to be made from pyrolitic graphite, laser cut as had been done on all klystrodes so far built at EIMAC. These earlier grids had been well developed and performed well, but they were flat, that is in one plane, and were used in an electron gun which produced a broom stick, or parallel beam. The gun required by the subject contract clearly had to be convergent so that the performance objectives of the program, especially bandwidth and



5-13-87

f (MHz)<sup>920</sup>

FIGURE 3-13 OUTPUT RESPONSE AT 920 MHz

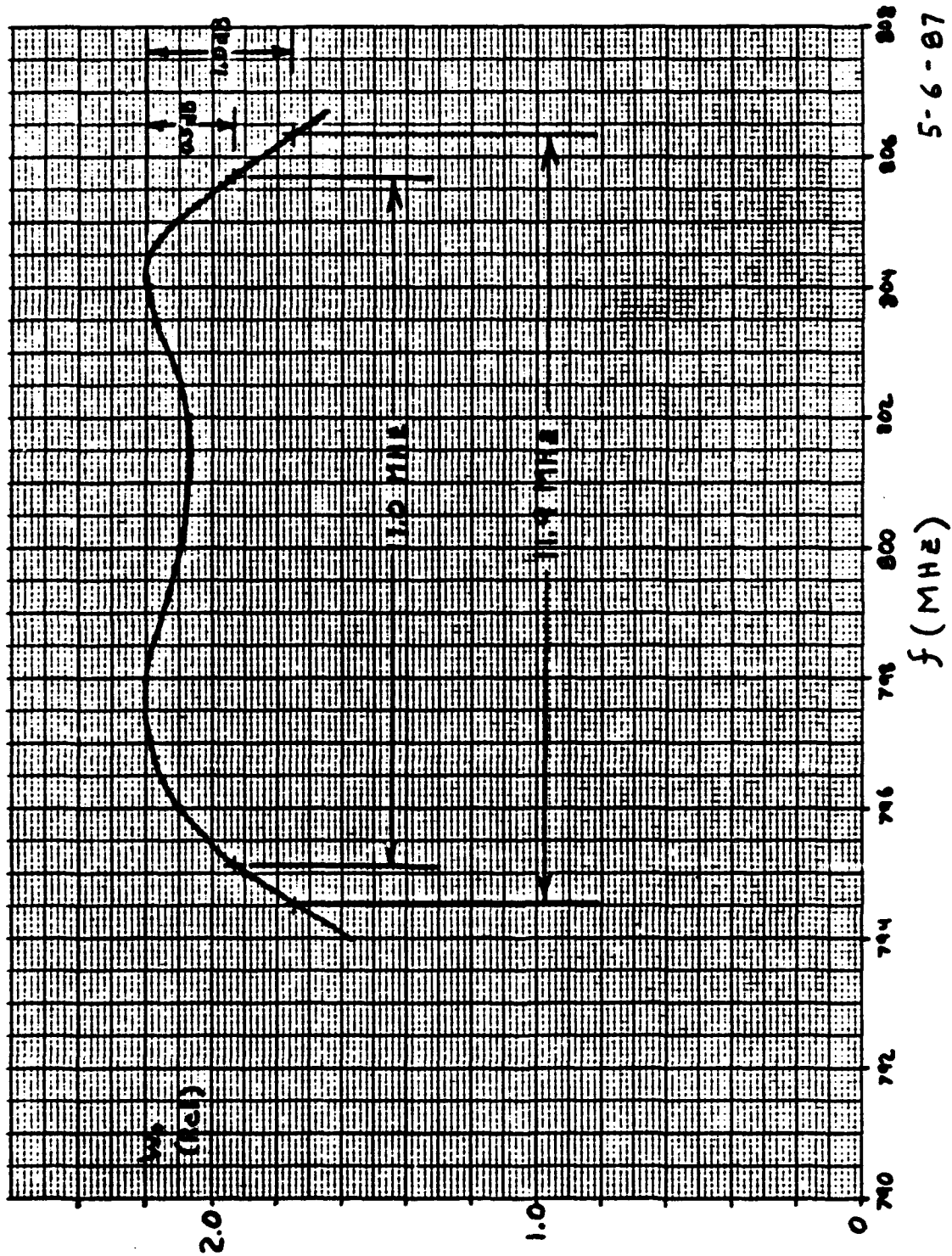


FIGURE 3-14. OUTPUT RESPONSE AT 800 MHz

efficiency, could be met. It therefore became necessary to develop techniques for the fabrication of grids which were portions of a spherical surface and solve the problems of mounting such a grid concentrically over a cathode with a similar spherical surface. Clearly the computer program which had been successfully used to cut planar grids would not be suitable for spherical grids.

In reality the development of a computer program for cutting spherical grids turned out to be much more arduous and complex than was at first realized, and in the course of solving all the problems, about 8 months were consumed. Having arrived at a satisfactory program, the next step was to implement it in terms of computer hardware. This apparently simple problem turned out to be very difficult, partly because of the need to use hardware situated in two divisions of Varian. The problems of compatibility between these various pieces of equipment was finally solved, but again a delay was involved amounting to about two more months. The final solution was completely satisfactory, and grids have been fabricated successfully since that time.

### 3.5 Future Engineering Programs

#### 3.5.1 Complete Amplifier Characterization

The program for which this report is being written did a great deal to develop a troposcatter Klystrode amplifier in the UHF region. However, time and funding did not allow the completion of the job. There are several subsystems which could be improved with further work. Also, the measured data is not complete. A program is necessary to complete the measurements across the operational band. This would allow the generation of tuning curves or tables.

#### 3.5.2 Input Coupling

Another area of improvement needed is input coupling. At present the best method of coupling is with a 4-stub tuner. An effort was made to develop an input coupling cavity similar to that which is used on the television Klystrode amplifier. The first version of this cavity fell short of expected performance. However, with a little more experimentation such a device could be completed.

#### 3.5.3 Collector Improvements

The collector on this experimental tube is the same water cooled collector used on the 30KW television Klystrode tube. Although this is over kill for its present use, it was expedient and inexpensive. Future programs could improve upon this design. There are two possible approaches. The first is to develop a vapor cooled collector similar to that of a klystron. However, the more

interesting approach would be to air cool the collector. This approach would again benefit from the UHF television program as EIMAC has developed a 15KW air cooled tube for the 600 to 800 MHz region. The same technology could easily be extrapolated to a 985 MHz troposcatter Klystrode tube.

#### 3.5.4 Permanent Pole Magnet

The magnetic field requirements for the X2255 are relatively simple. An experimental structure was made to see if it would be possible to generate the required field with permanent magnets. Figure 3-15 shows the measured axial field of this structure. A comparison of this figure with Figure 3-5 shows the two are quite similar. With a small amount of engineering design it may be possible to replace the electromagnet and its power supply with a permanent pole magnet.

#### 3.5.5 Productization

Finally, the structure shown in Figure 3-6 is really an experimental device. Although it operates exactly as a useful device would, in its present form, it is not usable as an actual amplifier at a real site. It would be very important to productize the circuit and hardware in a fashion similar to that which has been done to other Klystrode amplifiers. This is important in terms of usability, maintainability and safety.

#### 3.6 Summary and Conclusions

This contract projected the design of a new 12KW Klystrode for UHF Troposcatter applications. The (X2255) Klystrode device developed has met all of the requirements listed under "PROGRAM OBJECTIVES". These include a measured RF gain of 20 to 22 dB, an efficiency of greater than 50%, an operational bandwidth of 9 MHz, and a tuning range of 755 to 985 MHz. Other than the addition of a bias supply and a solid state RF driver amplifier, the Klystrode Amplifier, when fully productized, will be closely compatible with existing klystron sites. It should be noted that Comark Communications is marketing a transmitter for the television market which accepts klystrons and klystrodes interchangeably.

Although the (X2255) Klystrode Amplifier had some unique design problems, its' general structure came as a direct extrapolation of work completed by EIMAC on its UHF television Klystrode Amplifiers. This project benefited from the design of a convergent gridded gun and the design of an iris-coupled, double-tuned output circuit that operates up to 985 MHz. The program was not without its problems,

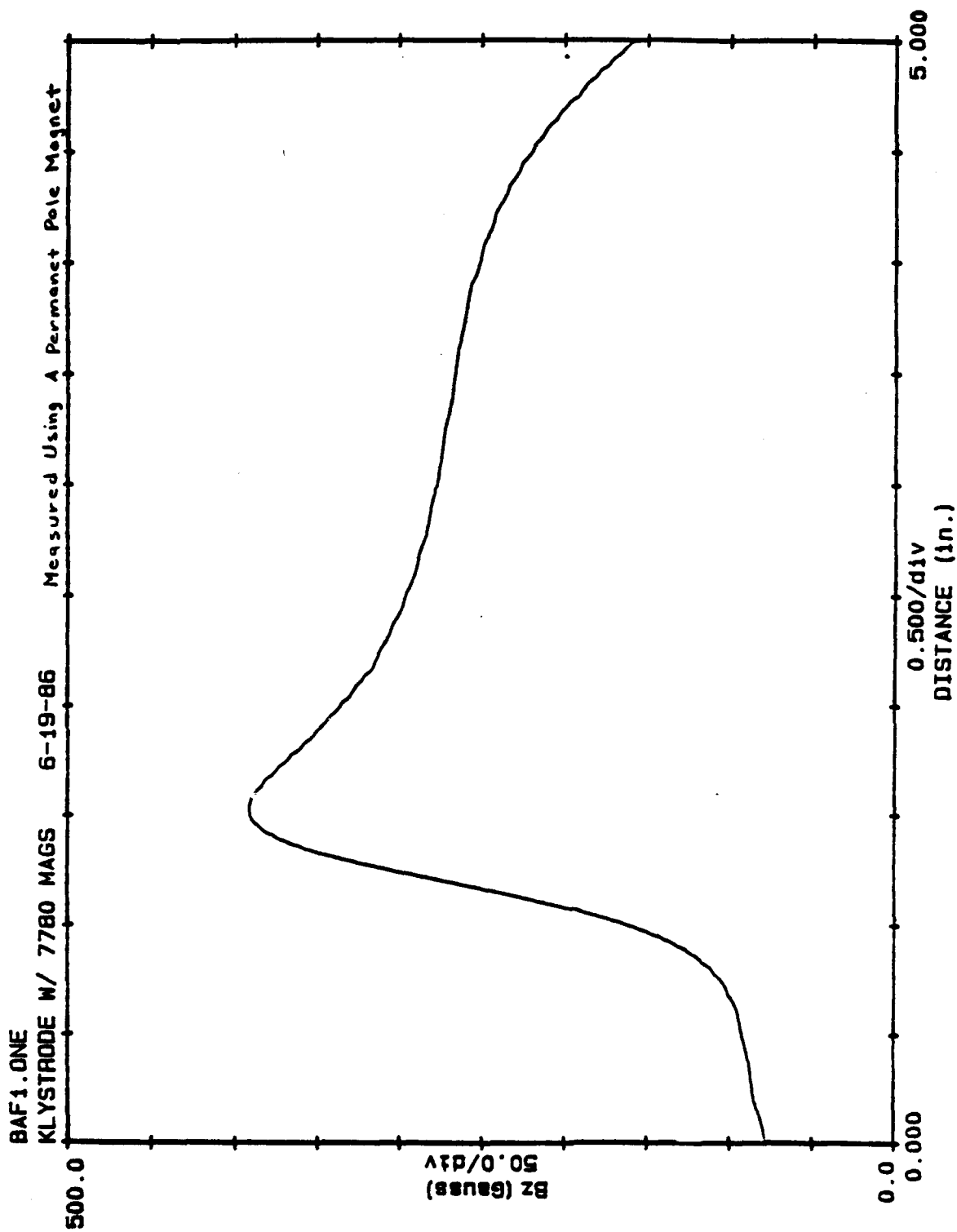
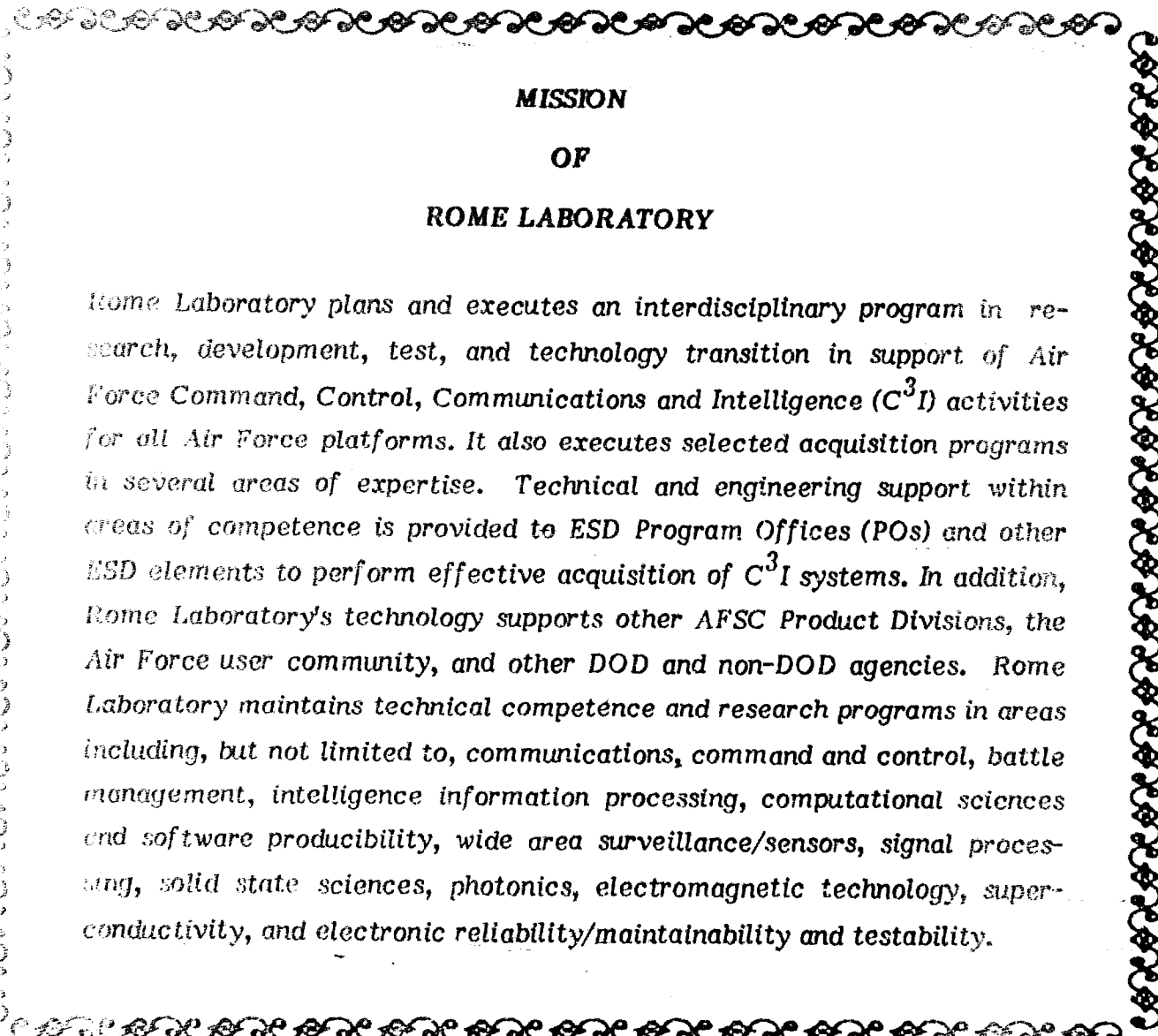


FIGURE 3-15. AXIAL MAGNETIC FIELD (PERMANENT MAGNET)

but all were overcome satisfactorily. EIMAC feels the present amplifier is a good design which can be improved upon.

Although the existing experimental Klystrode Amplifier met all requirements for troposcatter applications, the continued development of this device into a useable product is recommended. One practicable improvement would be the design of a permanent pole magnet focusing system. This would most likely reduce the Klystrode Amplifier's weight (which is already less than 100 lbs. magnet and circuit included), and would eliminate the magnet power supply. Other developmental foci should include: complete device characterization, input coupler design, and addition of an air cooled collector. With these recommended improvements the (X2255) Klystrode Amplifier would make a desirable and efficient Amplifier for troposcatter applications in the 755 to 985 MHz range.



**MISSION  
OF  
ROME LABORATORY**

Rome Laboratory plans and executes an interdisciplinary program in research, development, test, and technology transition in support of Air Force Command, Control, Communications and Intelligence (C<sup>3</sup>I) activities for all Air Force platforms. It also executes selected acquisition programs in several areas of expertise. Technical and engineering support within areas of competence is provided to ESD Program Offices (POs) and other ESD elements to perform effective acquisition of C<sup>3</sup>I systems. In addition, Rome Laboratory's technology supports other AFSC Product Divisions, the Air Force user community, and other DOD and non-DOD agencies. Rome Laboratory maintains technical competence and research programs in areas including, but not limited to, communications, command and control, battle management, intelligence information processing, computational sciences and software producibility, wide area surveillance/sensors, signal processing, solid state sciences, photonics, electromagnetic technology, superconductivity, and electronic reliability/maintainability and testability.